Robustness of steel frames further to a column loss: development of analytical methods for practitioners

Auteur : Jacques, Mathilde
Promoteur(s) : Demonceau, Jean-Francois; Jaspart, Jean-Pierre
Faculté : Faculté des Sciences appliquées
Diplôme : Master en ingénieur civil des constructions, à finalité
Année académique : 2018-2019
URI/URL : http://hdl.handle.net/2268.2/6784

Liège University
Faculty of Applied sciences
Academic year 2018-2019

Robustness of steel frames further to a column loss: development of analytical methods for practitioners.

Dissertation submitted as part requirement for the degree of Master in Civil engineering.

Written by Mathilde Jacques.

Jury members:
Jean-François Demonceau (promotor)
Jean-Pierre Jaspard (co-promotor)
Vincent Denoel
Sébastien Seret

I would like to thank one of my hometown friend, Emilie, and her mum for giving me support to take the engineer entrance test in the first place. Furthermore, I would like to thank my close friends and family, and in particular Julien, who have been supportive throughout my academic journey. Moreover, I would also like to thank Dave for reviewing the present work. Besides, I would like to thank Fantine for the support during the final step.

In addition, I would like to deeply thank my promoter, Jean-François Demonceau and my co-promoter, Jean-Pierre Jaspard for guiding me during the accomplishment of my master thesis. I would also like to thank Vincent Denoel for his constructive advice and help. Finally, I would like to thank Sebastien Seret and the preceding academical members for accepting to be part of the jury of the present master thesis.

Mathilde Jacques

Statement

The statement of this master thesis is written in French.

Titre du travail: Version anglaise: Robustness of steel frames further to a column loss : development of analytical methods for practitioners.
Version française: Robustesse des portiques en acier suite à la perte d'une colonne: développement de méthodes analytiques pour les praticiens.

A l'heure actuelle, les réglementations européennes en matière de robustesse des structures se limitent à l'énoncé de principes généraux. D'un point de vue purement pratique, seule l'une ou l'autre procédure directement utilisable pour assurer la robustesse requise est proposée aux ingénieurs-concepteurs.

Face à ce manque, des actions de recherches sont menées depuis une bonne quinzaine d'années et l'Université de Liège y contribue activement par des développements relatifs à la méthode dite "des chemins alternatifs d'efforts". Cette méthode étudie l'impact sur la structure de la perte d'un élément structurel consécutif à un évènement exceptionnel. La méthode vise à s'assurer que la redistribution des efforts suite à la perte de l'élément n'engendre pas la perte d'autres éléments, ce qui provoquerait un phénomène de ruine en chaîne.

Les recherches conduites à l'Université de Liège s'intéressent plus particulièrement, mais non exclusivement, à la réponse de portiques en acier suite à la perte de l'une de leurs colonnes. Dans ce cadre, une méthode analytique permettant de modéliser le comportement de la structure a été élaborée puis rapidement implémentée dans un code *Matlab*.

Le présent travaille visera, dans un premier temps, à valider cette procédure *Matlab* via des comparaisons avec le logiciel *FINELG*, mais également à en étendre la portée en termes de géométries de structures (entre autres via son couplage avec le logiciel *BeamZ*). Dans un second temps, le mémoire se donnera pour objectif de permettre au code *Matlab*, via une procédure analytique, d'intégrer la plastification progressive de la partie dite "non directement affectée" de la structure suite à la perte de la colonne, ce que la version actuelle du logiciel ne couvre pas. Ici aussi, une validation du code *Matlab* via des comparaisons avec le logiciel *FINEG* sera réalisée.

Membres du jury

J.-F. Demonceau (promoteur) — J.-P. Jaspart (co-promoteur) — V. Denoel — S. Seret

Abstract

In order to fill the lack of practical guidelines in the European recommendations regarding the structures robustness, research are conducted in Liège University on this topic. This master thesis focuses on the "alternative load path method" which analyses a structure further to the loss of a structural element due to an exceptional event. More specifically, the topic of this master thesis is the analytical model developed in Liège University designed to characterize the response of a steel frame further to the loss of one of its columns. A particular plastic mechanism is assumed to form in the "directly affected part" above the lost element while the rest of the structure is assumed to behave elastically [11].

The last version of the model and its implementation, after years of incremental modifications, have not yet been properly stated and verified. Therefore, the first part consists to detail and verify extensively the analytical model and its implementation developed so far. A particular emphasis was brought to the field of applications and the assumptions made during each development step.

Afterwards, a first improvement of the initial model is implemented to enhance its accuracy and to widen its field of application. This improvement includes the combination of *Matlab* and *BeamZ*. After clearly stated the methodology and its implementation, new developments are validated through the comparison of different scenarios with *Finelg* simulations. Besides, during the validation of the new implementation, the plastic mechanism assumed in the initial model have been adjusted due to inconsistencies with results obtained in *Finelg*.

Finally, a second implemented improvement aims to introduce the yielding of the "indirectly affected part" of the structure, that was not taken into account in the initial analytical model. Once the methodology developed in [8] and its implementation are clearly detailed, the implementation is verified and validated through comparison with *Finelg* simulations.

Résumé

Afin de combler le manque de recommandations pratiques dans l'Eurocode concernant la robustesse des structures, des recherches sont actuellement conduites à l'université de Liège sur le sujet. Ce TFE se concentre sur la "méthode des chemins alternatifs d'efforts" qui analyse la réponse d'une structure suite à la perte d'un élément structural lors de la survenue d'un évènement exceptionnel. Plus spécifiquement, le sujet de ce TFE concerne la méthode analytique développée à l'université de Liège pour caractériser la réponse d'une structure en acier suite à la perte d'une colonne. Un mécanisme plastique particulier est supposé se former dans la "partie directement affectée" tandis que le reste de la structure est supposé rester élastique.

La dernière version du modèle et son implémentation, après plusieurs années de modifications incrémentales, n'a jamais été correctement établie ni vérifiée. Par conséquent, la première partie consiste à détailler et vérifier de manière approfondie le modèle analytique et son implémentation réalisée jusqu'ici. Une attention particulière est apportée à la définition du champ d'applications et des hypothèses posées durant le développement.

Par la suite, une première amélioration du modèle initial est implémentée pour améliorer sa précision et élargir son champs d'applications. Cette amélioration se base sur la combinaison de *Matlab* et de *Beamz*. Après avoir clairement établi la méthodologie et son implémentation, les nouveaux développements ont été validés au travers de la comparaison des différents scénarios réalisés sous *Finelg*. Par ailleurs, durant la validation de la nouvelle implémentation, le mécanisme plastique supposé par le modèle initial a été ajusté à cause d'incohérences obtenus avec les résultats sous *Finleg*.

Finalement, une deuxième amélioration est implémentée afin d'introduire la plastification de la "partie indirectement affectée" de la structure, qui n'était pas prise en compte jusque là dans le modèle analytique. La méthodologie dévelopée dans [8] ainsi que son implémentation sont d'abord détaillées avant que l'implémentation ne soit vérifiée puis validée avec les résultats obtenus sous *Finelg*.

Contents

CHAPTER 1

Introduction and general concepts

In the following, firstly the subject of this thesis is introduced through the detailing of several catastrophic events which led to robustness research and codes to avoid such catastrophes. Then, the European codes are briefly detailed followed by the explanation of the behavior of a 2D frame further to the loss of one structural column. Finally, the objectives of the thesis are specified followed by the organization of the thesis.

1.1 Introduction to robustness of structures

The interest on robustness of structures started with the observation of the partial or total collapse of buildings after their exposure to an exceptional event. The latter is an event with a very small occurrence probability but which leads to large consequences and damages. In the following, the collapse of three structures are detailed.

The partial collapse of the Ronan Point is shown in figure 1.1. It is a tower situated in London which collapsed in 1968. The disaster had been initiated by a gas explosion in the kitchen at one corner of the 18^{th} story which caused excessive pressure on the walls. At that time, no particular attention was given to the connections between elements and the walls were not tied up to the flooring. As a consequence, the walls and flooring surrounding the kitchen had nothing to tie up to in order to withstand the excessive pressure. Therefore the walls surrounding the kitchen were ejected, as shown in figure 1.1. Further to which, the walls and flooring just above this kitchen were not resting on anything anymore, they collapsed and crashed onto the 17^{th} floor and so on for the stories above the 18^{th} floor. At some point, the 18^{th} story did not withstand the additional loads and collapsed. After that, all the stories below collapsed one after the other. This phenomenon in which a local event induces the

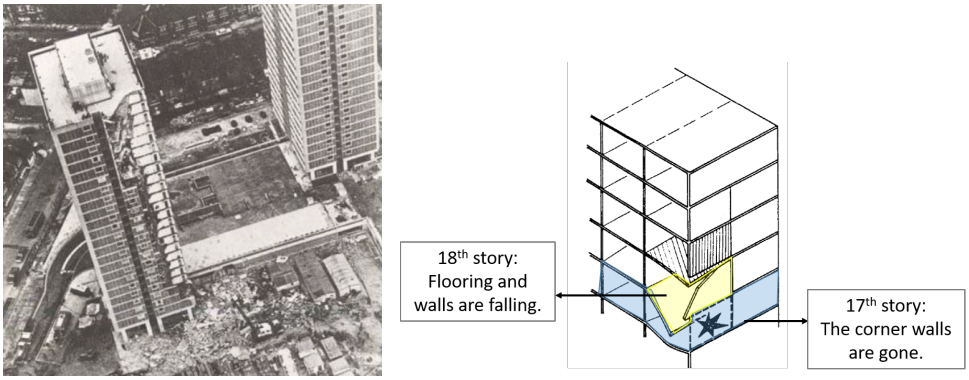

Figure 1.1 – Ronan Point's partial collapse [1].

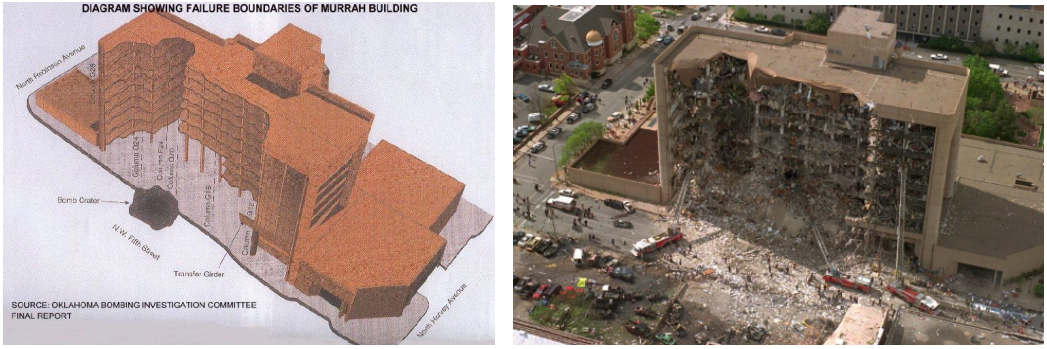

Figure 1.2 – Murrah building's partial collapse [1].

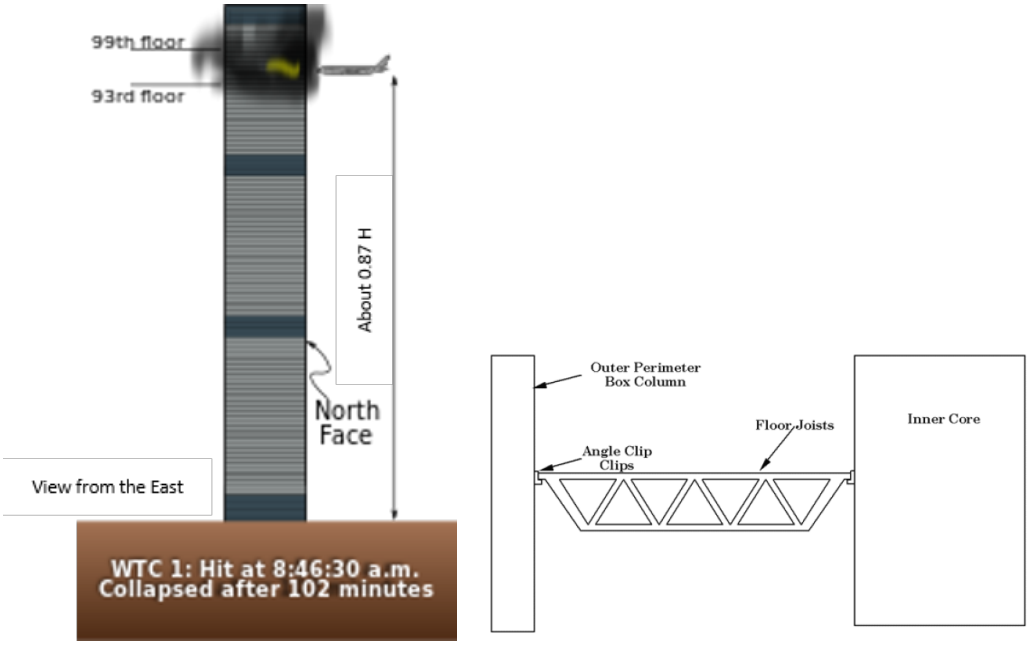

Figure 1.3 – World Trade Center towers' total collapse [1]. On the left, scheme of the tower. On the right, scheme of one story of the tower.

partial or total collapse of the structure is called progressive collapse and it has been observed for the first time during this incident.

Around 30 years after, the Murrah building, situated in Oklahoma city, partially collapsed in 1995 after the blast of a truck full of explosives situated at the front of the building (see figure 1.2). Again, the building could not withstand the additional pressures because its structural elements were not tied up to each other.

Another well known progressive collapse is the Wall Trade Center towers' attack in 2001 in New-York. These buildings were both made of a rigid concrete core surrounded by a mesh of beams resting on to the concrete core and on the structural facade (see figure 1.3). The beams were not tied up neither to the concrete core nor to the facade. This paragraph focuses on the tower named WTC1 which lasted the longest and collapsed after 102 minutes (see figure 1.3). The plane crashed into the building at about 90% of its height and damaged several stories. The building was designed to withstand an airplane crash: indeed, it did not fail due to the plane's collision. Furthermore, the WTC1 was designed as well to withstand a

standard fire appearing in a closed compartment of the building. However, the combination of both scenarios have not been verified and caused the progressive collapse of the structure. Indeed, the airplane impacted several stories and caused the spraying of jet fuel into those stories, the deterioration of the structural beams and their fire protection and the damaging of the electrical circuits. Following that, a fire ignited in the area where the plane hit the structure. As the beams were heated and as they were not tied up to the other elements, the structure could not withstand an additional tension force in the beams. These beams elongated towards the outer perimeter box column. This lead to second order phenomenon in the external columns in addition to the fire's presence and caused their collapse one after the other. As the beams were not tied up to the central core, they fell onto the floor below. In the mean time, the fire had expended to other stories: the floors onto which the beams fell were not strong enough and collapsed onto the floors below. This happened again until the total collapse of the structure.

In summary, these three buildings underwent an exceptional event leading to local damages and the loss of a structural element. This loss caused the loss of other structural elements and, at the end, provoked the partial or total progressive collapse of the structure. Furthermore, these catastrophes have been caused by the lack of ties between elements. But more generally, these catastrophes happened because the exceptional loads applied to these buildings had not been taken into account in the traditional verifications. Indeed, the probability of occurrence of an exceptional event is considered too small to justify its presence in the traditional checks.

However, these progressive failures led to detrimental material and human losses. In response to such catastrophes, the authorities opened research to create specific codes and standards which prescribe rules to avoid these progressive collapses in future buildings. In the next section, the recommendations added to the European codes are detailed.

1.2 Normative European context

As mentioned earlier, codes and standards made their apparition in order to avoid progressive collapse. In Europe, those are summurized in Eurocode 1 part 1-7: General actions - Accidental actions [2]. These recommendations mainly give definitions and good practice guidelines and are inspired by the British standards which made their apparition soon after the Ronan Point progressive failure. In the following, some important general concepts defined in the Eurocodes are explained, such as robustness and structural integrity, before the additional verification is detailed. It is followed by the listing of the means to reduce the risk of an exceptional event.

1.2.1 General concepts

The robustness of a structure is defined in [2] as "*The ability of a structure to withstand events like fire, explosions, impact or the consequences of human error, without being damaged to an extent disproportionate to the original cause*". In other words, the collapse of some of the structural elements of the structure are accepted as well as large displacements as long as the structure reaches a new equilibrium position for which the global structure remains globally stable. The structure is therefore said to have kept its structural integrity.

Furthermore, the robustness of a structure is also defined as its ability to keep its structural integrity when exposed to an exceptional event. For example, the Ronan Point tower partially collapsed almost immediately after the explosion and therefore had no structural integrity

faced to this blast. On the other hand, the WTC1 collapsed after 102 minutes. It had some structural integrity although it could be improved. For instance, we know that the elements should have been tied up to each other which would have increased the structural integrity of the structure.

1.2.2 Supplementary structural demand

As already mentioned in the introduction, these robustness recommendations add a supplementary structural demand to the traditional design of a structure. In the following, the traditional verifications are quickly remembered, followed by the reasons of the need of additional verifications.

Traditionally, a structure is designed through the ultimate limit state (ULS) and the serviceability limit state (SLS). In the ULS, the stability and the resistance of the structure are checked under design loads. Through the SLS, the structure's deflection is checked under service loads. The combinations of actions taken into account in those design and service situations are the permanent actions, the variable actions and the accidental actions with a relatively high probability of appearance.

However, the exceptional loads, i.e. accidental loads with a relatively low probability of occurrence, are not taken into account in those traditional verifications. Indeed, the probability of appearance of an exceptional event is considered too small to justify its presence in those traditional checks. Yet, an exceptional event may lead to detrimental consequences, as the exceptional events cited earlier highlighted it. Therefore, an additional check has been added to the traditional verifications: the verification of the structural integrity of the structure under accurate exceptional loads, defined with the client and the relevant authorities.

1.2.3 Means to reduce the risks of an exceptional event

The damages caused by an exceptional event may be decreased by reducing its risk of appearance. The risk of a hazard is defined in [2] as "*a measure of the combination (usually the product) of the probability or frequency of occurrence of a defined hazard and the magnitude of the consequences of the occurrence*". Two types of strategies are defined in the Eurocodes [2] to reduce the risk of an exceptional event, these are illustrated in figure 1.4.

On one hand, there exists methods "*based on identified accidental actions*". Among these are the protective measures which aim to prevent or reduce the accidental action such as a protection barrier against impacts, on figure 1.5. Another method is based on the design of the structure to sustain the action using the static equivalent load linked to the accidental action.

On the other hand, a second type of method is based on non-identified accidental action and consists in "*limiting the extent of localized failure*" using structural measures which increase the robustness of the structure. Two types of strategies are defined to improve the robustness of a structure: the direct methods and the indirect methods, both detailed in the following.

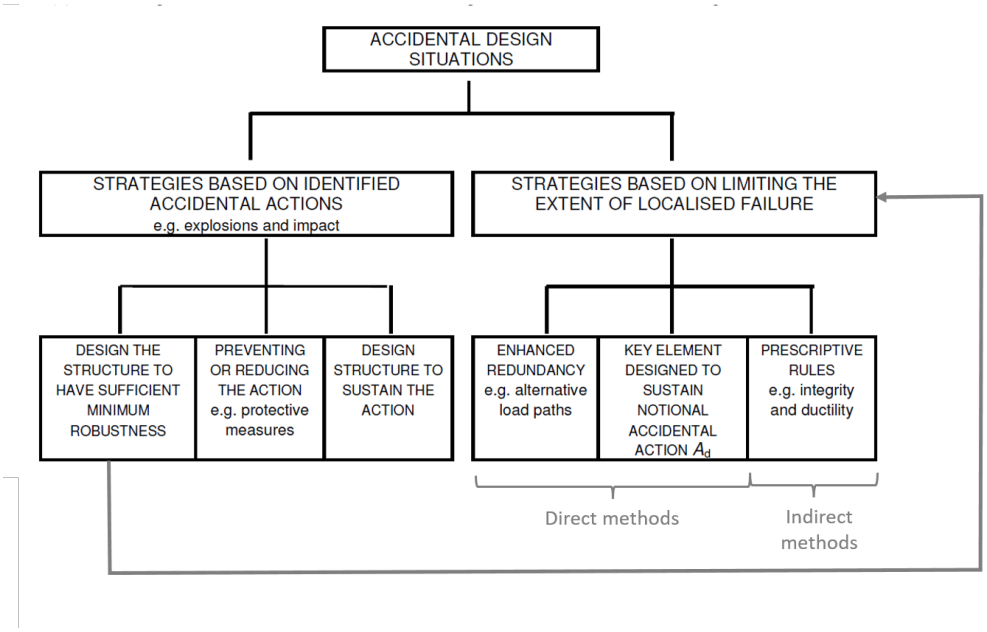

Figure 1.4 – Strategies to reduce the risk of an accidental event with a relatively low probability of appearance [2].

Figure 1.5 – Example of protection measure against impacts [1].

Indirect methods

The indirect methods give prescriptive rules, which means that there is no need to consider an explicit scenario to implement them, as explained in [1]. Furthermore, they may be implemented to the building after its conception as long as they are introduced in the project before the execution of the building.

The **tying method** is part of the indirect methods. This strategy encourages the continuity between horizontal and vertical elements and, in particular, the tying of vertical elements in two perpendicular directions. By this way, the structure acquires a certain redundancy and it allows a load redistribution between the stories.

Some examples to tie a column with the horizontal elements are given in figure 1.6. The first example on the left illustrates a solution for a slab poured on site after the columns are placed. In this case the continuity is brought by the additional reinforcement poured into the column and the slab. Figure 1.6(b) illustrates a solution applicable for a precast slab: the junction between the horizontal and vertical elements is made by a rod and mortar.

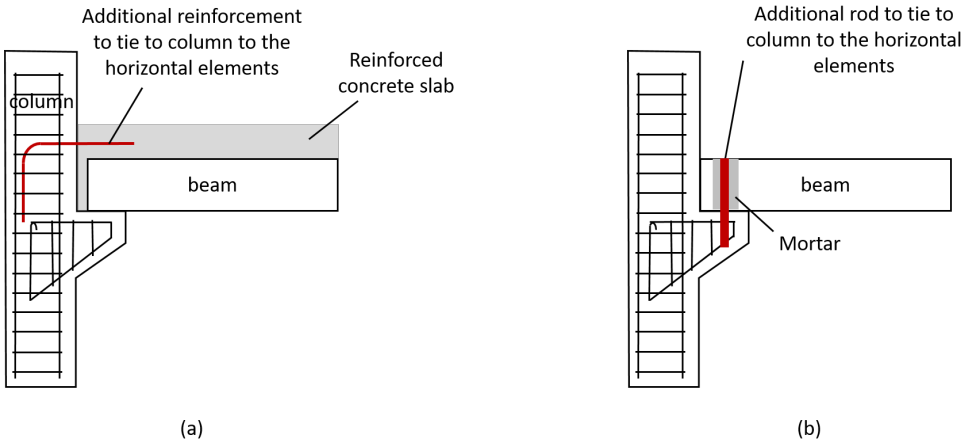

Figure 1.6 – Examples of continuity joints between a column and horizontal elements.

Note that the horizontal element needs to be able to withstand the supplementary loads. Figure 1.7 illustrates a column-beam continuity where reinforcement bars are added around the column to provide a ductile behavior to the reinforced concrete slab. In that aim, the removing of the column will cause large deflections without the local collapse of the slab. It activates membrane effects (more details in section 1.3) to withstand the additional loads.

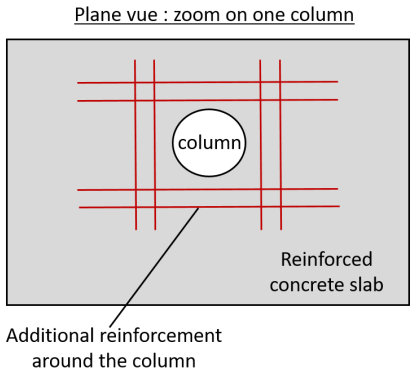

Figure 1.7 – Procurement of a ductile behavior to slab through additional reinforcements.

Direct methods

The direct methods are implemented at the beginning of the building conception and influence the whole building's structural conception.

The **key elements method** is a direct method which promotes the design of key elements to ensure the structural integrity of the structure. There are two types of key elements:

- On the one hand it may be an element that is designed to sustain the exceptional event, such as mega beams and mega columns as illustrated in figure 1.8 (type 1). In this case, the lost column does not affect the rest of the structure as the columns above the lost one are now suspended to the mega beam that is designed to withstand this supplementary load,

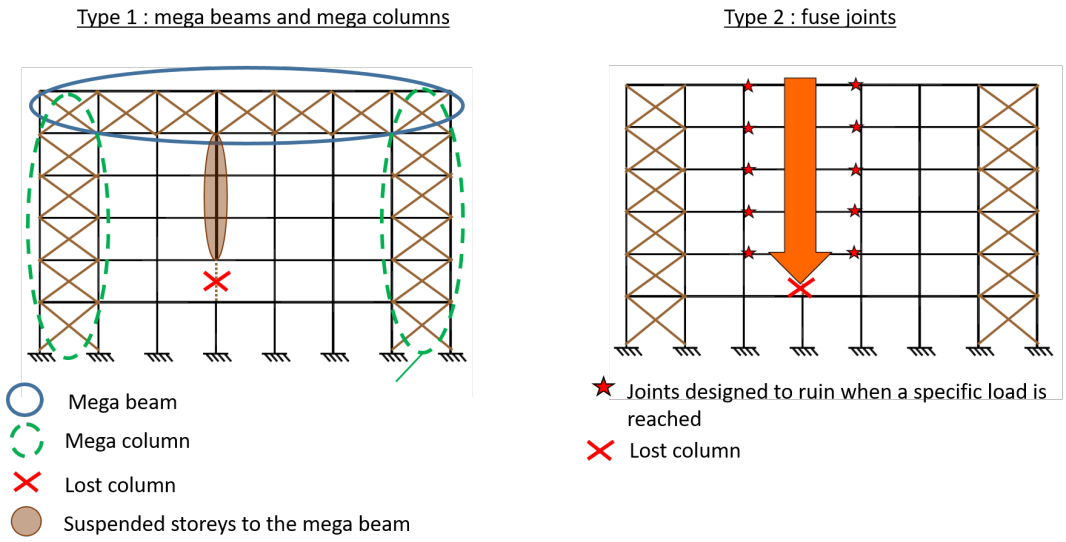

Figure 1.8 – Illustration of the two type of a key element [1].

- On the other hand, it may be an element designed to fail when it reaches a certain maximum allowed stress in order to avoid the spreading. Type 2 in figure 1.8 illustrates a structure losing one of its columns. In this case, a part of the structure is sacrificed in order to keep the structural integrity of the structure. To do so the joints are designed to fail for a specific load. Note that sacrificing a part of the structure is not conceivable for apartments as it would not be ethical. However, it is a good solution for storage racks.

The **alternative load path method**, a direct method as well, consists of the analysis of the structure in the domain of large displacements after the removal of one structural element. The structural integrity of a structure is ensured for the loss of one element if the structure is able to redistribute the load that was carried by the lost element and if the structure is ductile enough to find a new equilibrium state without its collapse. This operation should be repeated for all the structural elements that might be damaged by the relevant exceptional events. This method is time-consuming. However, it allows the engineer to analyze which elements need to be stronger and it allows the engineer to maximize the structural capacity of the building.

This master thesis focuses on the alternative load path method and more specifically on the loss of a structural column. In the next section, the response of a frame losing one column is detailed.

1.3 Behavior of a frame further to the loss of one column

In the following, the situation under investigation is first specified. Then, the response of the structure faced with this situation is detailed. Finally, the methodology followed to simulate the loss of a column is explained.

1.3.1 Studied situation

The studied response concerns a 2D steel frame exposed to an exceptional event leading to the loss of one structural internal column.

For a targeted column, the structure may be divided into two parts : the directly affected part (DAP) and the indirectly affected part (IAP). As illustrated in figure 1.9, the DAP is composed of all the columns just above the lost column, the adjacent beams to those columns and the beam-to-column-joints linking those beams and columns. The IAP it is composed of the rest of the structure. Explicitly, this corresponds to the stories under the lost column and the beams, columns and beam-to-column joints that are not just above the lost column. Both directly and indirectly affected parts influence each other.

In this case, the structure is assumed to collapse due to the formation of the complete plastic mechanism in the DAP shown in figure 1.10. This plastic mechanism is achieved when all the plastic hinges indicated in figure 1.10 are formed. This failure mode is assumed to occur before other failure modes. Namely, strength failure and local and global instabilities. Note that when the number of stories in the DAP increases, the higher levels of the DAP are more likely to not be affected by the loss of the column at first. Such a structure is part of the field of applications as long as the stress redistribution within the structure allows the formation of the complete plastic mechanism in the DAP.

Moreover, it is assumed that the IAP has not yielded by the time that the structure collapses. In that way, the restraint the IAP gives to the DAP does not decrease during the analysis of the phenomenon.

Moreover the exceptional event is assumed to not induce significant dynamic effects. Therefore, the following developments are based on a static approach and the column is assumed to be progressively removed from the frame[1].

Finally, before the column's removal, the structure is loaded by the accidental combination of the gravity loads, as prescribed in the Eurocodes. Also called normal loading in the following.

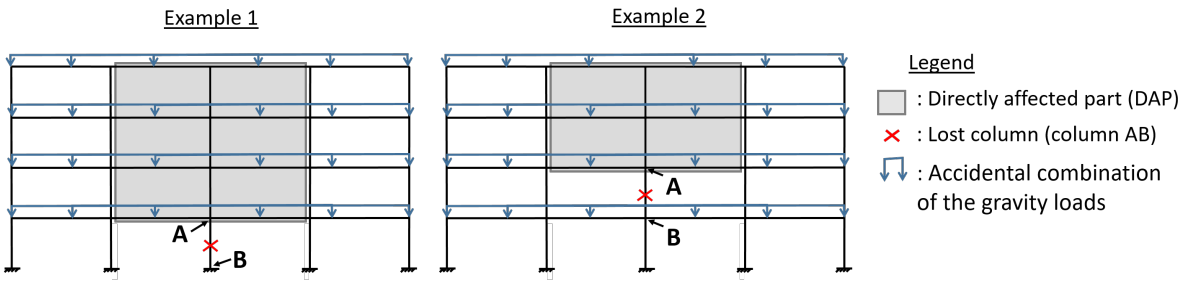

Figure 1.9 – Illustration of the DAP in two different situations.

[1] Note that the nature of the exceptional event may be any event that agrees with the assumptions mentioned above.

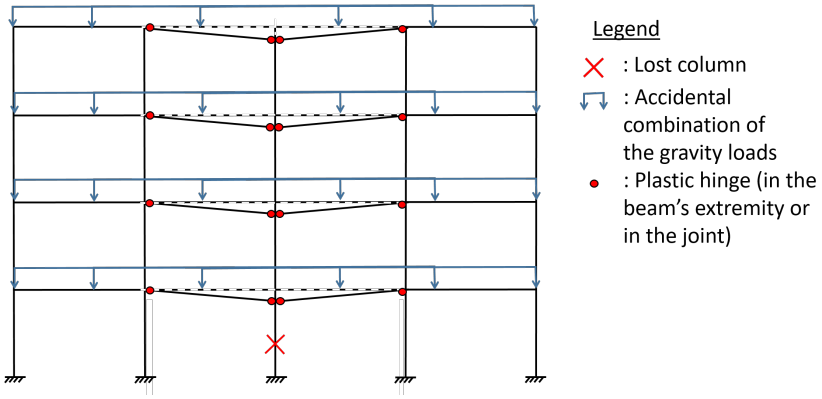

Figure 1.10 – Illustration of the plastic mechanism forming in the DAP of a frame losing one column.

1.3.2 Response of the frame

Under the presented situation, the behavior of the structure is studied through the evolution of the internal force at the top of the lost column (point A in figure 1.9), named N_{AB}. N_{AB} is positive when it is in traction and negative when it is in compression. The evolution of N_{AB} is studied as a function of the vertical displacement of point A, named u, positive downwards.

The general appearance of the $u - N_{AB}$ curve is given in figure 1.11 where three phases and five points are highlighted. The characteristics and the physics principles governing those phases are detailed hereafter.

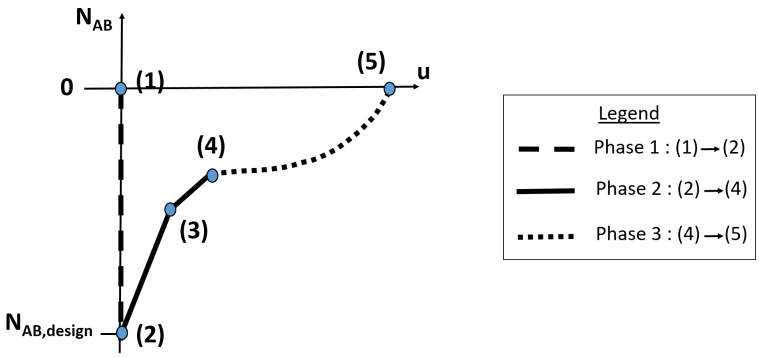

Figure 1.11 – Evolution of u, the vertical displacement at the top of the lost column (point A), in terms of the internal force at the top of the lost column, so-called N_{AB}.

Phase 1

Phase one extends from point (1) to point (2) and represents the normal loading of the frame. Point (1) represents the structure before being loaded, for which the internal force and vertical displacement of point A are null. The accidental combination of the gravity loads are then gradually applied, leading to the progressive compression of column AB. Hence, a progressive decrease of N_{AB} is observed in figure 1.11 during phase 1. Furthermore, the frame is assumed to remain fully elastic during phase 1 (i.e. no yielding appears in the column AB). Therefore, the vertical displacements at the top of the lost column associated to its compression are small and these may be neglected compared to the ones that appear during

the progressive loss of the column (phase 2 and 3). Therefore u is equal to zero during the whole phase 1 as it is seen in figure 1.11. At the end of phase 1, N_{AB} reaches $N_{AB,design}$, that is the internal force at the top of the lost column when the structure is subjected to the accidental design loads.

Phase 2

Phase 2 spans from point (2) to point (4). Point (2) indicates the beginning of the column's removal. This phase is characterized by the progressive formation of the DAP's plastic mechanism shown in figure 1.10.

Between points (2) and (3), the behavior of the DAP is linear. Point (3) highlights the formation of the first plastic hinge in the DAP. As a hinge is formed, the structure becomes less stiff which is characterized by a kink on the $u - N_{AB}$ curve and a decrease of its slope. After that, each subsequent change of slope in phase 2 characterizes the formation of a new plastic hinge in the DAP. Note that for reliability purposes, figure 1.11 shows only one change of slope within phase 2, which corresponds to a plastic mechanism induced by only one plastic hinge. This is a simplification to represent the $u-N_{AB}$ curve in a simpler way. For the example shown in figure 1.10, 16 plastic hinges are needed in order to form the plastic mechanism. Therefore the number of kinks within phase 2 would be 16 as well.

Finally, point (4) characterizes the formation of the last plastic hinge to be developed. Therefore it points out the moment when the plastic mechanism in the DAP is fully formed. As a consequence, from point (4), the DAP has no more first order rigidity.

Phase 3

Phase 3 extents from point (4) to point (5). This phase is characterized by the development of the catenary actions and membrane forces.

As already mentioned, phase 3 starts when the plastic mechanism in the DAP is totally developed. As the DAP loses all its first order rigidity at point 4, the slope of the $u-N_{AB}$ curve is null and large displacements appear. As shown in figure 1.12, when large displacements appear, the beam at the top of the lost column elongates and is not horizontal anymore. A part of the vertical force coming from the lost column may now be carried by the vertical component of the normal force in the beams. This effect is called membrane effect or catenary actions and provides a second order stiffness to the DAP. Those membrane forces may develop because the IAP acts as a lateral anchorage, or a spring, for the beams of the DAP. The stiffer the IAP, the bigger the membrane forces will be in the DAP. Remark that the catenary actions may only develop if the column is an internal column of the frame since the IAP needs to provide a lateral anchorage at both sides of the DAP in order for the catenary actions to develop and in order for the complete plastic mechanism to form in the DAP. As the second order stiffness of the DAP develops, the slope of the $u - N_{AB}$ curve increases and a bigger force may be applied to the DAP.

During this phase, the beams of the DAP lie on the IAP in order to generate the membrane forces, which induces the non braced IAP to horizontally shift towards the DAP, as shown in figure 1.13. This induces compression forces in the beams of the DAP that get bigger as the beam is higher in the DAP. Therefore, the beams, that were in tension without taking this

effect into account, are less in tension as they are upper and the ones at the very top of the DAP may be in compression. This phenomenon gains in importance when there are a larger amount of stories in the DAP and is the reason why the membrane forces develop the most in the bottom stories of the DAP (see figure 1.12).

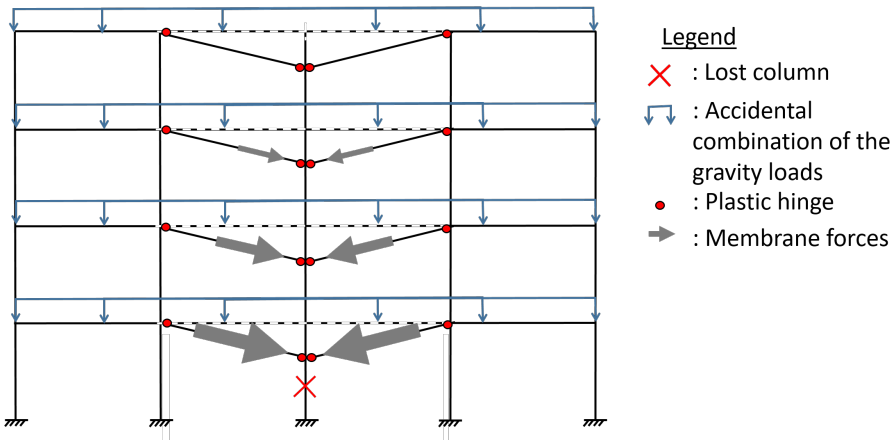

Figure 1.12 – Phase 3: development of the membrane forces.

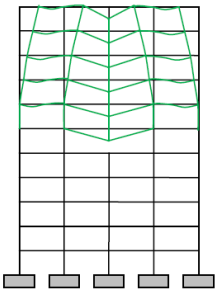

Figure 1.13 – IAP leaning on the DAP [11].

Finally, when the internal force in column AB is null, the column has fully disappeared. If the structure possesses sufficient ductility to reach this point without damaging any other elements than the lost column and without forming a plastic mechanism in the IAP, the structure has enough robustness or has sufficient structural integrity to face this exceptional event.

Note that for some structures it could be possible that the total removal of the column is reached before reaching phase 3.

1.4 Methodology followed to simulate the loss of the column

Hereafter, an equivalent methodology to simulate the loss of the column is detailed. This equivalent methodology models the structure without the future lost column for all three phases. In this modeling, the future lost column is represented by the internal forces that defines it.

The loading process of this methodology is separated into two steps: the normal loading of the structure, corresponding to the phase 1 of the $u-N_{AB}$ curve, and the progressive removal of the column, corresponding to phases 2 and 3 of the $u-N_{AB}$ curve. These steps are detailed in the following.

Step 1: Normal loading of the structure

The first step consist of the progressive application of the accidental combination of the gravity loads during phase 1.

At the end of phase 1, $N_{AB} = N_{AB,design}$ and the situation with the total structure is represented in figure 1.14. This situation is equivalent to the modeling of the frame in which the future lost column is represented by its reactions forces ($M_{AB,design}$, $N_{AB,design}$ and $T_{AB,design}$) acting on the frame (see figure 1.14). Note that as, in this example, it is the central column that is removed, $M_{AB,design}$ and $T_{AB,design}$ are both null. Remark as well that as the column is in compression, its reaction axial force on the rest of the structure acts upwards.

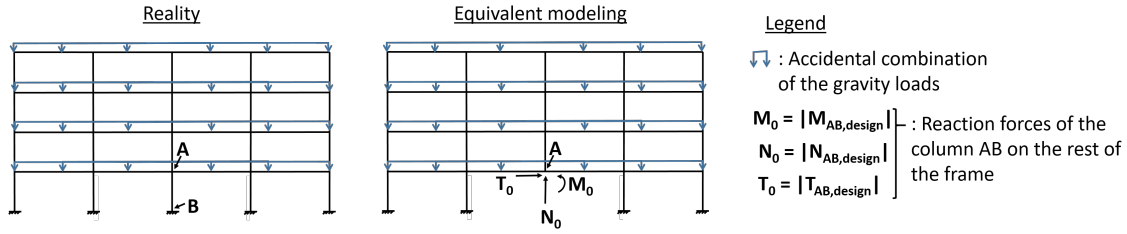

Figure 1.14 – Modeling of the structure at the end of phase 1.

Therefore, the loads progressively applied during phase 1 to the structure without the future lost column are the accidental combination of gravity loads and the reaction forces of the removed column AB in order to simulate its presence.

Step 2: Loading of the column's removal

The second step consists in the modeling of the column's removal during phases 2 and 3.

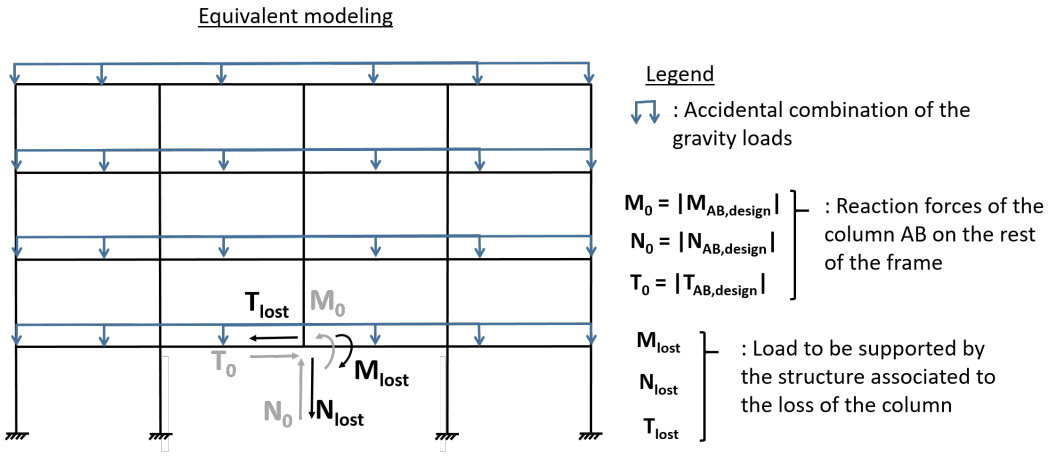

Figure 1.15 – Modeling of the structure during phases 2 and 3.

As already explained, the removal of the column induces the diminution of the internal forces in the column AB, and therefore, the diminution of its reaction forces acting on the rest of the frame. The column is totally removed once the internal forces at the top of this column are null. Therefore, the removal of the central column may be modeled by a force acting downwards which represents the load to be supported by the structure associated to the loss of the column, N_{lost} defined in (1.2), in addition to the forces acting on the structure at the end of phase 1 (see figure 1.15)[2]. The internal force in the central column progressively removed N_{AB} is therefore given by:

$$N_{lost} = \lambda_d \left| N_{AB,design} \right|, \text{ with } 0 \leq \lambda_d \leq 1 \tag{1.1}$$

$$N_{AB} = N_{AB,design} + N_{lost} \tag{1.2}$$

Using the equivalent modeling, at point (2) in figure 1.11, the force simulating the loss of the column, N_{lost}, is null and therefore, using equation (1.2), $N_{AB} = N_{AB,design}$. When the column is totally removed, point (5) in figure 1.11, $N_{lost} = N_{AB,design}$ and therefore $N_{AB} = 0$ as N_{lost} counteracts the force N_{AB}.

Finally, The loading scenario shown in figure 1.15 may be dissociated into the superposition of two loading scenarios: the normal loading of the structure and the loading of the column removal, as shown in figure 1.16. This separation allows the drawing of the $u - N_{lost}$ curve shown in figure 1.17. This curve is the $u - N_{AB}$ curve without the phase 1 represented which is shifted upwards.

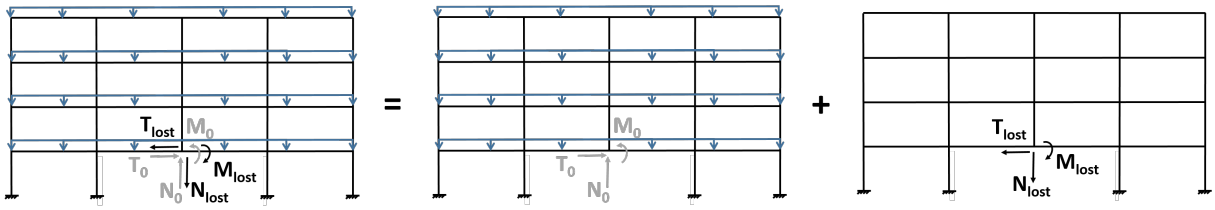

Figure 1.16 – Application of the superposition method to the equivalent modeling of the structure.

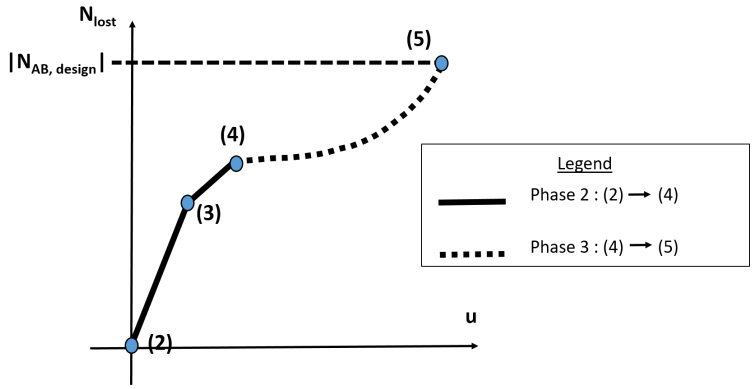

Figure 1.17 – Axial force at the top of the lost column that has to be carried by the rest of the structure, N_{lost}, in function of the vertical displacement at the top of the lost column, u.

[2] Note that if the column removed is not a central column, M_{lost} and T_{lost} need to be taken into account in addition to N_{lost}.

1.5 Objectives and organization of the thesis

Nowadays the inspection and assurance offices demand structural integrity verification. Furthermore, the authorities want the disasters that happened due to a lack of robustness to be avoided. In Europe, the European codes part 1-7 [2] present all the directives to ensure structural integrity, and therefore robustness, to a structure. However, as explained earlier, these recommendations present a lack of practical methods to ensure robustness of structures. Hence, in the aim to provide practical guideline to the design offices, Liège university has been developing robustness research. One topic under investigation in these research is the alternative load path method. In particular, for 15 years, Liège University has been elaborating an analytical model to represent the response of steel frames after the loss of one column. The method aims to reproduce the 3 phases previously explained and illustrated in figures 1.11 and 1.17. Phase 1 is easily reproduced and there is no need to develop a model for that phase. Then, Hai has been developing a method to determine the second phase in his PhD thesis [4]. Finally, Demonceau and Hai in their PhD thesis, respectively [3] and [4], have been expending an analytical method to reproduce phase 3.

This master thesis focuses on the analytical method developed to determine phase 3. The method is a simplified method based on the understanding of the physical phenomenon governing the different phases. After Demonceau and Hai worked on this analytical method, it has been improved and implemented in *Matlab* by different PhD students and researchers, namely, Huvelle [11] and [12], Cameliau [13] and [14] among others. However, as they all helped to add or improve a small part of the model, they all explained well what they added to the model but none took the time to settle the model itself. Furthermore, parts of the implementation have neither been explained through an article nor is commented on in the code. Therefore, for someone who does not know the code, it may be very work intensive to put his mind into it and understand all the things the model involves.

Therefore, the first objective of this master thesis is to detail the existing model and its implementation in chapter 2. A particular attention will be brought to differentiate the analytical model and its implementation, in terms of hypothesis and methodology. Through this focus on the existing model, the model will be reviewed, fully understood and explained.

Then, the structures under study to comment, verify and validate the analytical model are explained in chapter 2. Furthermore, the reference response to which the analytical model will be compared is explained.

Afterwards, chapter 4 will be devoted to the second task consists of the validation and improvement of this model. The first improvement aims to enlarge the choice of the elements of the structure as well as the choice of the supports, and improve the accuracy of the model. This enrichement will be reached by coupling the existing implementation of the model with *BeamZ*. During this task, the initial model is as well validated through a comparison between the results obtained with the initial model, the new model, and the modeling of the situation in *Finelg*, a finite element software [5].

Finally, the last objective of the thesis, presented in chapter 4, is to introduce the yielding of the IAP in the model implementation. As detailed later in chapter 2, the model is based on the assumption that the IAP does not yield during phase 3. This unlikely hypothesis will be lifted as the analytical method developed by Dewez [8] shall be implemented into the model.

this inclusion is enabled by the enhancement aimed in the second task that will be realized in chapter 4.

CHAPTER 2

Analytical model developed in Liege University

Liège University is developing an analytical model which reproduces the response of the frame during phase 3. As already mentioned, the first goal of this master thesis is the deep understanding of the analytical model and its implementation in *Matlab* in order to gather and synthesize all previous incremental developments. Indeed, this method has been developed and enhanced through different master's and PhD theses, among which Demonceau's PhD thesis [3], Hai's PhD thesis [4], Huvelle's master thesis [9] and her research in Liège [11] and [12].

For this purpose, the analytical model developed in Liège University is firstly summarized and detailed in this chapter. Its implementation in *Matlab* is then explained. Then, difficulties encountered during this task are depicted. Finally, inferences on the restrictions of the analytical model and its *Matlab* implementation are drawn before concluding with the possible enhancements of the model.

2.1 Analytical model

In this section, the hypothesis at the base of the model and its field of application are firstly detailed. Afterwards, the substructure, representing the DAP and the surrounding elements, involved in the analyze to compute the response of the total structure is detailed. Finally, the methodology followed to determine the response of the substructure is explained.

2.1.1 Field of application

The analytical model applies to 3D steel frames for which the structural elements are beams and columns only. This implies that the structural effect of any slab is neglected.

Furthermore, the model determines the response of the structure during phase 3 after to its exposure to an exceptional event leading to the loss of one of its internal columns (see figure 2.1). Furthermore, the dynamic effects associated to the loss of the column are neglected. The model is therefore based on a static approach in which the lost column is assumed to be progressively removed. This is an important assumption which allows the research to focus on the loads redistribution inside the structure. Note that complementary research have been conducted to determine the impact of the dynamic effects on the model and to implement these dynamic effects to the model explained in this chapter. For more information, see [13] and [14].

In addition, Demonceau demonstrated in his PhD thesis [3] that the gravity loads applied to the structure does not affect the third phase of the frame. Hence, the phase 3 of the $u - N_{AB}$ curve (see figure 1.11) is studied through the $u - N_{lost}$ curve (see figure 1.17).

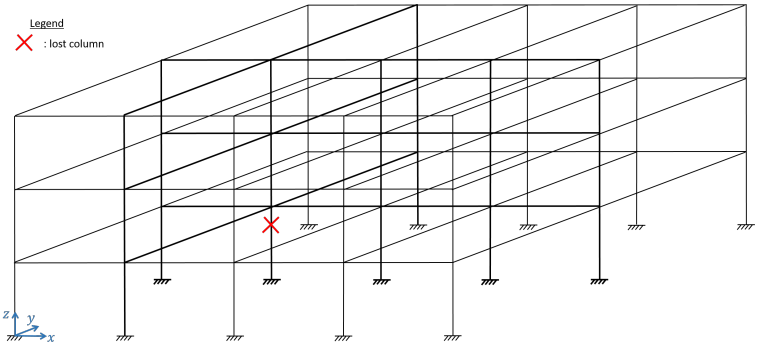

Figure 2.1 – Example of a 3D structure within the field of application of the analytical model.

Besides, the 3D couplings effects of a steel frame losing one of its column have been studied in Sergii Kulik's master thesis [10]. He concluded that the $u - N_{AB}$ curve of a 3D steel frame may be determined by the superposition of the $u_x - N_{AB,x}$ curve of the 2D frame in the (x,z) plane and the $u_y - N_{AB_y}$ curve of the 2D frame in the (y,z) plane, as illustrated in figure 2.2. Indeed, the vertical displacement compatibility between the (x,z) and the (y,z) planes constrains u_x to be equal to u_y and to u. And the $u - N_{AB}$ curve may be determined by summing $N_{AB,x}$ and $N_{AB,y}$ for each u. The same reasoning may be applied to the $u - N_{lost}$ curve. Therefore, the initial 3D frame analysis is replaced by the analysis of two 2D frames and the analytical model is based on a 2D analysis.

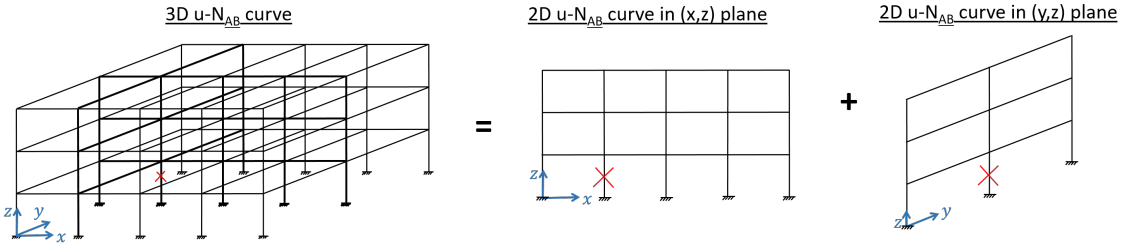

Figure 2.2 – Superposition of the $u_x - N_{AB,x}$ curve and the $u_y - N_{AB_y}$ curve to obtain the $u - N_{AB}$ curve of the 3D structure.

The model is based on the hypothesis that the phase 3 starts when the complete plastic mechanism in the DAP, showed in figure 1.10 in section 1.3, is formed. Furthermore, the analytical model on the hypothesis that all the plastic hinges will form at the same time. Besides, this hypothesis entails that the load redistribution does not induce either local instability or resistance failure of the elements of structure. Secondly, it implies a plastic mechanism will not form in the IAP before the formation of the complete plastic mechanism in the DAP. Moreover, if the column removal does not firstly affect all the stories of the DAP, the load redistribution of the structure must allow the formation of the complete plastic mechanism of the DAP. Finally the lost column must be an internal column of the frame in order for the frame to collapse further to the development of a complete plastic mechanism in the DAP, as illustrated in figure 1.10.

Furthermore the analysis of the model is assumed and only the elastic axial elongation of the beams is taken into account.

Then, the material's law of the frame's elements need to be specified. On one hand, the elements composing the IAP are assumed to follow a fully elastic material law, shown on the

left of figure 2.3. On the other hand, the elements composing the DAP follow an elastic-perfectly plastic material law, shown in figure 2.3, and are assumed to be infinitely ductile. Furthermore, as the flexural elongation of the beam is neglected, only the axial elongation of the latter elements is taken into account in the model. This hypothesis makes sense as the model aims to represent phase 3, governed by the development of the membrane forces.

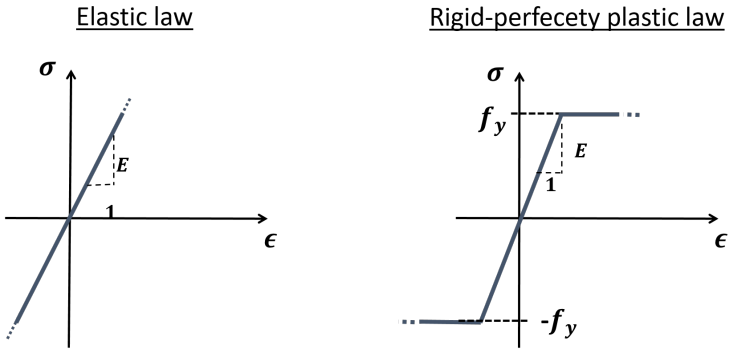

Figure 2.3 – Illustration of the elastic and the rigid-perfectly plastic material laws.

Moreover, the analytical model analyzes a substructure representing the DAP and the elements around it (see figure 2.4). This substructure and the supplementary hypothesis linked to the later are defined in the following section.

Finally, the analytical model is based on the second order elastic- perfectly plastic analysis of the defined substructure. Indeed, as already mentioned, large displacements occur during phase 3. Therefore, a second order analysis is required. Besides, the analysis is elastic-perfectly plastic as the elements of DAP (and therefore all the elements composing the substructure) are assumed to follow an elastic-perfectly plastic material's law.

2.1.2 Definition of a substructure and additional hypothesis

Figure 2.4 illustrates the substructure characterizing the 2D structure in the (x,z) plane shown in figure 2.2. In the following, all the characteristics of the substructure are detailed.

This substructure is composed of all the stories of the DAP in order to take into account the couplings effects between them. For instance, figure 2.5 shows two opposite situations for which the compression forces in the columns above the lost column either increase or decrease and lead to opposite coupling effects. The origin of the coupling effects is the same for both structures: in order to activate the membrane forces in the beams of the DAP, these beams lie on the IAP. From there, in the case of a non braced structure, the IAP is free to move horizontally and sags on the DAP. This horizontal displacement induces the upper stories to fall on the lower stories (see figure 2.5) and induces compression stresses in the columns above the lost column which causes the compression force to increase in the upper columns. On the other hand, if the structure is braced, the IAP will not horizontally shift on the DAP. The IAP will instead provide a very good anchorage for the beams of the DAP such that the upper stories of the DAP will provide a support for the lower stories of the DAP. In this case, the compression force decreases in the columns above the lost column and tension forces might even develop in the upper columns.

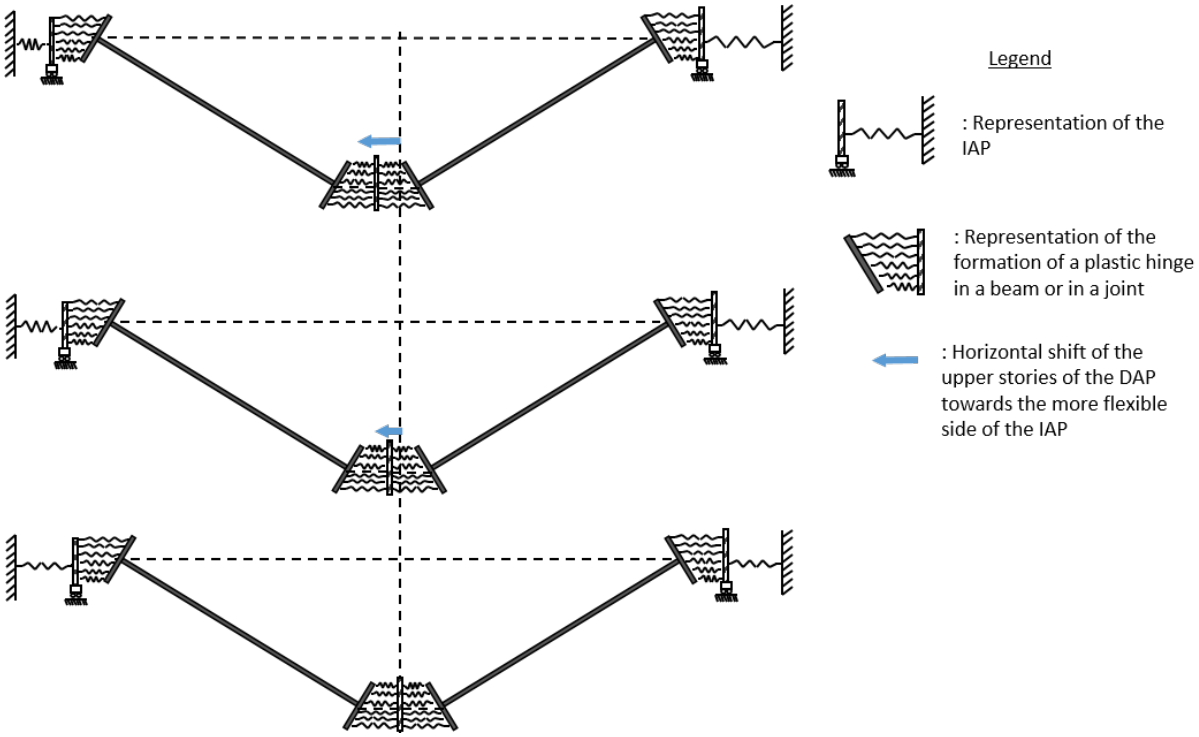

Figure 2.4 – Substructure of the 2D structure in the (x,z) plane given in figure 2.2.

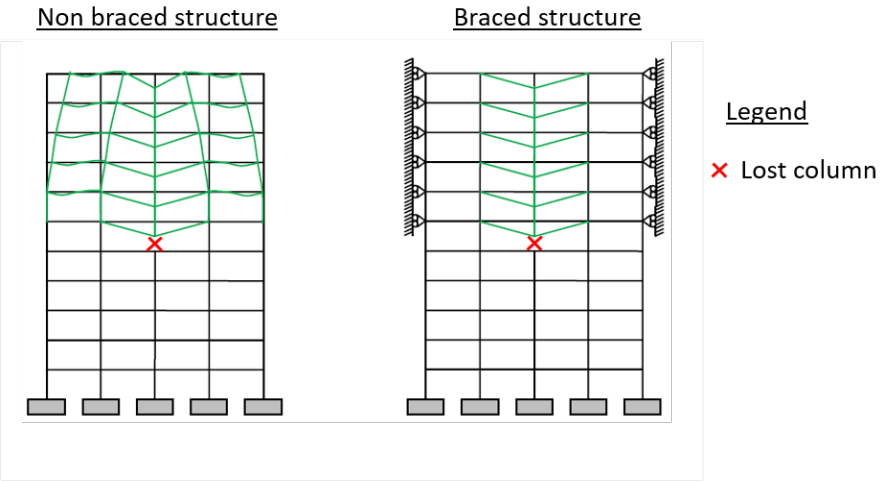

Figure 2.5 – Variation of the compression force in the upper columns [11].

Furthermore, the coupling effects between the IAP and the DAP are represented by horizontal single springs placed at each side of each story of the DAP, as shown in figure 2.4. Furthermore, there exists coupling effects between the stories of the IAP. These coupling effects are due to the dependence of the displacements at one point of the structure on all the forces applied to the structure. This induces the horizontal force applied by the DAP at a story of the IAP to influence not only the displacements of that specific story of the IAP, but also the displacements of the other stories. In order to take into account these coupling effects, the single horizontal spring at the left (right) end of the i^{th} story is in fact a series of N springs characterized by a flexibility S_{gji} (S_{dji}), N being the number of stories in the DAP and $i, j = 1, 2, ..., N$. S_{gji} (S_{dji}) characterizes the displacements at the left (right) of the story i of the DAP relative to the horizontal force acting on the IAP at the left (right)

of the story j of the DAP. This is equivalent to having a flexibility matrix characterizing the displacements of the left side of the DAP, S_g, and an other flexibility matrix characterizing the displacements of the right side of the DAP, S_d. These two are N by N size. Besides, they do not take the interaction between the movements occurring at one side of the substructure and the forces acting at the other side of the substructure. Indeed, if the lost column is not the bottom column, this coupling effect between the left and right end of the substructure exists and is neglected in the model. Note that as the IAP is assumed to stay in the elastic range during phase 3, these matrices are constant during the whole phase 3. These stiffness matrices may be determined through a first order analysis of the IAP which depends on the implementation of the analytical method. Therefore, the details of their determination are given later in the explanation of the implementation of the analytical model in *Matlab*.

Besides, the substructure does not take into account the distributed load acting on the beams (see figure 2.4) because Demonceau demonstrated in his PhD [3] that the influence of the normal loading on the structure does not affect the third phase of the frame, as already mentioned.

Moreover, each set of parallel springs placed at both extremities of each beam represents one plastic hinge of the complete plastic mechanism formed during phase 2 (and therefore already formed during the phase 3 which is being analyzed). The analytical model allows these plastic hinges to form either in the beams' extremities in the case of full-strength joints or in the joints if the latter are partial-strength joints.

If the plastic hinges form in the joints, each spring composing the parralel set of springs represents either a joint row or a part of the slab that is part of the joint. The springs are assumed to follow a non-symmetrical elastic-perfectly plastic law (the components are assumed to have an infinite ductily). As explained in [12], each component law is not symmetric in tension and compression because the bolts are assumed to have no compression strength and therefore they are only activated in tension. Whereas the concrete (slab) is assumed to activate only in compression. Furthermore, as the yielded zone is localized in the joints and as the joint length may be neglected with respect to the beam's length, the hinge length is assumed to be equal to zero. Lastly, the characteristics (stiffness and strength) of the springs representing a bolt row are determined through the application of the component method, whereas the characteristics of the springs representing a part of the slab are determined through Demonceau's method [3].

If the plastic hinges form in the beams, each spring composing the set of parallel springs characterizes a part of the plastic hinge's section. These springs are assumed to follow a symmetrical elastic perfectly plastic law. Furthermore, the yielded zone is assumed be finite and constant during phase 3 (therefore the plastic hinge's length is assumed to be constant). Finally, this spring model developed to characterize such plastic hinges is based on the Bernoulli assumption (the section at the extremities of the springs remain straight) and is detailed in the following section.

As shown in figure 2.4, the columns are not modeled in the substructure. Indeed, the model is based on the hypothesis that the plastic hinges do not form in the columns. Hence, the columns of the DAP are assumed to not yield. Furthermore, their elastic elongation is neglected to simplify the modeling of the substructure. Using that hypothesis, they are assumed to not influence the model which explains why they are not modeled in the substructure.

Finally, if the lost column is not a central column of the frame, the IAP is not symmetrical. Therefore, the flexibility matrices S_g and S_d defined earlier are not equal and a horizontal shift will appear towards the most flexible side of the IAP (as seen in figure 2.4). However, to simplify the model, these horizontal shifts are neglected. In practice, the displacements at the left and right side of the story i ($i = 1, 2, ..., N$) of the symmetrical substructure, named $\delta_{H,i}$, are given in equation (2.1). In this equation, $\delta_{Hg,i}$ is the displacement at the story i at the left side of the non symmetrical substructure. $\delta_{Hd,i}$ is the counterpart on the right side. The substructure is illustrated at the left of figure 2.6. Furthermore, with the assumption that the two beams of each story of the substructure are identical, the substructure may be assumed to have a symmetrical response and only half of the structure is studied in the analytical model as illustrated at the right of figure 2.6.

$$\delta_{Hi} = 0.5\,\delta_{Hgi} + 0.5\,\delta_{Hdi} \tag{2.1}$$

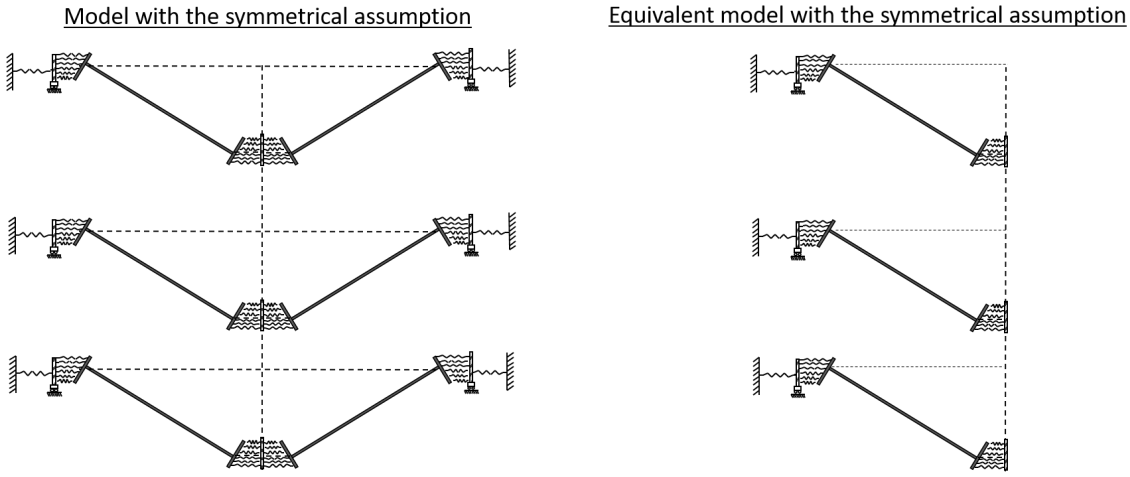

Figure 2.6 – At the left, studied substructure with the symmetrical displacements hypothesis. At the right, studied substructure with the assumptions that the displacements are symmetrical and the beams of each story of the substructure are identical.

2.1.3 Prediction of the substructure's response: full-strength joints

In this section, the analytical method is particularized to the assumption of full-strength joints and for which the beams' section of the DAP are assumed to be IPE or HE. First, the spring model characterizing the plastic hinges is detailed. The substructure is then analyzed. In particular, a zoom on one story is given and all the known, unknown and equations governing the analysis of the substructure are detailed.

Characterization of the plastic hinges

The spring model of a plastic hinge forming at the extremity of a beam have been defined in [12]. This model is illustrated in figure 2.7. It is characterized by the length of the plastic hinge, L_{rot}, the springs axial strength and the springs stiffness. These are defined hereafter.

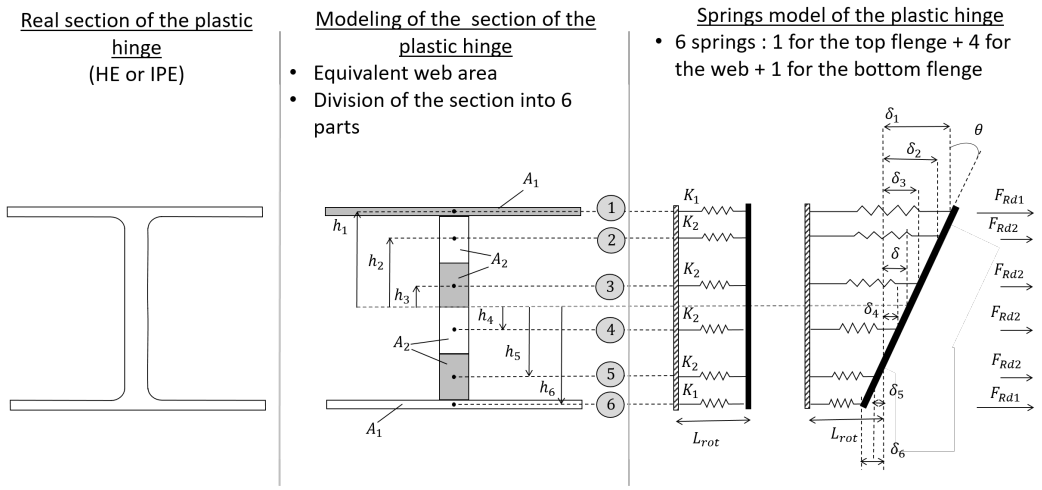

Figure 2.7 – Spring model characterizing a plastic hinge formed in a beam's extremity.

First, the length of the plastified zone in the beam due to the apparition of a plastic hinge, L_{rot}, is assumed to be constant during phase 3 and its value is given by:

$$L_{rot} = \frac{L}{2}\left(1 - \frac{M_{el}}{M_{pl}}\right) \tag{2.2}$$

Where L is the length of the beam in which the plastic hinge is forming and M_{el} and M_{pl} are respectively its elastic and plastic momentum. For more details, see [12] and [15].

Figure 2.7 shows the spring model, which is formed by 6 parallel springs. Four of them represent the web and are all characterized by an axial strength F_{Rd2} and a stiffness K_2. The two last springs represent the top and bottom flanges and are characterized by an axial strength F_{Rd1} and a stiffness K_1.

The values of F_{Rd1} and F_{Rd2} are determined by solving (2.3) for F_{Rd1} and F_{Rd2} which is given in (2.4). Where $N_{pl,Rd}$ is the axial strength of the beam's section, $M_{pl,Rd}$ is the plastic momentum of the beam's section and h_1, h_2 and h_3 are respectively the level arms of portion 1, 2 and 3, illustrated in figure 2.7.

$$\begin{cases} N_{pl,Rd} = 4\,F_{Rd2} + 2\,F_{Rd1} \\ M_{pl,Rd} = 2\,F_{Rd1}\,h_1 + 2\,F_{Rd2}\,(h_2 + h_3) \end{cases} \tag{2.3}$$

$$\begin{cases} F_{Rd1} = \dfrac{2\,M_{pl,Rd} - 0.25\,(h_2 + h_3)\,N_{pl,Rd}}{h_1 - 0.5\,(h_2 + h_3)} \\ F_{Rd2} = 0.25\,(N_{pl,Rd} - 2\,F_{Rd1}) \end{cases} \tag{2.4}$$

The values of K_1 and K_2 are defined in by:

$$\begin{cases} K_1 = \dfrac{E\,A_1}{L_{rot}} \\ K_2 = \dfrac{E\,A_2}{L_{rot}} \end{cases} \tag{2.5}$$

Where E is the Young modulus of the steel and A_1 and A_2 are respectively the area of portions 1 and 2, illustrated in figure 2.7. The elastic-perfectly plastic force-displacement laws followed by these springs are illustrated in figure 2.8.

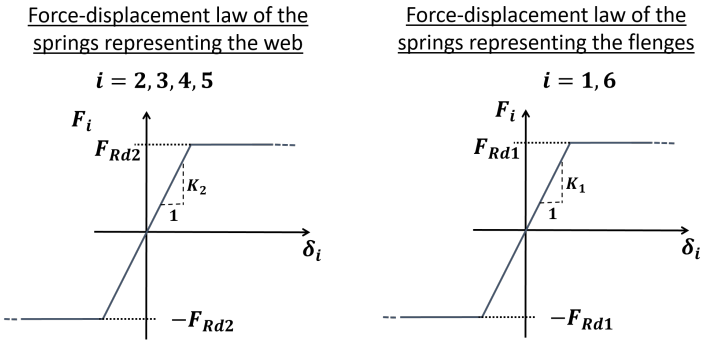

Figure 2.8 – Elastic-perfectly plastic force-displacement law characterizing the six parallel springs of a plastic hinge forming at the beam's extremity.

Analysis of the substructure

To determine the phase 3 of the $u - N_{lost}$ curve, an increasing vertical displacement, u, is applied downwards at the bottom story at the right of the beam (at the middle of the two beams), which simulates the displacement of the bottom story further to the column's loss. Since the columns are staying in the elastic range and are assumed to follow a rigid-perfectly plastic material law, the vertical displacement applied at the other stories is the same as the one applied at the bottom story of the DAP. Therefore, the increasing displacement, u, is applied to all the N stories of the substructure. And at each step u is analyzed through a second order rigid plastic analysis of the substructure for which N_{lost} is one of the unknowns.

Each of the stories of the substructure is modeled the same way and figure 2.9 illustrates the modeling of the story i. Furthermore, figure 2.10 shows the equilibrium of the forces and the internal forces in the beam's extremities of the i^{th} floor of the substructure. The known variables and the unknowns of the model are respectively listed in tables 2.1 and 2.2.

To determine these unknowns, the following equations are solved: the kinematic equations (equations (2.6) and (2.7)), the equation characterizing the elastic axial elongation of the beam (equation (2.8)), the equations characterizing the plastic hinges (equations (2.9), (2.10) and (2.11)), the force compatibility equations between the beam and one of its plastic hinges (equations (2.12) and (2.13)), the equilibrium momentum equation of the beam (equation (2.14)), the displacement compatibility equations between the DAP and the IAP (equations (2.15), (2.16) and (2.17)) and the force compatibility equation between the stories of the substructure (equation (2.18)).

$$\sin(\theta_i) = \frac{u}{L_0 - 2\,L_{rot,i} + \Delta L, i} \tag{2.6}$$

$$\cos(\theta_i) = \frac{L_0 - 2\,L_{rot,i} - \delta_{H,i} - 2\,\delta_i}{L_0 - 2\,L_{rot,i} + \Delta L, i} \tag{2.7}$$

$$\Delta_{L,i} = F_{H,i}\,\frac{L_0 - 2\,L_{rot,i}}{E\,A_i} \tag{2.8}$$

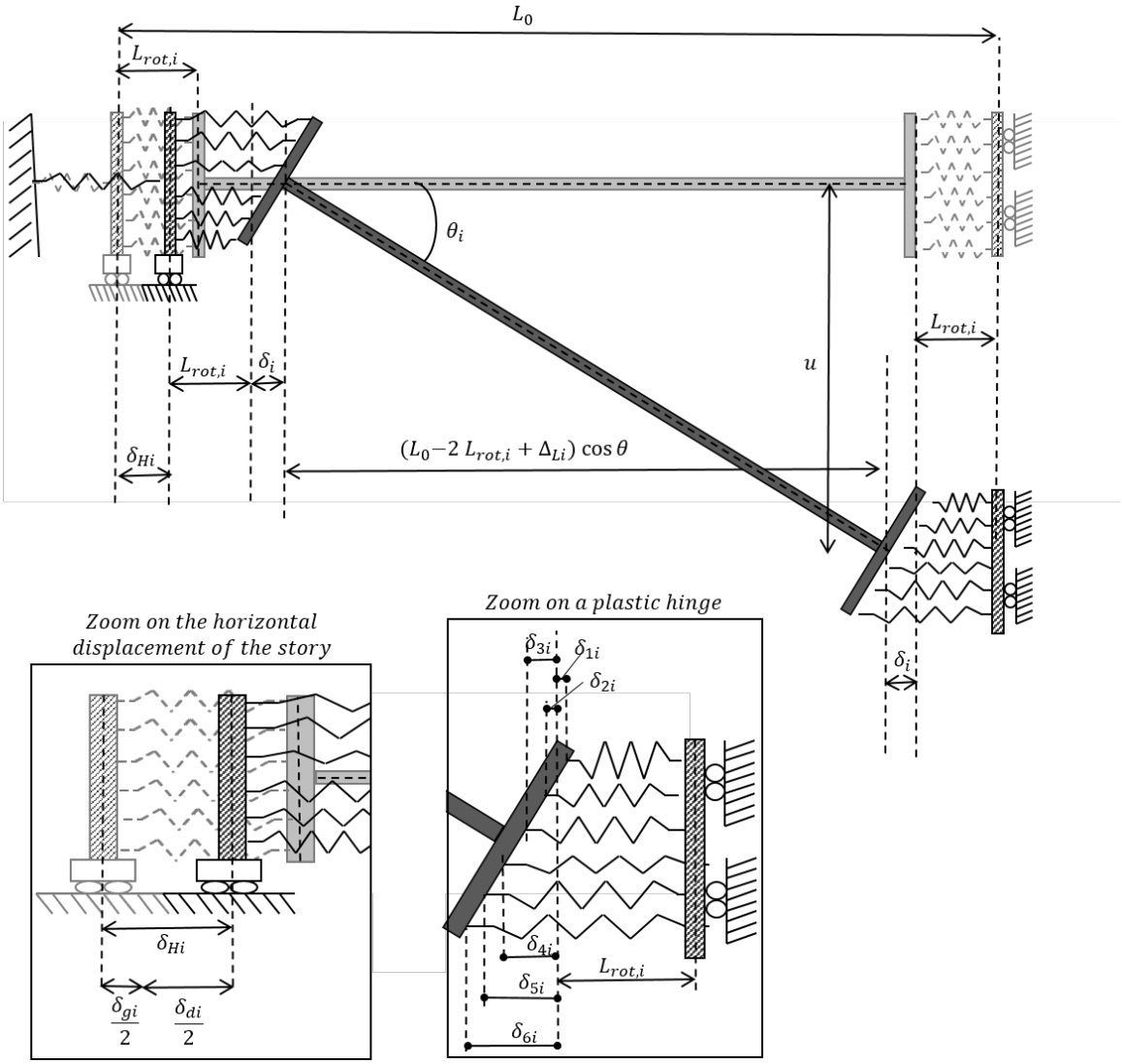

Figure 2.9 – Modeling of the i^{th} story of the substructure (inspired by [12]).

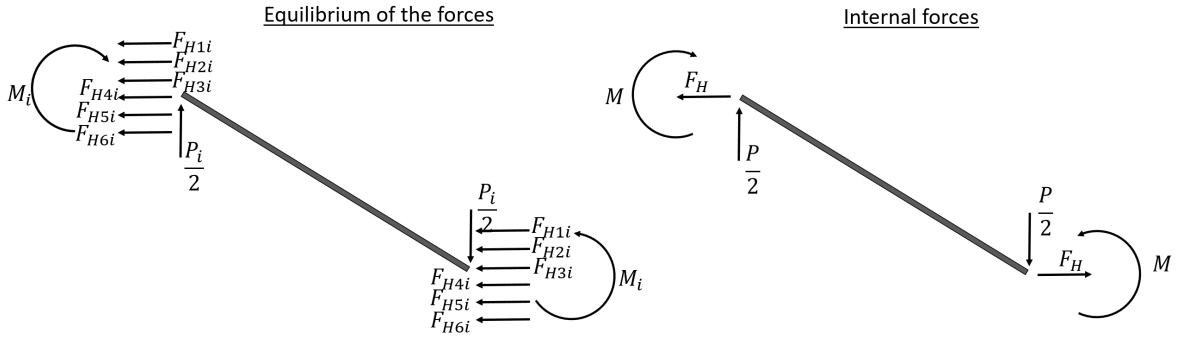

Figure 2.10 – Equilibrium of the forces and internal forces at the beam's extremity of the i^{th} story of the substructure.

Where A_i is the area of the beam at the story i of the substructure.

$$\delta_{j\,i} = \delta_i + h_{j\,i}\,\theta_i \text{ with } j = 1, ..., 6 \tag{2.9}$$

Known variables linked to the considered i^{th} story of the substructure	
$L_{rot\,i}$	Length of the plastic hinge appearing at the beam's extremity.
$h_{j\,i}$	Lever arm of the spring j ($j = 1, 2, ..., 6$) characterizing the part j of the plastic hinge's section (see figure 2.7).
$F_{Rd1,i}$	Axial strength of each flange of the plastic hinge's cross section and therefore axial strength of the springs 1 and 6 (see figure 2.7).
$F_{Rd2,i}$	Axial strength of one fourth of the web of the plastic hinge's cross section and therefore axial strength of the springs 2 to 5 (see figure 2.7).
Known variables linked to the hole substructure	
u	Vertical displacement applied at each story above the lost column.
L_0	Beam's length.
E	Yong modulus of the steel.
S_g	Flexibility matrix linking the horizontal forces and displacements at the left side of the substructure. Note that the component $S_{g\,j\,i}$ is the horizontal displacement appearing in the IAP at the left of the story i of the DAP when a unitary force is applied at the story j of the DAP.
S_d	Flexibility matrix linking the horizontal forces and displacements at the right side of the substructure. Note that the component $S_{d\,j\,i}$ is the horizontal displacement in the IAP appearing at the right of the story i of the DAP when a unitary force is applied at the story j of the DAP.

Table 2.1 – Known variables of the analytical model.

Unknowns linked to the considered i^{th} story of the substructure	
θ_i	Rotation angle of the beams' extremities.
$\delta_{j\,i}$	Horizontal displacement of the spring j ($j = 1, 2, ..., 6$) due to the rotation of the plastic hinge.
δ_i	Horizontal displacement at the middle of the beam's extremity due to the plastic hinge's rotation.
$\delta_{Hg\,i}$	Horizontal displacement of the IAP (and DAP) at the left of the studied story due to all the horizontal forces acting on the left side of the DAP.
$\delta_{Hd\,i}$	Horizontal displacement of the IAP (and DAP) at the right of the studied story due to all the horizontal forces acting on the right side of the DAP.
$\delta_{H\,i}$	Equivalent horizontal displacement equal at each side of the story.
$\Delta_{L\,i}$	Elastic elongation of the beam between the yielded zones.
$F_{j\,i}$	Horizontal force applied on the spring j ($j = 1, 2, ..., 6$) characterizing the portion j of the plastic hinge's section (see figure 2.7).
$F_{H\,i}$	Internal horizontal force at the beam's extremities.
M_i	Internal bending moment at the beam's extremities.
P_i	External vertical force applied above the lost column. Note that as P_i is applied to the two beams of the DAP, the internal vertical force at the beam' extremity is given by $\frac{P_i}{2}$.
Unknowns linked to all the stories of the substructure	
N_{lost}	Vertical force carried by the substructure (and therefore carried by the structure) due to the column's progressive removal.

Table 2.2 – Unknowns of the analytical model.

$$Fj\,i = max\left\{ \begin{array}{c} -F_{Rd1\,i} \\ min\left(F_{Rd1\,i}\,, F_{pre\,j\,i} + K_{1\,i}\,\delta_{pre\,j\,i}\right) \end{array} \right\} \text{with } j = 1,6 \tag{2.10}$$

$$Fj\,i = max\left\{ \begin{array}{c} -F_{Rd2\,i} \\ min\left(F_{Rd2\,i}\,, F_{pre\,j\,i} + K_{2\,i}\,\delta_{pre\,j\,i}\right) \end{array} \right\} \text{with } j = 2,3,4,5 \tag{2.11}$$

$$F_{H,i} = \sum_{j=1}^{6} F_{j\,i} \tag{2.12}$$

$$M_i = \sum_{j=1}^{6} F_{j\,i}\,h_{j\,i} \tag{2.13}$$

$$-\,0.5\,P_i\,\left(L_0 - \delta_{H,i}\right) + F_{H,i}\,u + 2\,M_i = 0 \tag{2.14}$$

$$\delta_{g\,i} = \sum_{k=1}^{N} K_g\,F_{H,k} \text{ with } K_g = \frac{1}{S_g} \tag{2.15}$$

$$\delta_{d\,i} = \sum_{k=1}^{N} K_d\,F_{H,k} \text{ with } K_d = \frac{1}{S_d} \tag{2.16}$$

$$\delta_{H,i} = 0.5\,\left(\delta_{g,i} + \delta_{d,i}\right) \tag{2.17}$$

$$N_{lost} = \sum_{i=1}^{N} P_i \tag{2.18}$$

Unknowns	Equations	number
θ_i	(2.6)	N
δ_i	(2.7)	N
$\Delta_{L\,i}$	(2.8)	N
$\delta_{j\,i}$	(2.9)	$6\,N$
$F_{j\,i}$	(2.10) and (2.11)	$6\,N$
$F_{H\,i}$	(2.12)	N
M_i	(2.13)	N
P_i	(2.14)	N
$\delta_{g\,i}$	(2.15)	N
$\delta_{d\,i}$	(2.16)	N
$\delta_{H\,i}$	(2.17)	N
N_{lost}	(2.18)	1
TOTAL		$21\,N + 1$

Table 2.3 – Summary of the system of equations and unknowns to solve.

Unknowns	Equations	number
θ_i	$\sin(\theta_i) = \dfrac{u}{L_0}$	N
$\delta_{SAG\,i}$	$L_0\ (\cos(\theta_i) - 1) + \delta_{SAG\,i} + +\delta_{HOG\,i}$	N
$\delta_{HOG\,i}$	$F_{H\,i} = \sum_{j=1}^{n_s} F_{SAG\,j\,i}$, n_s is the number of parallel springs.	N
$F_{H\,i}$	$F_{H\,i} = \sum_{j=1}^{n_s} F_{HOG\,j\,i}$, n_s is the number of parallel springs.	N
$\delta_{g\,i}$	(2.15)	N
$\delta_{d\,i}$	(2.16)	N
$\delta_{H\,i}$	(2.17)	N
$M_{SAG\,i}$	$M_{SAG\,i} = \sum_{j=1}^{n_s} F_{SAG\,j\,i}\, h_{j\,i}$	N
$M_{HOG\,i}$	$M_{HOG\,i} = \sum_{j=1}^{n_s} F_{HOG\,j\,i}\, h_{j\,i}$	N
$F_{SAG\,j\,i}$	$F_{SAG\,j\,i} = f\,(\delta_{SAG\,j\,i})$	$n_s\,N$
$F_{HOG\,j\,i}$	$F_{HOG\,j\,i} = f\,(\delta_{HOG\,j\,i})$	$n_s\,N$
$\delta_{SAG\,j\,i}$	$\delta_{SAG\,j\,i} = \delta_{SAG\,i} + h_{j\,i}\,\theta_i$	$n_s\,N$
$\delta_{HOG\,j\,i}$	$\delta_{HOG\,j\,i} = \delta_{HOG\,i} + h_{j\,i}\,\theta_i$	$n_s\,N$
N_{lost}	$N_{lost}(L_0\,\cos(\theta_i))\ (F_{H\,i}\,u + M_{HOG\,i} - M_{SAG\,i}) = 0$	1
TOTAL		$(9 + 4\,n_s)\,N + 1$

Table 2.4 – System to solve in the case of partial-strength joints.

2.1.4 Prediction of the substructure's response: partial-strength joints

In this section, a quick focus is made on the analytical method particularized to partial-strength joints. Indeed, both methods are almost identical and emphasis is brought here regarding their differences, especially the system of equations and unknowns relative to partial and full-strength joints. The system of unknowns and equations relative to partial-strength joints are given in table 2.4. First, a lot of the known variables are the same (as for S_g and S_d) and some are determined with different equations (as for the spring model which is different). Then, the unknowns and their related equations are mostly identical but some are different because of two reasons. The first difference resides in the fact that the plastic hinges form in the joints. Therefore, it induces a yielded length assumed to be null. Furthermore, the beam's elongation due to the formation of a plastic hinge is now null as well, as the plastic hinges do not form in the beams. These two unknowns are therefore not in the system of equations. Secondly, the joint's components activated in tension are different than those activated in compression. Therefore, if the joint is non symmetrical, the hogging and sagging moments, appearing respectively at the left and right of the beam in figure 2.9, are now not equal anymore. This induces the unknowns relative to the hogging and sagging moments to be multiplied by two, in comparison with the first model presented.

However, the spring model of the concrete part of the joints are still under investigation. In fact, another student is studying this topic this semester in parallel to the work done in this master thesis.

To conclude, as the rest of this master thesis is based on a code implementing the analytical method particularized to full-strength joints, the particularizing of the method to partial strength joints stops here. For additional information on the analytical method particularized to partial-strength joints, see Huvelle's article [12].

2.2 Implementation of the analytical model in *Matlab*

This section presents the implementation of the analytical model particularized to full-strength joints. Firstly the additional hypothesis made to simplify the implementation of the model is detailed. Afterwards, the organization of the implementation is explained in detail.

2.2.1 Additional hypothesis

In addition to the hypothesis of the analytical model, some supplementary hypotheses have been brought to facilitate the implementation of the model. The aim of these additional hypotheses is to avoid as much as possible a complicated structure and to be able to implement the method without the implementation of a finite element method.

First, some additional hypotheses have been made on the elements of the structure themselves. All the elements (beams and columns) of the structure are placed according to their strong axis and they all have the same steel grade. The columns of the IAP at the left of the lost column are assumed to be identical. The same hypothesis is made for the columns of the IAP at the right of the lost column. Moreover, all the beams of the IAP are assumed to be identical. However, there is the possibility to choose a different beam for the different stories of the DAP. Furthermore, all the beams have the same length, L_0, and all the columns have the same length as well, H_0.

Secondly, some supplementary assumptions have been made on all the joints of the structure: they are assumed to be fully rigid in addition to being full-strength joints. Furthermore, the joints at the base of the structure are assumed to be embedded in the foundation.

Finally, some additional hypotheses are made on the methodology used to determine S_g and S_d, explained in the next section.

2.2.2 Organization of the *Matlab* code

The global framework of the *Matlab* code is shown in figure 2.11 where four main subdivisions are highlighted: the inputs, the characterization of the DAP, the characterization of the IAP and the analytical resolution.

First, all the necessary inputs to run the code are detailed in table 2.5. This table is divided into three categories: the properties specific to the whole structure, those specific to the DAP, those specific to the IAP and those specific to the column removal. The inputs relative to the global aspect of the structure are illustrated in figure 2.12.

Then, the characterization of the DAP contains the determination of the plastic hinge's properties that are needed for the resolution of the system summarized in table 2.3. As the beams of one story in the DAP are identical, the plastic hinges forming at one story have the same properties and there are N plastic hinges to characterize. The inputs and outputs of this part of the framework are detailed in figure 2.13. The details to determine these characteristics have already been explained in section 2.1.3.

After that, the characterization of the IAP aims to determine both S_g and S_d, the flexibility matrices governing respectively the displacements at the left and at the right of the defined substructure. The determination of these matrices depends on the chosen hypothesis at the

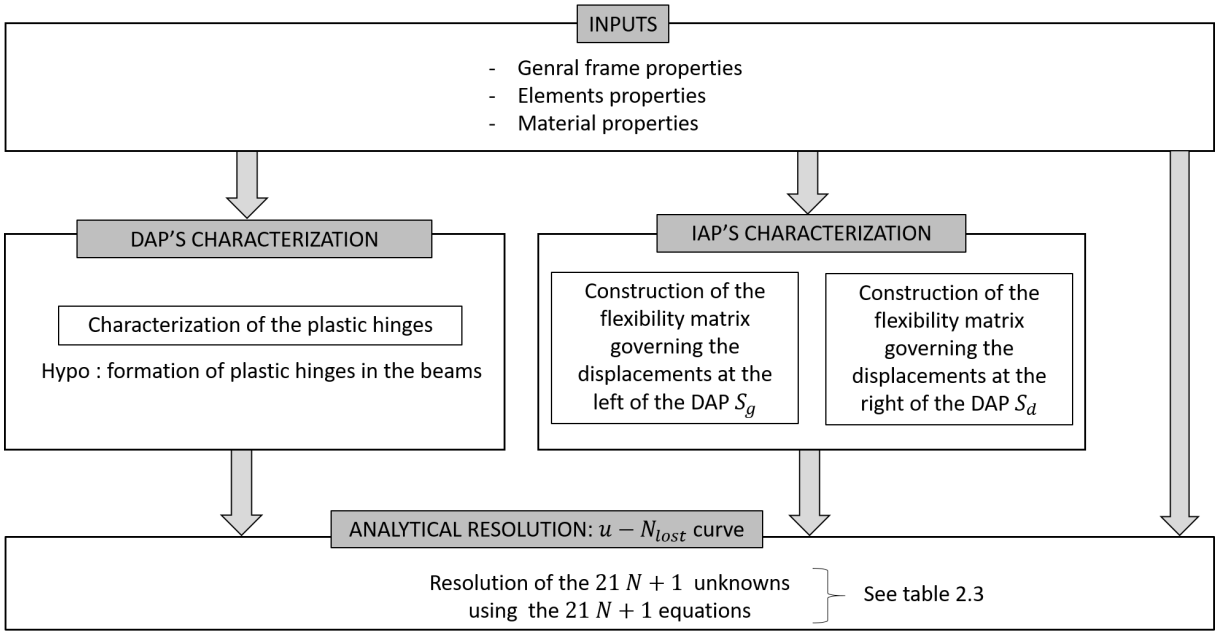

Figure 2.11 – Global framework of the *Matlab* code.

Properties specific to the hole structure	
N	Number of stories above the lost column/ Number of stories composing the DAP/ Number of stories composing the substructure.
n	Number of stories below the lost column.
$bracing_g$	Characterizes whether there is a bracing at the left side of the frame or not. If there is one $bracing_g = 1$, if not $bracing_g = 0$.
$bracing_d$	Characterizes whether there is a bracing at the right side of the frame or not. If there is one $bracing_d = 1$, if not $bracing_d = 0$.
c_g	Number of columns at the left of the lost column (per story).
c_d	Number of columns at the right of the lost column (per story).
L_0	Length of the beams.
H_0	Height of the columns.
E	Young modulus of the steel.
f_y	Yielding stress of the steel grade.
Properties specific to the DAP	
$beam_i$	Beams' type of the i^{th} $(i = 1, 2, ..., N)$ story of the DAP. For example 'HE 100 b'.
Properties specific to the IAP	
$beam_{IAP}$	Type of the beams composing the IAP.
col_{left}	Type of the columns composing the IAP at the left the lost column.
col_{right}	Type of the columns composing the IAP at the right of the lost column.
Properties specific to the column's removal	
u_{max}	Maximum vertical displacement necessary to reach for the drawing of the $u - N_{lost}$ curve.

Table 2.5 – Inputs of the *Matlab* code.

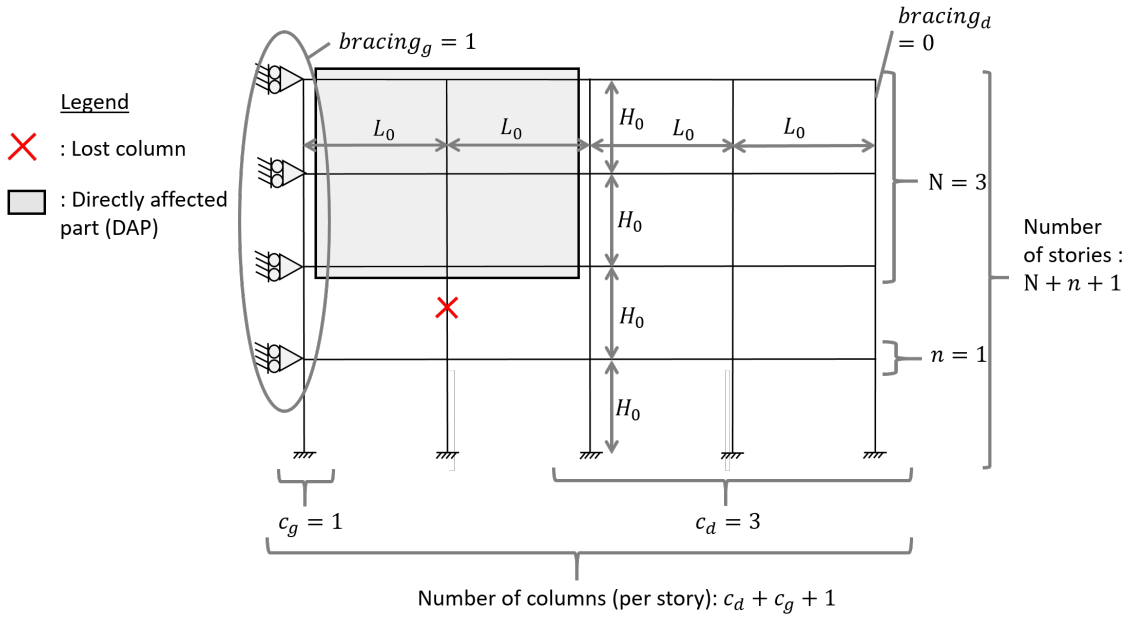

Figure 2.12 – Illustration of some of the inputs of the *Matlab* code.

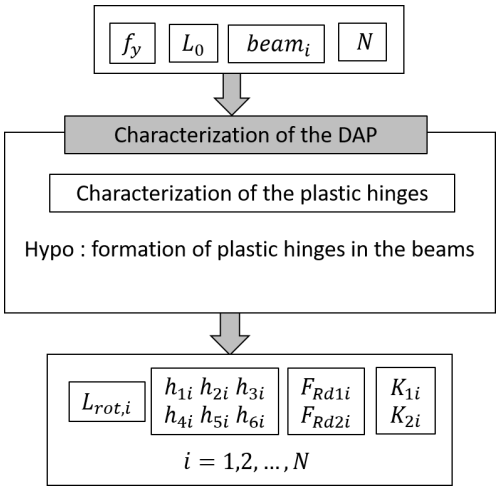

Figure 2.13 – Inputs and outputs linked to the characterization of the DAP.

base of the implementation of the model. In this code, it has been chosen to avoid the implementation of a finite element code by simplifying the structure, as explained in 2.2.1. In the following, the method used to determine these flexibility matrices is detailed. The inputs and outputs related to this specific part of the code are highlighted in figure 2.14.

S_g (S_d) is determined through the analysis of a portion of the IAP composed of the part at the left (right) of the DAP, named IAPL where "L" stands for left (IAPR with "R" standing for right). Figure 2.15 illustrates this division between the IAPL and IAPR relative to a given example. The structure on the left shows the whole analyzed frame. The structure on the middle shows the total IAP during phase 3 to which the DAP does not bring any stiffness anymore (because the complete mechanism plastic of the DAP has fully formed). Finally, the two frames at the right of the figure illustrate the IAPL and the IAPR of the example. The rotational springs of the IAPL (IAPR) take into account the stories of the IAP at the left (right) of the lost column and the columns under the lost colum and are determined using Hai's

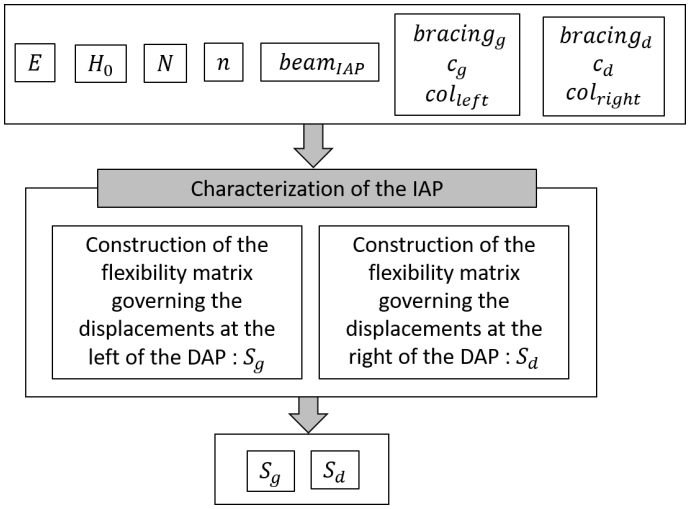

Figure 2.14 – Inputs and outputs linked to the characterization of the IAP.

method [4]. The methodology to determine the rotational spring for the IAPL is identical to the one applied for the determination of the rotation springs of the IAPR. Therefore, the methodology is only explained for the IAPL in the following. Figure 2.16 details what have been implemented in the code and figure 2.17 illustrates the 2 principles forming the basis of Hai's methodology.

As highlighted in figure 2.16, a mistake has been made during the implementation of the method. A mistake that I found and corrected while I was implementing a new method to determine S_g and S_d. More details are given in chapter 4.

Furthermore, I found another issue in the code. The columns under the lost column are assumed to be of type col_{right} when determining S_d and are assumed to be of type col_{left} which causes some confusion.

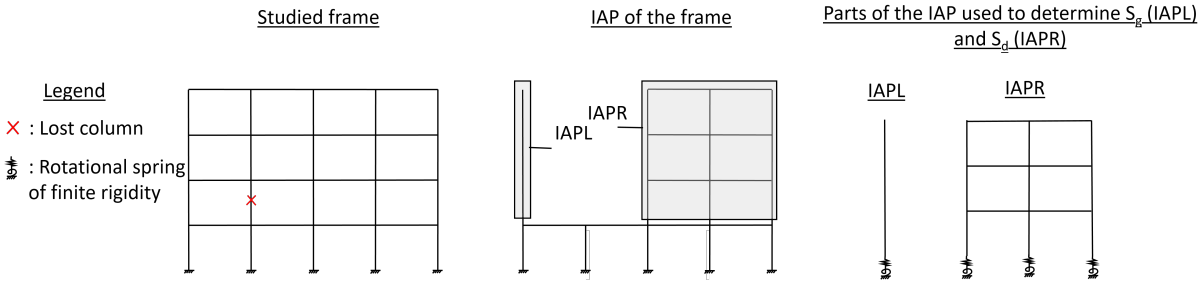

Figure 2.15 – Illustrtaion of how the frame is divided into the IAPL and IAPR.

Again, as the same methodology is used to determine S_g and S_d, in the following, the methodology is developed for the IAPL to determine S_g. The global methodology to determine this stiffness matrix is given in figure 2.18.

First, the code distinguishes two cases, depednding if the IAPL is braced or not. If it is braced, all the components of S_g are null. If not, components of S_g are different than zero.

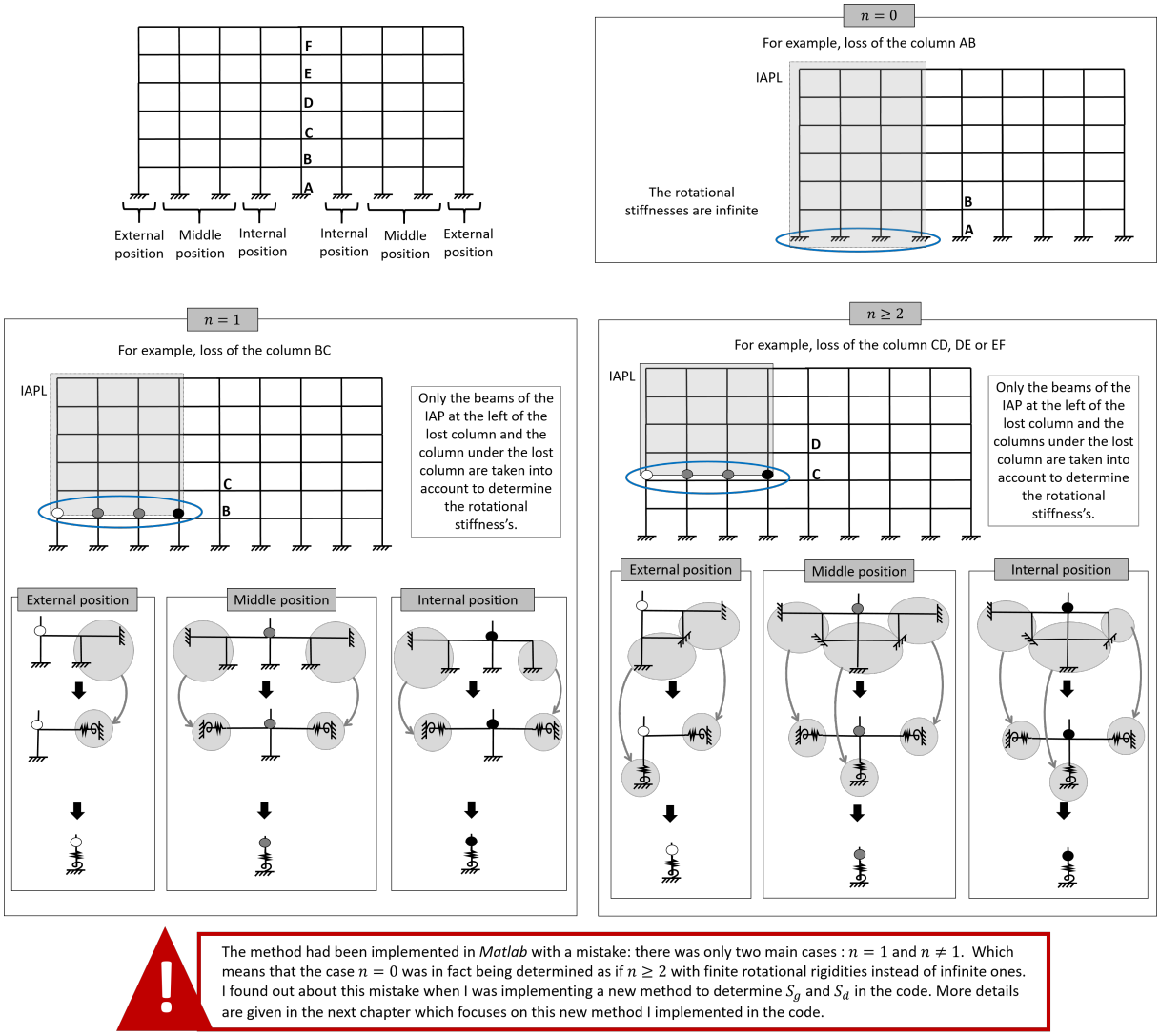

Figure 2.16 – Illustration of the methodology applied to determinate the finite rotational stiffness's at the bottom of the IAPL, determined by Hai is his PhD thesis.

Second, if the left end of the structure is not braced, the code analyzes the number of columns present in the IAPL. If there is only 1 column ($c_g = 1$), the flexibility matrix is found through the application of the unitary force theorem to a cantilevered column with a correction added in the case of $n \geq 1$ to take into account the finite rigidity of the bottom column's base of the IAPL (see figure 2.15). The major steps of this method are explained in figure 2.19.

If each story of the IAPL is composed of more that one column ($c_g \geq 2$), the unitary force method is applied as a matrix problem. So firstly the rigidity matrix of the IAPL is determined. To do so, all the fully rigid joints are characterized by a very large rotational stiffness. Moreover, the stiffness's rigidity at the bottom of the bottom columns of the IAPL are determined using Hai's method (see figures 2.16 and 2.17). Afterwards, once the rigidity matrix is constructed, the terms of S_g are determined as illustrated in figure 2.20.

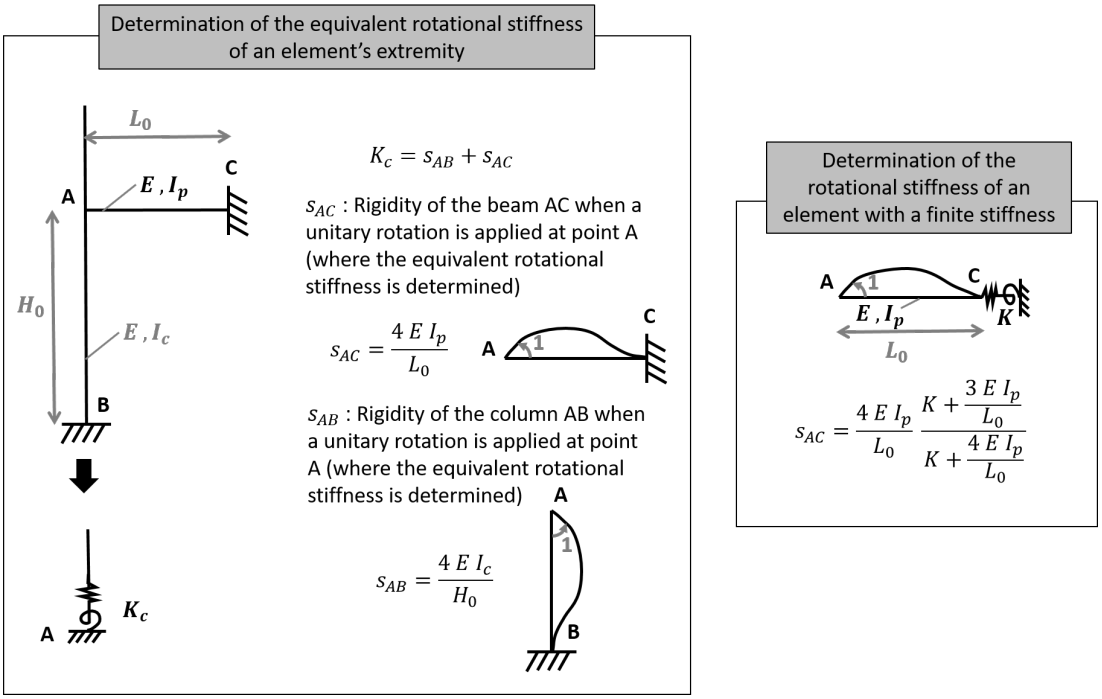

Figure 2.17 – Illustration of the 2 principles governing Hai's methodology studied during his PhD.

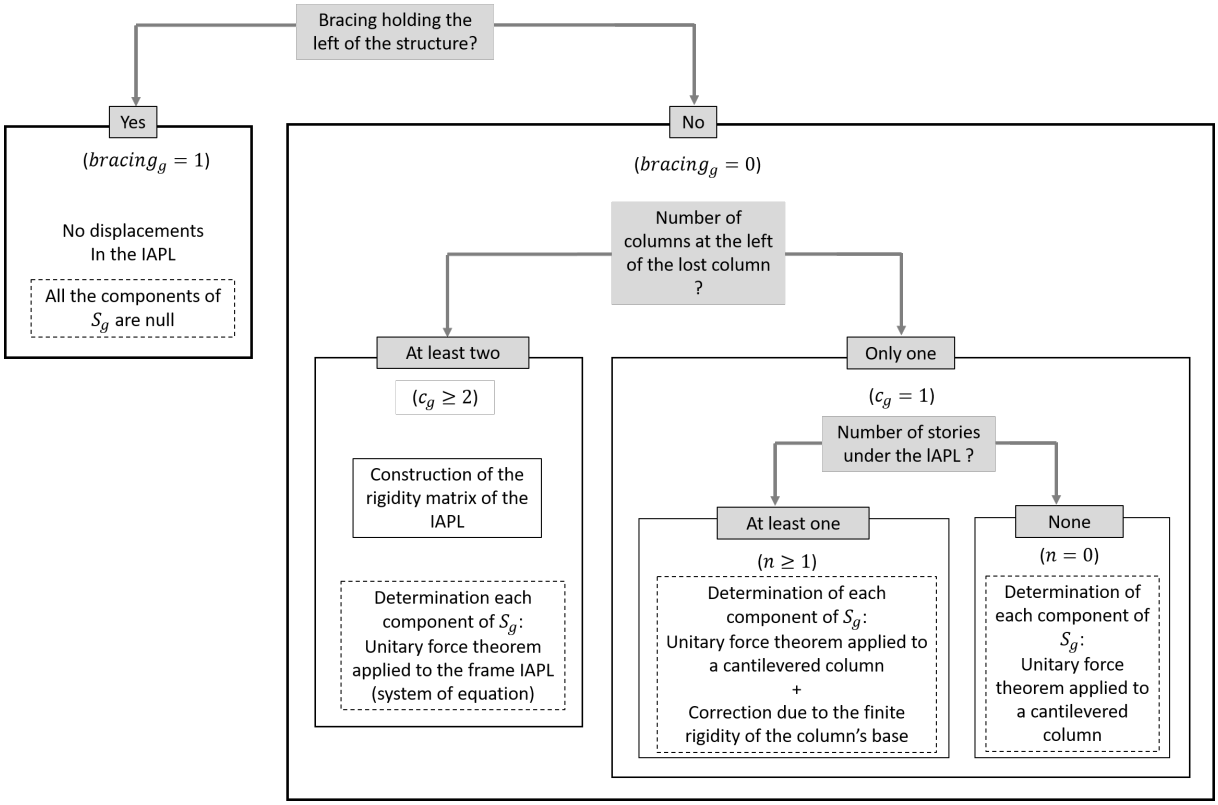

Figure 2.18 – Organization chart of the determination of the flexibility matrix S_g.

Finally, now that all the inputs needed to solve the system of $21\,N + 1$ equations are determined, the system summarized in table 2.3 is resolved for each step u for $u > 0$ to

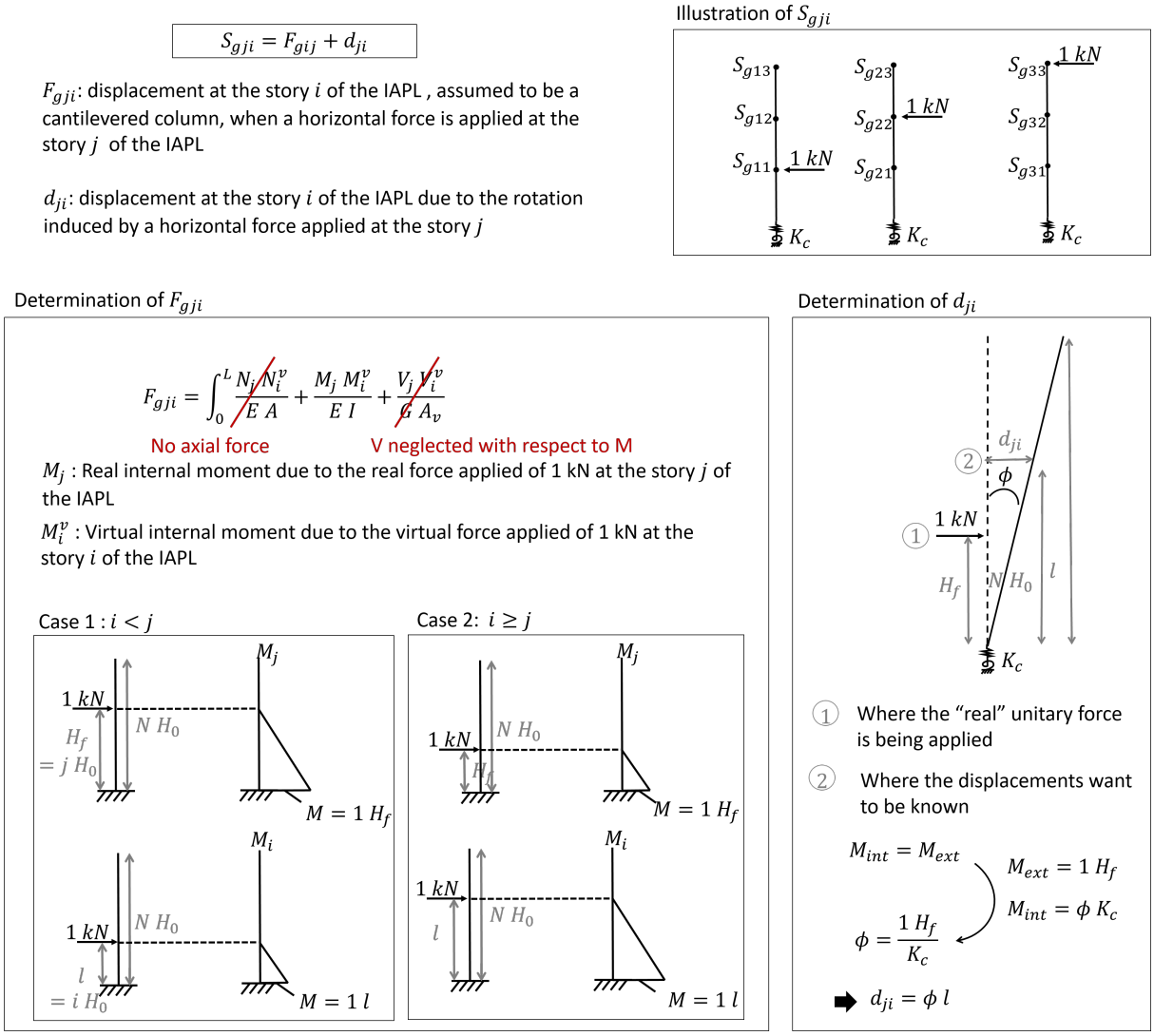

Figure 2.19 – Determination of $S_{g\,j\,i}$ $(i, j = 1, 2, ..., N)$ if the structure is not braced at its left and if $c_g = 1$.

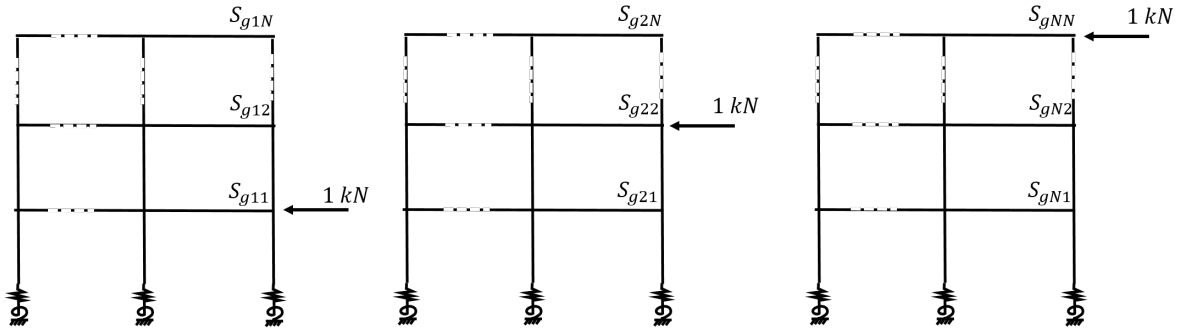

Figure 2.20 – Unitary force applied to the frame IAPL to determine the terms $S_{g\,j\,i}$ $(i, j = 1, 2, ..., N)$ if the structure is not braced at its left and if $c_g \geq 1$.

$u = u_{max}$. The inputs of the analytical resolution part of the code are highlighted in figure 2.21. The outputs of the analytical resolution are the unknowns detailed in table 2.2 and more specifically, N_{lost} so that the $u - N_{lost}$ curve is now determined.

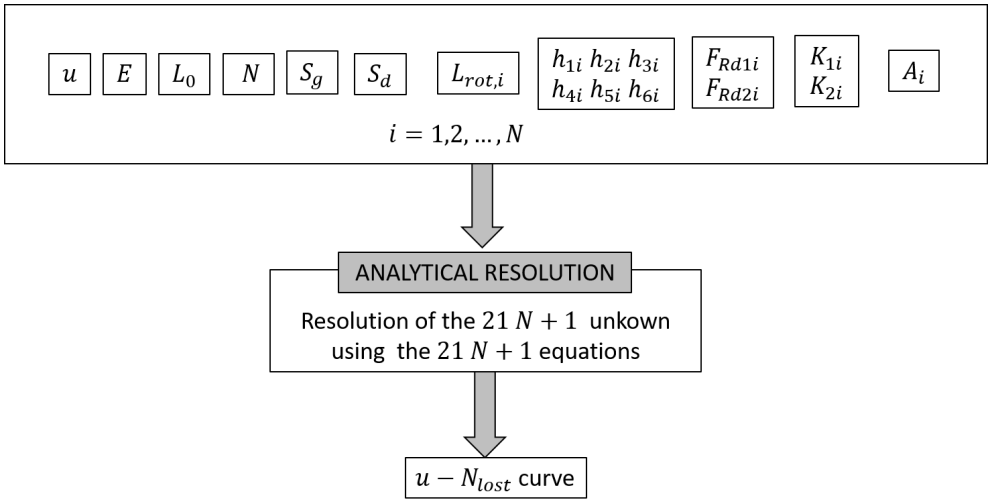

Figure 2.21 – Inputs for the resolution of the system given in table 2.3 at each step of u.

2.3 Conclusive remarks

During this chapter, it worth mention let's focus on the encountered difficulties during this task. Globally, it was work intensive for me to deeply focus on this model and its implementation, as I was new in this research field concerning the robustness of structure. The difficulties confronted concerning the understanding of the field of application, hypotheses and theoretical explanations of the analytical method developed so far are first detailed in the following. The hypotheses of the analytical model have been especially difficult to clarify. Indeed, the small improvement brought by each researcher led to changes in the hypotheses and these were not always clearly set up in the existing literature on the subject. Furthermore, although the origins of the system of equations to solve in the analytical resolution (see table 2.3) and the spring model (see figure 2.7) were detailed in the existing literature, some inconsistencies in the variables names and the lack of clarification regarding the variables were a handicap for the model's understanding. Then, difficulties were encountered during the comprehension of the implementation itself. Conciling the incremental implementation done by several persons and the absence of explanations or comments, the most difficult part of the code to understand was the characterization of the IAP (see figure 2.11) within which the flexibility matrices are determined. The difficulties of understanding this part were due to the lack of an article or paper explaining specifically the method illusrated in figure 2.16. Indeed, Hai has explained his method in his PhD thesis [4], however, the method explained in figure 2.16, inspired by his method, have not been explicitly detailed. Therefore, this made the understanding of all the equations and the code difficult.

In spite of everything, the model was entirely and deeply inspected and detailed. Indeed, the hypotheses at the base of the analytical model are now settled and the variables governing the system of equation summarized in table 2.3 are as well clearly defined and represented. Furthermore, the system of equation to be solved in the case of full-strength joints and partial-strength joints are clearly differentiated. Besides, the hypotheses of the model's implementation were first distinguished from the hypothesis of the analytical model itself. Moreover, the implementation of the analytical method is clearly defined and gives a rich basis for the future students or researchers who will work on this model. Moreover, all the formula implemented have been verified and the mistake found in the implementation of Hai's method has been corrected. Besides, I rearranged the code in order to facilitate its use.

In conclusion, the contribution of this task to the analytical model is an essential work for all the future persons who will use and/or continue to improve the analytical model and its implementation.

Now that the analytical method based on full-strength joints and its implementation are fully understood and explained, the next work consists in the improvement of this implementation. More particularly, a new method to characterize the restrain brought by the IAP to the DAP will be implemented in chapter 4. While the effects of the yielding of the IAP will be investigated in chapter 5.

CHAPTER 3

Presentation of the studied situations

In this chapter, the structures under investigation are first presented. Then, some details are given on the simulations under investigation in this master thesis.

3.1 Studied structures

In the following, the reference structure is first presented, followed by a synthesis of its design. Then, the other similar structures that will be investigated in this work are detailed.

3.1.1 Presentation of the reference structure

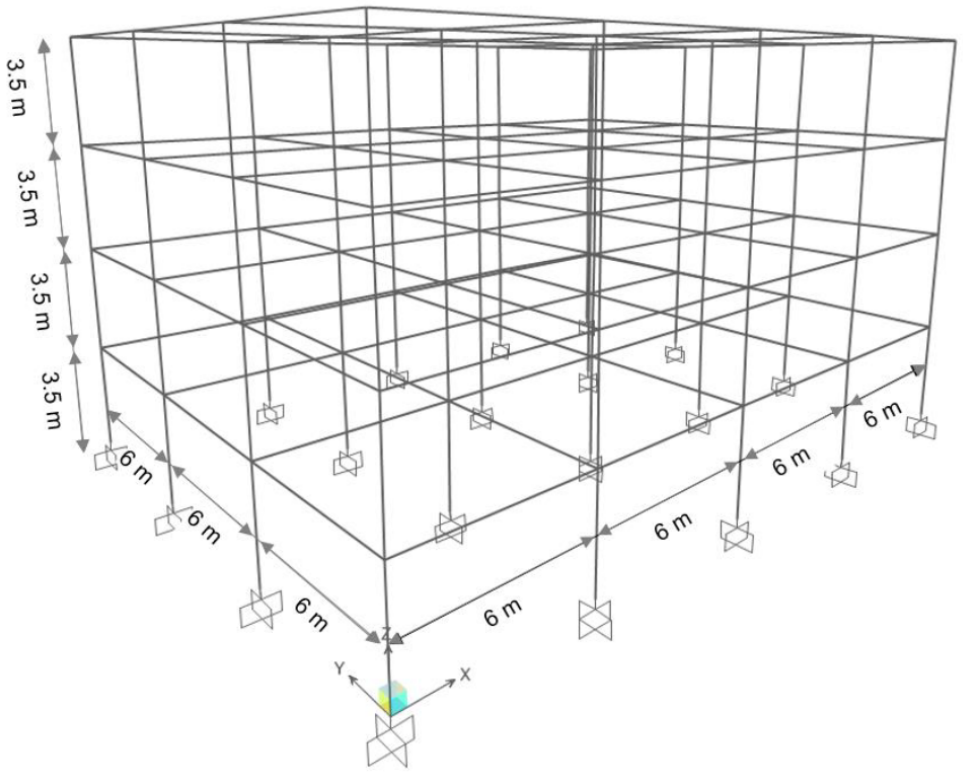

Figure 3.1 – 3D reference frame [17].

The reference structure is the same as the one adopted in Hjeir and Dewez master thesis, respectively [17] and [8]. The structure is assumed to be an office building situated in the area

of Brussels. The structure is a 3D steel frame and is illustrated in figure 3.1. Furthermore, the secondary beams lay in the Y direction (see figure 3.1) and are simply supported by the primary beams[1] of the structure, which lay in the X direction. On the top of the secondary beams, there is a two-ways concrete slab of 25 cm thickness. The latter is put on each story and on the roof. Moreover, the slab is not connected to the steel beams such that it does not have any structural effect on the frame. In addition, concerning the joints: the joints between the columns and beams are assumed to be fully rigid and fully resistant; and the bottom columns are embedded in the ground.

In the following, this frame is analyzed in the (X, Z) plane only, without the consideration of the 3D effects in the behavior of the 2D frame. The 2D frame is shown in figure 3.2. This 2D analysis makes perfect sense considering that the analytical model is a 2D model.

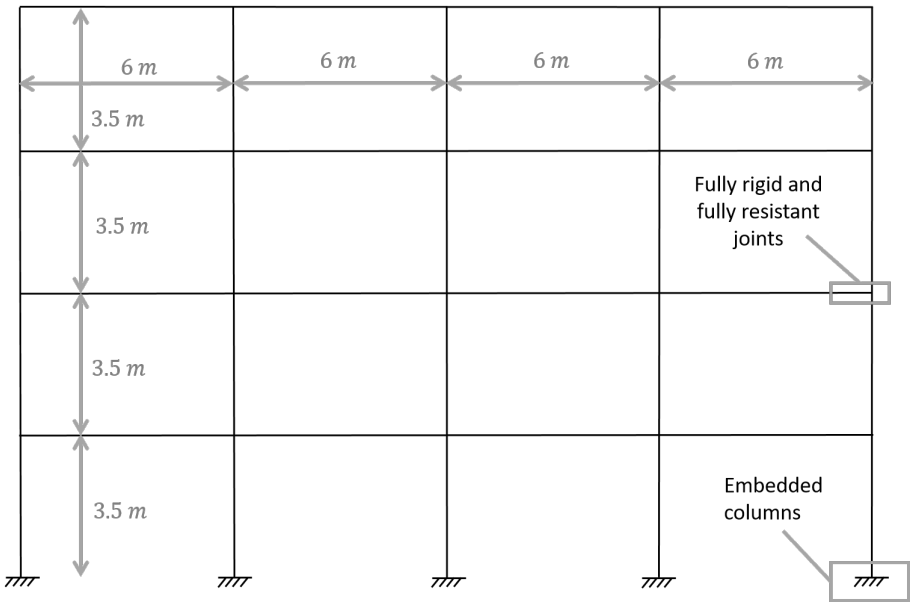

Figure 3.2 – 2D reference frame.

3.1.2 Design of the reference frame

The 2D struture shown in figure 3.2 has been designed under SLS and ULS according to the Eurocode. In the following, only the general hypotheses are stated. The complete design procedure may be found in Dewez's master thesis [8].

The loads determination in the Eurocodes are based on the hypothesis that the structure under investigation is an office building in the area of Brussels. Furthermore, the loads taken into account in the design of the structure are the variable loads, namely the live load and the snow load, the permanent loads and the wind load which is an accidental load.

The SLS verification follows the directives given in the Eurocode EN 1990 [18]. The maximum allowable transverse displacement between two adjacent stories is $\frac{H}{250}$, where H is the height of the story under consideration. Furthermore, the maximum allowable floor deflection is $\frac{L}{300}$ where L is the length of the considered beam.

[1] This assumption aims to simplify the analysis of the frame.

As for the ULS, they are as well verified by following the directives of the Eurocode EN 1990 [18]. Furthermore, in order to simplify the verification, it is assumed that there is no out of plane instabilities. Moreover, the structural imperfections have been taken into account in the design, as the structure has been classified as a sway structure.

The design of the structure is shown in figure 3.3. This structure is named structure Ib. However, as the existing analytical model, explained in chapter 2, may only be applied to structures with identical columns, a variance of this design has been developed. In this variance, all the columns are identical. This structure is shown in figure 3.4 and is named structure Ia.

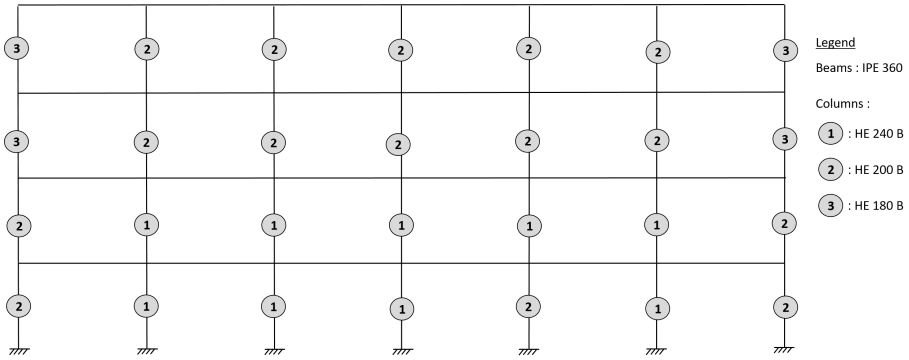

Figure 3.3 – Design of the 2D reference frame. Also called structure Ib.

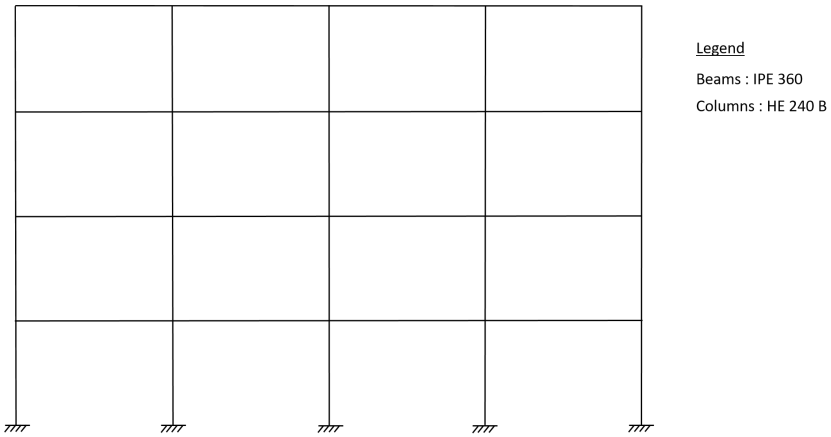

Figure 3.4 – Design of the 2D reference frame with all the same columns. Also called structure Ia.

3.1.3 Other structures under investigation

In order to test the analytical model on different structures, two other structures and their homologous with identical columns are defined. These additional structures are illustrated in figures 3.5 and 3.6. Note that as the number of stories is identical, the design of these structures is similar.

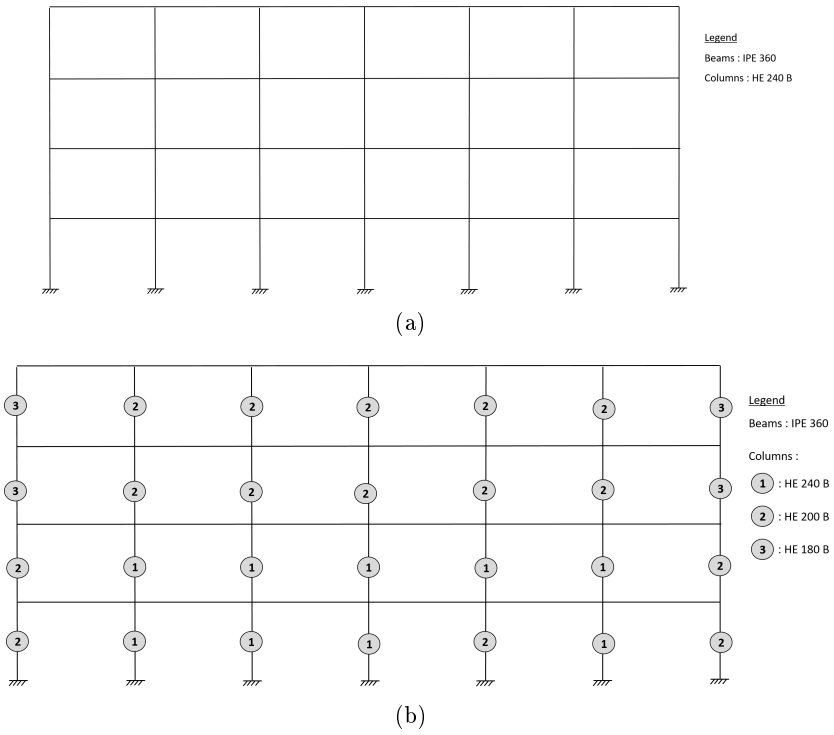

Figure 3.5 – Design of the structure IIa (a) and the structure IIb (b).

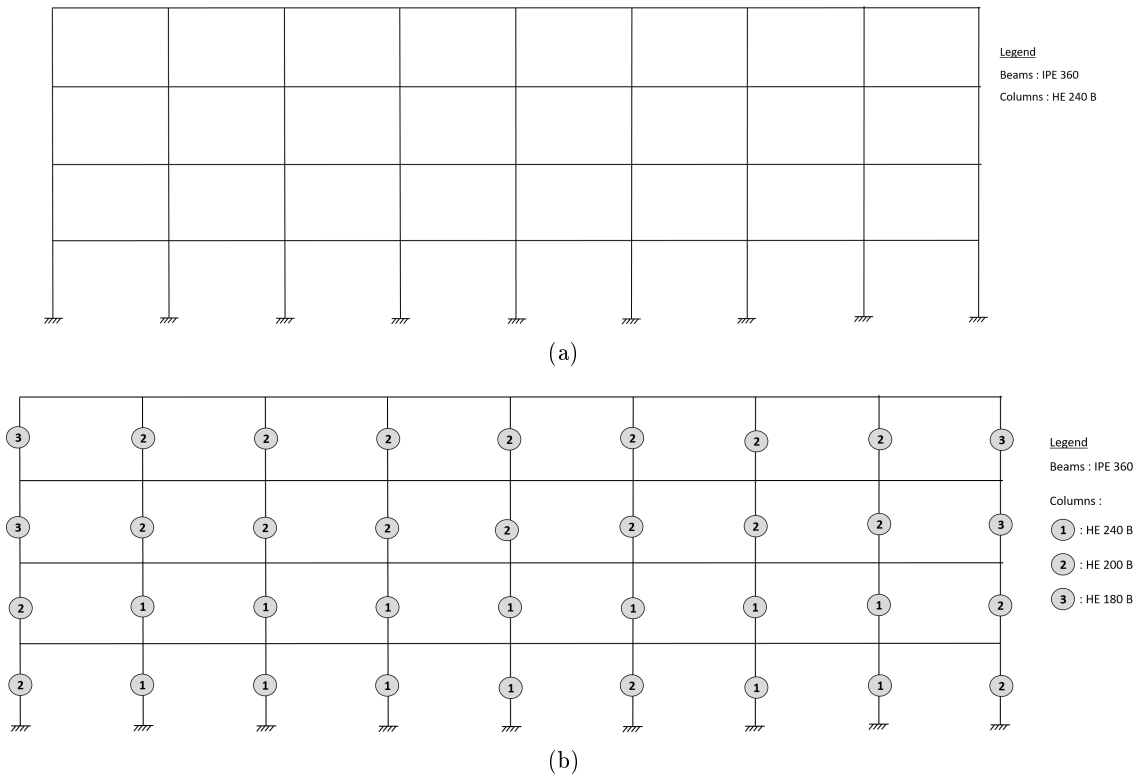

Figure 3.6 – Design of the structure IIIa (a) and the structure IIIb (b).

3.2 Structural analysis further to a column loss

In order to test the analytical model, two different situations are under investigation, named scenarios 1 and 2. The scenario 1 of each structure represents the situation in which the removed column is the bottom column at the middle of the structure. The scenario 2 is the situation in which the structure IIa or IIb is studied for the loss of the column next to the middle bottom column. For all these scenario, the structure is submitted to the accidental load case scenario determined in Dewez thesis [8] and illustrated for structures Ia and Ib in figure 3.7.

Furthermore, the response of a structure obtained with the analytical method will be compared to the same response determined with the finite element software *Finelg*. The latter is the reference for the structure's behavior under a given situation.

Finally, the modeling of the frame in *Finelg* is detailed briefly. For more information, see Dewez's master thesis [8]. The modeling in *Finelg* is based on a 2D non linear analysis which includes material non linearities and geometrical non linearities. Furthermore, each of the beams and columns are modeled with fifteen elements. About the element's material law, the elements of the DAP are following a linear-perfectly elastic law for all the simulations. The elements of the IAP are following a perfectly elastic law when it is wished to determine the response of the structure with the IAP assumed to not yield. However, when it is wished to determine the behavior of the structure with the IAP that may yield, the elements of the IAP are following an elastic-perfectly plastic law. Finally, the simulation of the lost column in *Finelg* is done through the method already explained in section 1.4. Furthermore, the accidental combination of load includes only the gravity loads to simplify the analysis of the frame's behavior.

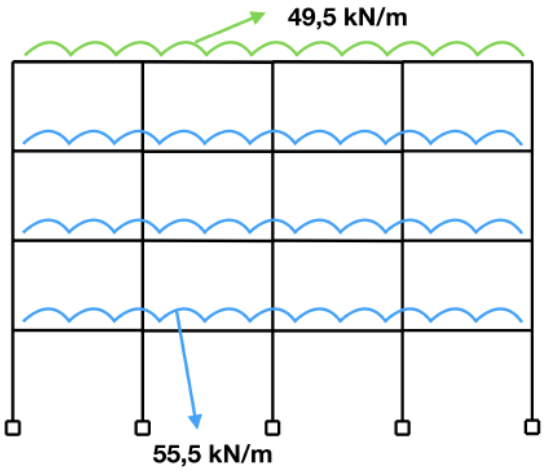

Figure 3.7 – Accidental loading, in addition to the self load, to be applied to the structures Ia and Ib in addition to the self load of the structure [8].

CHAPTER 4

Combination of the model with *BeamZ*

In this chapter, a first improvement of the initial code is implemented. The motivations and the strategy of this new implementation, as well as the software with which the *Matlab* implementation will be coupled, are first presented. The theoretical, implementation and verification methodologies are then detailed. After that, the response of the structure obtained with both the initial and the new implementations are compared to the structure's behavior obtained with *Finelg*. After that, the new implementation is validated through comparison with the initial implementation (see chapter 2) for situations for which both implementations should lead to the same results. The new model is then applied to some structures that could not be tested with the initial model. Finally, conclusive remarks are drawn on the staff contribution and the possible enhancements of the model.

4.1 Motivation and strategy of the improvement

Two main objectives encouraged the implementation of this improvement: improve the accuracy of the determination of S_g and S_d and widen the field of application of the model, and in particular enlarge the field of application of the IAP.

In the initial implementation, S_g and S_d are determined respectively through the analysis of the IAPL and IAPR (see figure 2.15) for which the bottom stiffnesses are determined using the hypothesis that some beam and column end are embedded (see figure 2.16). This implementation aims to make this determination more accurate by analyzing the total IAP instead of only the IAPL and IAPR. To do so, it is necessary to use a finite element method instead of the approximate method used before. In order to avoid the complete implementation of such a method, it is chosen to combine the implementation with *BeamZ*.

Thanks to the coupling with a finite element code as *BeamZ*, the related hypothesis added to avoid the use of a finite element code may now be raised. For instance, the columns and beams of the IAP may now be different from one to another, the bottom columns of the IAP (and therefore of the structure) do not have to be embedded anymore, other additional support may be put anywhere in the IAP, only some of the stories may now be braced with other stories not braced. In conclusion, a lot more possibilities open to the user.

Note that the IAP is still assumed to stay elastic during all three phases of the structure's response and therefore during the whole phase 3.

4.2 Presentation of the software *BeamZ*

BeamZ is a finite element software designed and implemented in *Matlab* by V. Denoel and his researchers. *BeamZ* solves the reaction forces, internal forces and displacements of 2D structures. For instance, it allows for linear elastic analysis which will be used in this implementation.

For the specific purpose of this improvement of the analytical model using *BeamZ*, this software has been improved by V. Denoel to allow for the extraction of a series of information defining the implemented structure. Among these, the stiffness matrix of the structure, the nodes number, the elements number,... When the user click on the knob "extraction", he is invited to save this information in a *Matlab* file.

4.3 Methodology followed in the new implementation

The general idea of the method is the application of the unitary force method on the whole IAP, instead of the application of the unitary force method on an approximate substructure, the IAPL and IAPR.

The first thing to determine with this new methodology is the stiffness matrix of the IAP, on which the unitary force theorem will be applied to determine the flexibility matrices, S_g and S_d. The stiffness matrix of the IAP is found trough the linear analysis of the IAP using *BeamZ*. The details of the implementation of the IAP in *BeamZ* are given in the next section.

However, this stiffness matrix outputted from *BeamZ* does not have "infinite" stiffness terms to characterize the fixed DOFs. Therefore, the second step is to add those. The terms to change are the terms of the diagonal corresponding to a fixed DOF. The amount added to these terms has to be large enough to seem infinite with respect to the other terms of the diagonal but cannot be too big in order to avoid numerical problems due to bad conditioning.

Then, the unitary force method is applied. The same global idea is adopted as the one applied in the initial implementation of the model but using the stiffness matrix of the IAP for both the determination of S_g and S_d instead of the stiffness matrix of the IAPL and IAPR. Figure 4.1 illustrates this method application on the IAP.

Note that if the lost column is situated above the ground floor, the IAP is composed of one single structure and there exists coupling effects between the forces acting on one side of the substructure and the displacement appearing at the other side of the structure, which are not taken into account in the original analogical model. However, those coupling effects are here neglected. Indeed, the system governing the substructure, resumed in table 2.3, does not take these coupling effects into account.

4.4 Organization of the new implementation

The global frame of the code is shown in figure 4.2. It is observed that one step has been added to the implementation before the code's implementation: the use of *BeamZ*. Within the second step, the code itself is partitioned in the same main divisions that were observed in the initial implementation of the code. However, the divisions are not all identical to the initial code. In the following, those differences are highlighted.

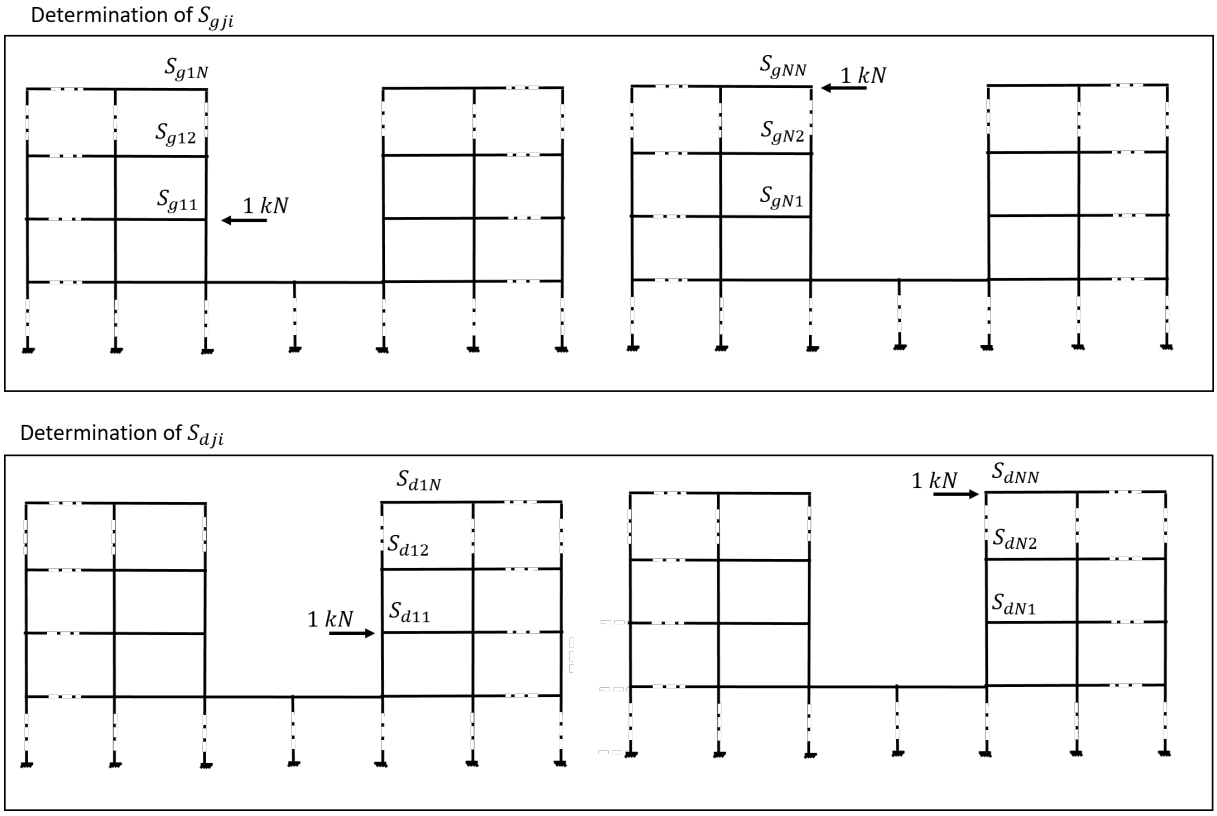

Figure 4.1 – Application of the force method to determine the terms of S_g and S_d.

Step 1 : *BeamZ*

First, let's take a closer look to the first new step. In this step, the IAP is first modeled in *BeamZ*. Note that only the nodes, the elements (numbering, material, geometries) and the supports of the IAP need to be introduced in the modeling. Furthermore the nodes and elements numbering is open.

Then, the IAP is analyzed through a linear elastic analysis with *BeamZ*. In the results, this specific version of *BeamZ* allows the writing of a *Matlab* file which, among others, defines the nodes, elements and stiffness matrix of the model. This stiffness matrix has a size $[3\,n_{nodes} \times 3\,n_{nodes}]$, n_{nodes} being the number of nodes of the IAP.

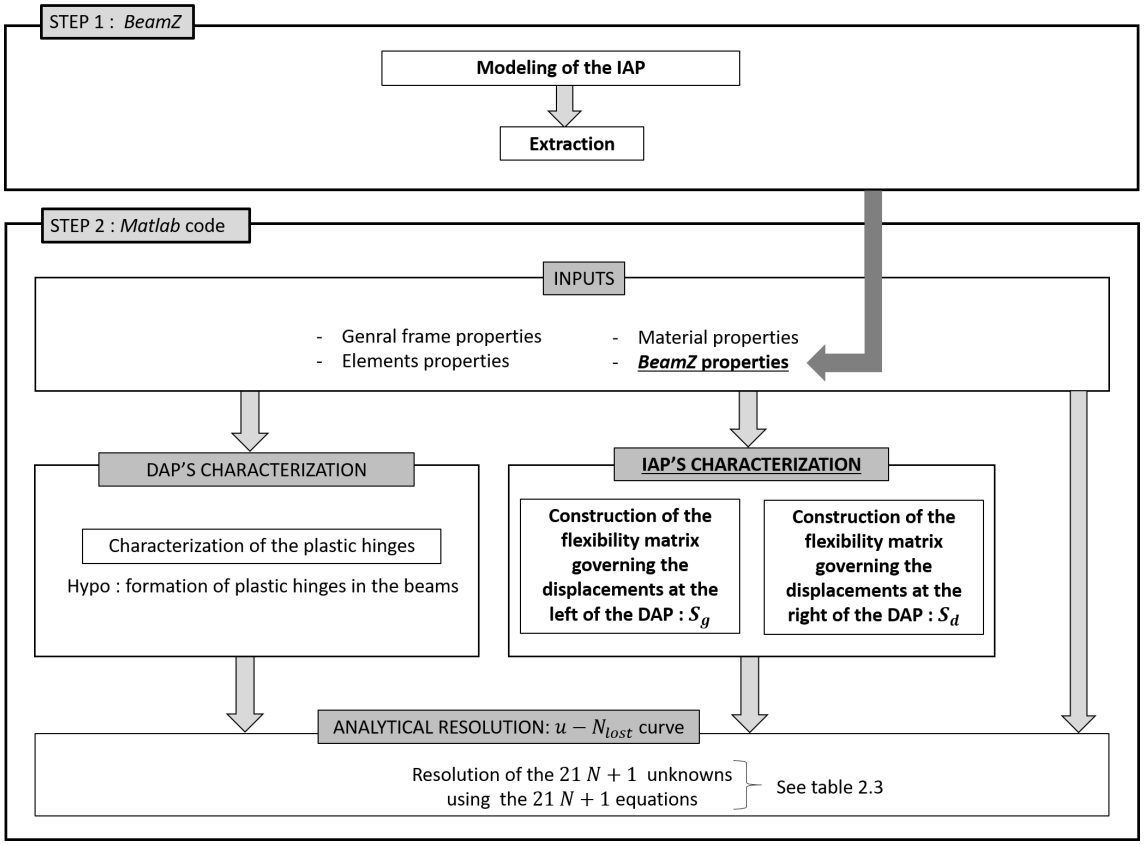

Figure 4.2 – Organization chart of the new implementation of the analytical model.

Step 2 : *Matlab* code

Now, let's take a closer look to the code's implementation itself. The inputs are summarized in table 4.1 in which the new inputs are in grey. First, the new inputs, appearing in the properties specific to the whole structure, aim to impose the fixed DOF of the IAP. Those boundary conditions may be manually set using H_{fixed}, V_{fixed} and R_{fixed}. For some specific configurations, they also may be defined semi-automatically using $Bracing_g$, $Bracing_d$ and $Embedded$. Furthermore, the *Matlab* implementation is based on the enumeration of the IAP nodes illustrated for two different structures in figure 4.3. Therefore, $node_{order}$, one of the new inputs in the IAP properties, makes the conversion between the *BeamZ* enumeration and the *Matlab* enumeration. Finally, the *Matlab* file named *file.mat* is the file in which the *BeamZ* information has been extracted. From this file, the code will extract the stiffness matrix $K_{IAP,mess}$ and the number of nodes in the IAP n_{node}.

To illustrate these inputs, let's focus on two different examples. The inputs applied to the structure on the left of figure 4.3 are first presented. The node order is identical to the one chosen in the *Matlab* code. Therefore, the vector $node_{order}$ is given by:

$$node_{order} = [1\,2\,3\,4\,5\,6\,7\,8\,9\,10\,11\,12\,13\,14\,15\,16\,17\,18\,19\,20\,21\,22]$$

Furthermore, all the bottom beams are embedded: that is the supports numbered 1, 6, 8 13 and 18. The first way (semi-automatic way) to impose these boundary conditions are set down by:

$$Embedded = 1 \text{ and } H_{fixed} = V_{fixed} = R_{fixed} = 0\,.$$

Properties specific to the whole structure	
N	Number of stories above the lost column/ Number of stories composing the DAP/ Number of stories composing the substructure.
n	Number of stories below the lost column.
c_g	Number of columns at the left of the lost column (per story).
c_d	Number of columns at the right of the lost column (per story).
L_0	Length of the beams.
H_0	Height of the columns.
E	Young modulus of the steel.
f_y	Yielding stress of the steel grade.
Properties specific to the DAP	
$beam_i$	Beams' type of the i^{th} $(i = 1, 2, ..., N)$ story of the DAP. For example 'HE 100 b'.
Properties specific to the IAP	
file.mat	*Matlab* file extracted from the BeamZ linear analysis of the IAP.
$Bracing_g$	If the user wants the code to automatically fix the horizontal DOF of the nodes of the left column of the structure. If yes $bracing_g = 1$, if no $bracing_g = 0$.
$Bracing_d$	If the user wants the code to automatically fix the horizontal DOF of the nodes of the right column of the structure. If yes $bracing_d = 1$, if no $bracing_d = 0$.
$Embedded$	If the user wants the code to automatically have embedded bottom columns. If yes $Embedded = 1$, if no $Embedded = 0$.
H_{fixed}	Vector manually provided by the user. It itemizes the nodes for which the horizontal DOF is fixed. The numbering is relative to the modeling of the IAP in *BeamZ*.
V_{fixed}	Vector manually provided by the user. It itemizes the nodes for which the vertical DOF is fixed. The numbering is relative to the modeling of the IAP in *BeamZ*.
R_{fixed}	Vector manually provided by the user. It itemizes the nodes for which the rotational DOF is fixed. The numbering is relative to the modeling of the IAP in *BeamZ*.
$node_{order}$	Vector provided by the user. It gives the numbering of the nodes in the order illustrated in figure 4.3.
Properties specific to the column's removal	
u_{max}	Maximum vertical displacement necessary to reach for the drawing of the $u - N_{lost}$ curve.

Table 4.1 – Inputs of the *Matlab* code.

The second way (manual way) is set down by:

$$Embedded = 0 \text{ and } H_{fixed} = V_{fixed} = R_{fixed} = [1\ 6\ 8\ 13\ 18]\,.$$

Note that the enumerating of the nodes in H_{fixed}, V_{fixed} and R_{fixed} is relative to the *BeamZ* enumerating. Then, let's assume that this structure has been implemented in *BeamZ* using the node order illustrated in figure 4.4. In this case, $node_{order}$ is given by:

$$node_{order} = [1\ 2\ 3\ 4\ 5\ 6\ 7\ 8\ 9\ 10\ 11\ 12\ 13\ 14\ 15\ 16\ 17\ 18\ 19\ 20\ 21\ 22]\,.$$

And in the case of the manual imposition of the fixed nodes, the boundary conditions are set down by:

$$Embedded = 0 \text{ and } H_{fixed} = V_{fixed} = R_{fixed} = [1\ 2\ 3\ 4\ 5]\,.$$

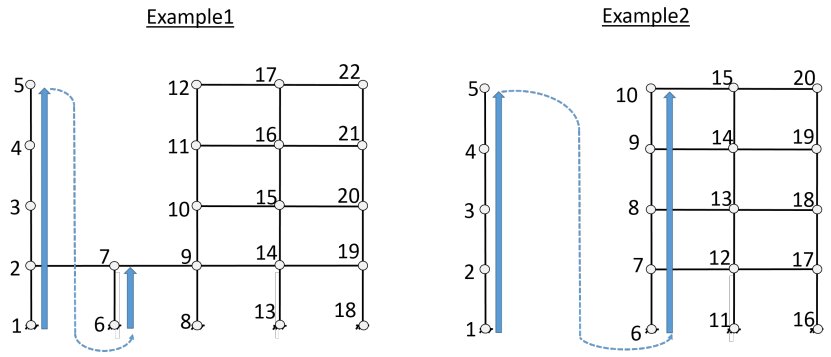

Figure 4.3 – Illustration of the numbering of the IAP used in the *Matlab* implementation.

Let's assume this structure is braced on its left, meaning that the horizontal DOF of nodes 1, 6, 11, 15 and 19 are fixed. The manual way to set these boundary conditions is given by:

$$Bracing_g = 0\,,\ V_{fixed} = R_{fixed} = 0\ textand\ H_{fixed} = [1\ 6\ 11\ 15\ 19]\,.$$

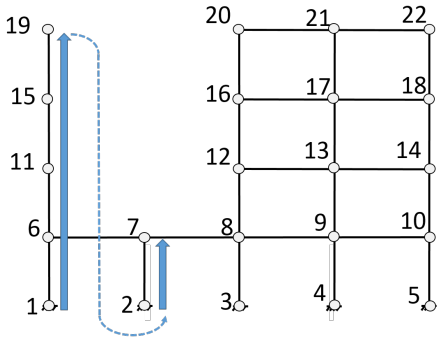

Figure 4.4 – Illustration of the *BeamZ* numbering of the IAP.

Lets focus now on the characterization of the IAP. The terms characterizing the fixed DOF in the stiffness matrix are first changed according to the vectors H_{fixed}, V_{fixed} and R_{fixed}. Note that the term to add to the fixed node is given by: $1000 \times max(diag(K_{IAP}))$ so that it is neither too small nor too big. Then, the stiffness matrix is rearranged, followed by the addition of the term $1000 \times max(diag(K_{IAP}))$ to the corresponding terms if $Embedded = 1$ and/or $Bracing = 1$ and/or $Bracing_d = 1$. Finally, the unitary force method applied to the stiffness matrix K_{IAP} in which all the characteristics of the IAP have been implemented. There is not anymore different ways to determined S_g (S_d) in function of c_g (c_d) and n.

Then, the characterization of the DAP and the system to solve are exactly the same as in the initial implementation of the analytical model. More details are given in section 2.2.

4.5 Verification of the new implementation

This section focuses on the verification of the new implementation. To do so, the new implementation was first tested for a case which should lead to the same results as the ones obtained with the initial implementation. So, first of all, the situation has to be applicable to the new and the initial implementation. This is the case for structure Ia for example.

Furthermore, in a situation such as scenario 1 of structure Ia, for which the structure loses one bottom column, the initial and the new implementations both theoretically should lead to the same flexibility matrices S_g and S_d (see section 2.2 for some refreshing of the initial implementation). It is therefore this situation that is under study in this section.

Therefore, to verify the implementation, the two implementations are compared through the $u - N_{lost}$ curve relative to the scenario 1 of structure Ia. Furthermore, as the aim is to compare the two curves, they are shown from the beginning of phase 2 until after the end of phase 3, even though the analytical model aims to represent phase 3 only. Moreover, both curves will be compared to a reference curve obtained with the modeling of the same situation in *Finelg*. The latter curve is chosen to show only phases 2 and 3 of the structure's response. For more details on these curves, see section 4.6.

Figure 4.5 illustrates the results of scenario 1 of structure Ia obtained with the new implementation, the initial implementation and *Finelg*. It reveals that the initial and the new implementation do not lead to identical $u - N_{lost}$ curves, which means that there should be a mistake somewhere. Moreover, looking at the graphical interpretation of the results, the initial implementation is more accurate than the new implementation, which is even more puzzling. In the following, the methodology followed to verify the code is detailed.

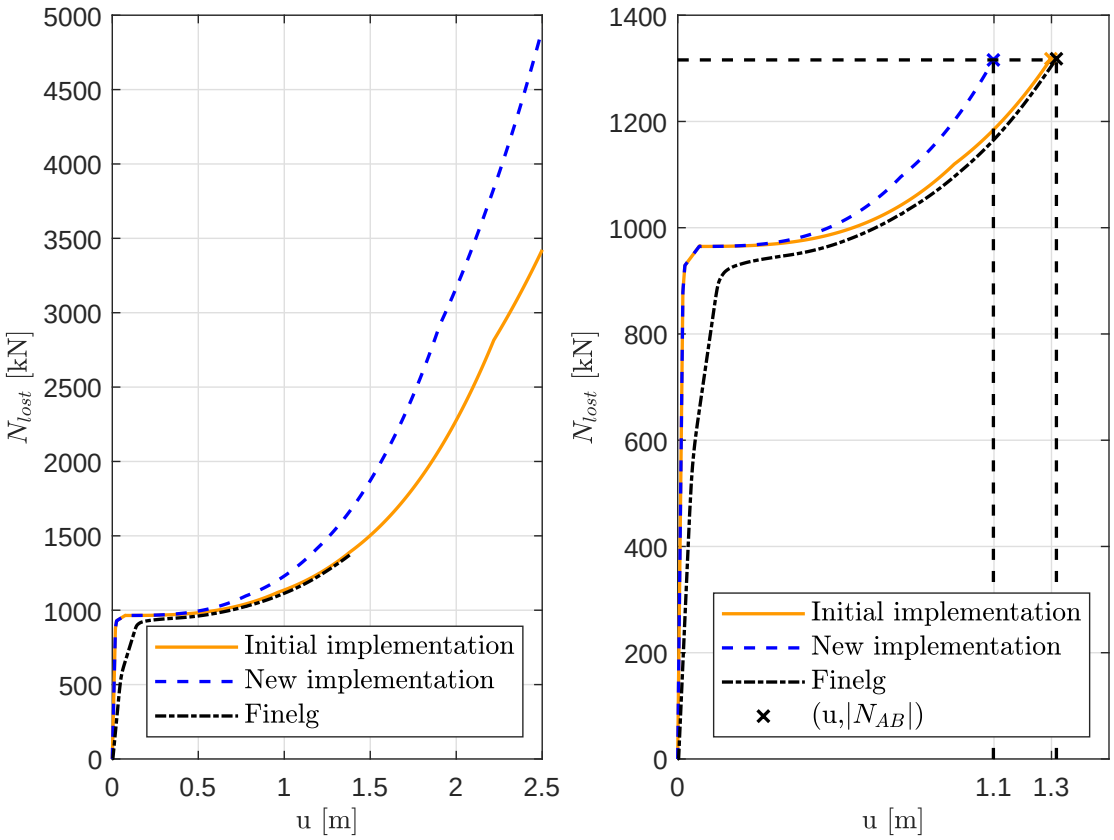

Figure 4.5 – Evolution of the internal vertical force carried by the structure at the top of the lost column, so called, N_{lost} in terms of u, the vertical displacement above the lost column. Comparison between the initial implementation, the improved implementation and the *Finelg* modeling of the scenario 1 of structure Ia.

First, I made sure that the new way to determine S_g and S_d was the cause of the differences between the curves and not due to something I would have changed outside the characterization of the IAP. To do so, in the new model implemented, just after the determination of S_g and S_d, I added two lines to command both S_g and S_d to be equal to their respective flexibility matrix obtained with the initial implementation of the analytical model. By doing so, both curves are identical. Therefore, the part of the code to be checked is indeed the characterization of the IAP.

The curve obtained with the new model is further from the curve obtained with *Finelg*, in comparison with the curve obtained with the initial model. Therefore, a lot of time has been consecrate to verify that the IAP was correctly implemented in *BeamZ* and to verify line by line the new implementation's code. Without any mistake found, it has been decided to verify the new implementation in a more "objective" kind of way. As the problem was coming from the flexibility matrices, I started to verify the step just before: the transition between the stiffness extrapolated in *BeamZ* and the flexibility matrices obtained which is characterized by the implementation of the unitary force theorem. Each term determined with the new implementation has been compared to the horizontal displacements obtained by applying a force of $1kN$ in the *BeamZ* modeling of the IAP. Such that the unitary force theorem was applied in *BeamZ* and compared to the one implemented in the new implementation of the model. Both ways led to the same flexibility matrices and therefore the manipulations made with the stiffness matrix of the IAP and the unitary force method were well implemented. Afterwards, I looked at the step just before that: the modeling of the IAP in *BeamZ*. To do so, the same IAP has been modeled in *OSSA2D*, a 2D linear elastic finite element program. Then, to compare the two modelings, one would think to compare the stiffness matrices. However, *OSSA2D* does not allow the extraction of the stiffness matrix. Hence, instead, the horizontal displacements obtained for a force of 1kN applied on the *OSSA2D* modeling (applicaton of the unitary force theorem to the structure modeled in *OSSA2D*) were compared to the two flexibility matrices obtained with the new model. Those were close and therefore the modeling in *BeamZ* was correct.

All these checks led to the conclusion that the new implementation was correct. So a closer look has been given to the initial implementation of the analytical method. Indeed, until this time, the initial implementation was assumed to be correctly carried out. Finally, a mistake was found in the implementation of Hai's method. More particularly, the case of the loss of a bottom column ($n = 0$) was carried out in the initial implementation as if there were at least two stories below the lost column in addition to the ground floor, so as if $n \geq 2$ (see figure 2.16). This mistake induced the IAPR and IAPL to be more flexible than what they were in reality. The behavior of the $u - N_{lost}$ curve was as well more flexible than it should be, spuriously bringing it closer to the *Finelg* results and improving artificially the results of the initial implementation.

After correcting this mistake, both the initial and the new implementations led to identical results, as illustrated in figure 4.6. In the next section, these curves are compared to the reference curve obtained with *Finelg*.

4.6 Validation and limitations of the analytical model

In this section, the *Finelg* curve showed in Figure 4.6 is first detailed. The results obtained with the analytical method are then analyzed with a particular attention on the validity of the analytical model explained in chapter 2.

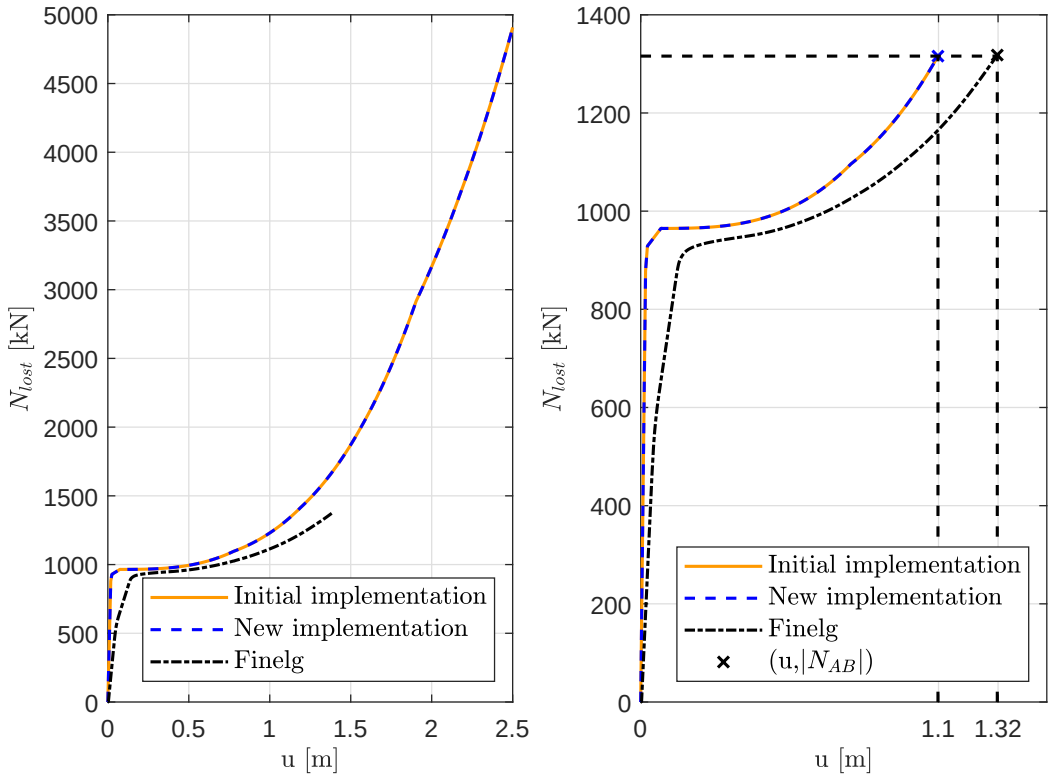

Figure 4.6 – Evolution of the internal vertical force carried by the structure at the top of the lost column, so called, N_{lost} in terms of u, the vertical displacement above the lost column. Comparison between the **corrected** initial implementation, the improved implementation and the *Finelg* modeling of the scenario 1 of structure Ia.

4.6.1 Analysis of *Finelg* results

The $u - N_{lost}$ curve obtained with *Finelg* is shown from the beginning of phase 2, when the column starts to be removed until the end of phase 3, when the column has been totally removed. Furthermore, the curve is outputted with an elastic-perfectly plastic material's law for the beams and columns of the DAP, and a fully elastic law for the elements of the IAP, in order to compare the curves of 2 identical situations. Indeed, to recall, the analytical model is based on a structure with an IAP assumed fully elastic.

The *Finelg* curve is in accordance with the theoretical explanations given in section 1.3. Indeed, at the beginning of the second phase, the behavior of the curve is stiff by comparison with the behavior of the rest of the curve. Then, when a first set of plastic hinges forms, a first kink appears on the cruve and soften the curve's behavior. Then, each change of slope represents the formation of one, or more, plastic hinges. Finally, when N_{lost} equals more or less $930\,kN$, the structure rigidity drastically decreases, which marks the end of phase 2 with the fully formed complete plastic mechanism of the DAP. As a consequence, the DAP lost all its first order rigidity. It leads to large displacements (see the plateau on figure 4.6). Then, as large displacements appear, the membrane forces develop thanks to the anchorage supplied to the DAP by the IAP. This second order rigidity of the DAP brought by the IAP is highlighted by the increase of the slope of the $u - N_{lost}$ curve. Finally, when N_{lost} reaches $|N_{AB,design}|$, the column has collapsed (is completely removed). At this point, if nor resistance failure nor

ductility failure nor instability failure has occured, the structure is said to be robust enough to keep its structural integrity faced to this exceptional event. However, the hypothesis of an IAP totally elastic during phase 3 is not realistic, as shown in Dewez's thesis [8]. Indeed, Dewez showed that a panel plastic mechanism will form in the IAP and will speed up the structure collapse and the structure will fail before the complete removal of the column. Therefore, no conclusion can be drawn regarding the structural integrity of the structure Ia further to scenario 1.

4.6.2 Analysis of phase 2 obtained with the analytical model

Now, a closer look is given to the curves obtained with the analytical model. The aim of the model is to reproduce phase 3 only. However, in order to comment the entire curve, figure 4.6 illustrates the curve from the beginning of phase 2 up to after the end of phase 3.

During phase 2, the analytical model reproduces a stiffer structural behavior than the one obtained with *Finelg*. This is a consequence of the hypotheses forming the basis of the analytical model[1]. Indeed, the flexural deformation of each beam is only taken into account in the yielded zones of the beam assumed to have a fixed length. The rest of the beam is assumed to have an infinite flexural rigidity. As phase 2 is governed by the flexural deformation of the beams, this hypothesis has a big impact on the flexural deformations reprodued by the model during phase 2. Besides, the progressive decrease of stiffness of the DAP is not taken into account in the model as it is based on the assumption that all the plastic hinges of the complete plastic mechanism of the DAP form at the same time. In conclusion, given those reasons, it is only logical that phase 2 is not well represented by the model. To take it into account, the analytical model should be combined with the analytical model reproducing phase 2, for more information see Hai's PhD thesis [4].

Then, the analytical model estimates the complete plastic mechanism to form more or less at $N_{lost} = 965\,kN$, as seen in figure 4.6. The analytical model evaluates the formation of the complete plastic mechanism to be $35\,kN$ above the N_{lost} for which the plastic mechanism is forming with *Finelg*. This is questioning because the moment when the plastic mechanism should be well determined using a rigid perfectly plastic analysis. Here we talk of a rigid plastic analysis as the axial elongation of the beams does not influence phase 2. In the following, the issue concerning incorrect determination of the plastic mechanism onset by the analytical model is addressed.

4.6.3 Plastic mechanism onset discussion

To answer this questioning, the rigid plastic analyzes supposedly implemented in the model is first verified. The complete plastic mechanism relative to scenario 1 of structure Ia is shown on figure 4.7. The internal and external work, respectively W_I and W_E, of this latter are given by:

$$\begin{cases} W_I = 4\,\theta\,N\,M_{pl} \\ W_E = N_{lost}\,u = N_{lost}\,\theta\,L_0 \end{cases} \tag{4.1}$$

where $N = 4$ (as the DAP is formed of 4 stories), $M_{pl} = w_{pl\,IPE360}\,f_y = 1019 \times 10^3\,mm^3 \times 355\,N/mm^2 = 361.745\,kNm$, $N_{lost} = \lambda_d\,N_{AB\,design}$, θ is the rotation angle of the beams when a vertical displacement u is imposed (see figure 4.7) and $L_0 = 6\,m$. Besides, the angle θ is assumed to be small enough for $\tan\theta$ to be equal to θ.

[1] Note that the analytical model under study in this master thesis aims to reproduce the phase 3 only. but in its implementation, it determines phase 2 as well but not very accurately.

The value of N_{lost} for which the plastic mechanism will form is then determined by equalizing the internal and external works and is given by:

$$N_{lost} = \lambda_d \, N_{AB\,design} = \frac{4\,N\,M_{pl}}{L} = \frac{4 \times 4\,361.745}{6} = 964\,kN\,. \tag{4.2}$$

The analytical value obtained for N_{lost} coincides with the graphical value observed. So, it is indeed this plastic mechanism that is implemented in the equations of the analytical model.

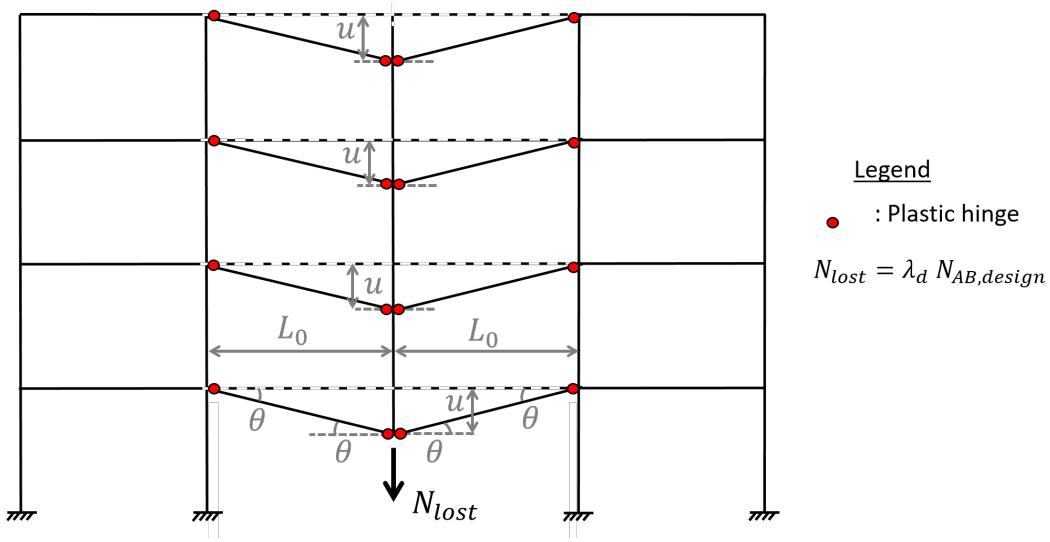

Figure 4.7 – Complete plastic mechanism of the DAP relative to the scenario 1 of structure Ia assumed to form in the analytical model.

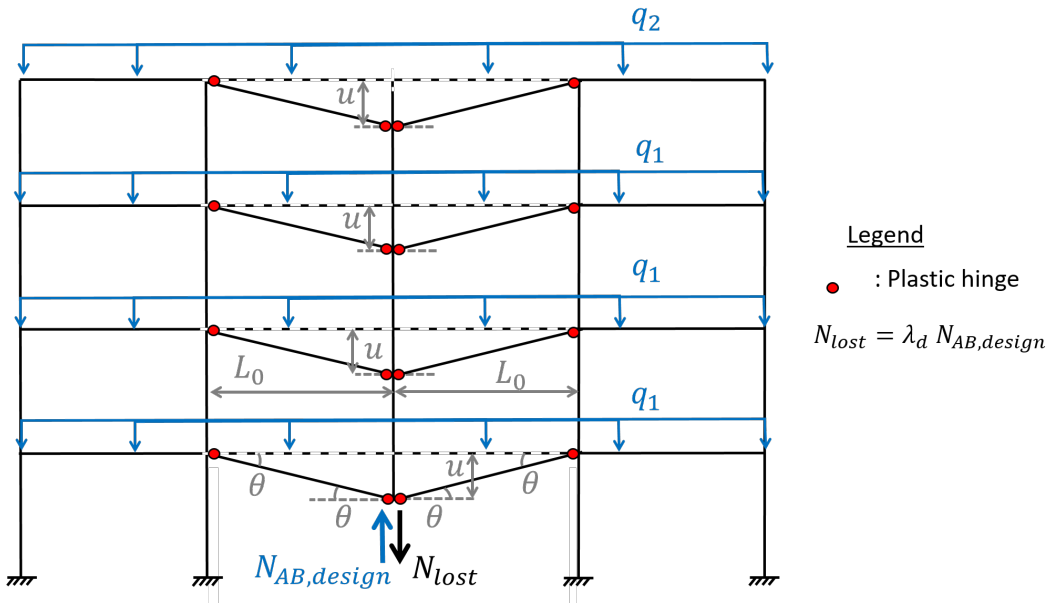

Figure 4.8 – Complete plastic mechanism of the DAP relative to the scenario 1 of structure Ia to analyze when the initial loading of structure is not neglected.

Let's now focus on what is not taken into account in the model that could explain the wrong determination of the DAP plastic mechanism onset. The analytical model does not take into

account the initial loading (accidental combination of gravity loads), which is however taken into account in the simulation in *Finelg*. Let's see how these terms influence the rigid plastic analysis of the DAP. The adjusted plastic mechanism to analyze is illustrated in figure 4.8. The internal work is identical the the one determined earlier. The updated external work is given by :

$$W_E = N_{lost}\,\theta\,L_0 + (3\,q_1 + 1\,q_2)\;L_0\,\theta\,L_0 - N_{AB\,design} \tag{4.3}$$

where $q_1 = 55.5 + 0.56 = 56.06\,kNm$ is the self load and the accidental combination of loads applied to the 3 bottom stories of the DAP, $q_2 = 49.5 + 0.56 = 50.06\,kNm$ is the load applied to the last story of the DAP. The updated N_{lost} characterizing the formation of the DAP plastic mechanism is then given by:

$$\begin{aligned} N_{lost} = \;& \lambda_d\,N_{AB\,design} = \frac{4\,N\,M_{pl} - (3\,q_1 + 1\,q_2)\;L_0^2}{L} + N_{AB\,design} \\ = \;& \frac{4 \times 4 \times 361.745 + (3 \times 56.06 + 1 \times 50.06) \times 6^2}{6} + 1302.5 \\ = \;& 957\,kN\,. \end{aligned} \tag{4.4}$$

This raised assumption lower the value of N_{lost} characterizing the plastic mechanism onset of only $7\,kN$. This difference may be neglected and therefore, the choice to neglect the initial loading in the determination of the value of N_{lost} characterizing the DAP plastic mechanism onset was a valid choice. However, there is still about $30\,kN$ difference between the analytical and the *Finelg* identification of the DAP plastic mechanism onset.

The next step consists of the verification that the plastic mechanism at the base of the model is the plastic mechanism that forms in *Finelg*. To do so, a closer look to the model in *Finelg* is taken in order to analyze the position where plastic hinges of the DAP are forming. The position of the plastic hinges with the *Finelg* model are shown in figure 4.9. The resultant plastic mechanism does not correspond to the one assumed in the analytical model. The positions where the plastic hinges form are the consequence of the accidental combination of distributed gravity loads that influence the shape of the moment diagram. Therefore, it may lead the plastic hinges to not form in the extremities of the beams when the distributed loads are leading to large hogging moments. And in fact the plastic hinges form at the distance $L' \approx 0.8\,m$ from one extremity of each beam.

To confirm these explanations, the N_{lost} of the plastic mechanism shown in figure 4.9 is determined. The internal load is exactly the same than the one determined earlier and the updated external load is given by:

$$W_E = N_{lost}\,\theta\,L' + (3\,q_1 + 1\,q_2)\;L'\,\theta\,L' - N_{AB\,design} + (3\,q_1 + 1\,q_2)\;L'\,\theta\,2\,(L_0 - L')\,, \tag{4.5}$$

where $L' = 0.7\,m$ is the distance from the beam extremity at which the plastic hinge forms (see figure 4.9). The N_{lost} characterizing the DAP plastic mechanism onset is therefore given by:

$$\begin{aligned} N_{lost} = \;& \lambda_d\,N_{AB\,design} \\ = \;& \frac{4\,N\,M_{pl} - (3\,q_1 + 1\,q_2)\;\left(L'^2 + 2\,(L_0 - L')\,L'\right)}{L'} + N_{AB\,design} \\ = \;& \frac{4 \times 4 \times 361.745 - (3 \times 56.06 + 50.06) \times (5.3^2 + 1.4 \times 5.3}{5.3} + 1314.5 \\ = \;& 939.86\,kN\,. \end{aligned} \tag{4.6}$$

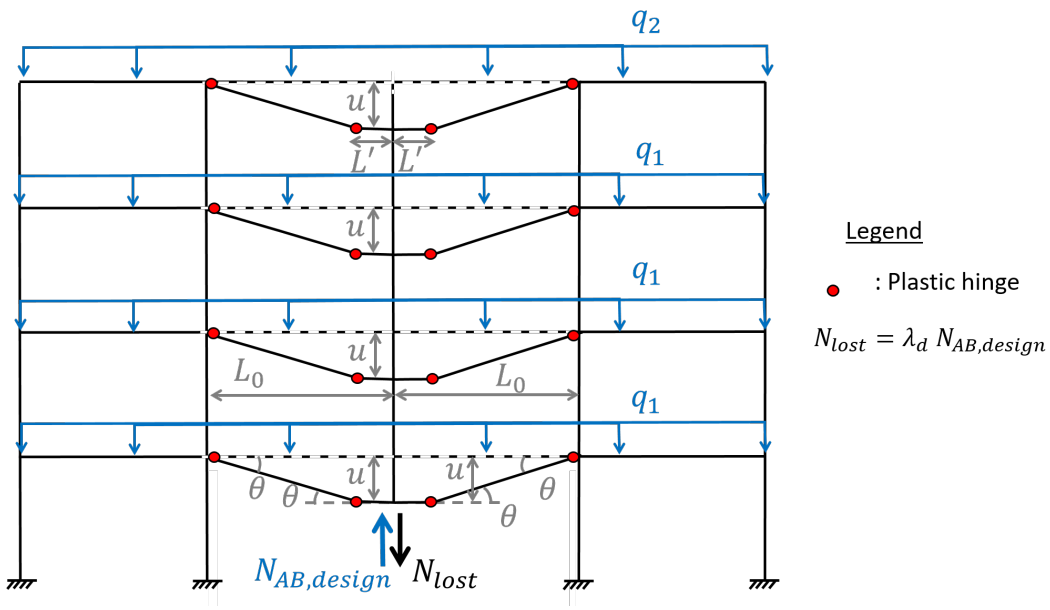

Figure 4.9 – Complete plastic mechanism of the DAP relative to the scenario 1 of structure Ia forming in the simulation with *Finelg*.

The value obtained ($N_{lost} = 939.86\,kN$) is consistent with the graphical value obtained earlier by reading the *Finelg* curve. This confirms that the plastic mechanism that induces the collapse of the DAP is the one shown on figure 4.9 and not the one illustrated in figure 4.7. Indeed, the plastic mechanism forming the first is the one for which N_{lost} is the smallest, which is, in this case the one shown in figure 4.9. The mechanism that is considered in the initial model is thus not the one leading to the smallest values of N_{lost}. The beginning of the phase 3 of the analytical curve is not correctly determined with the model.

Besides, the $u - N_{lost}$ curve obtained in obtained with *Finelg* without the initial loading is shown on figure 4.10 and leads to the same results obtained with the rigid plastic analysis of the plastic mechanism shown in figure 4.7. This confirms once again that it is the distributed loads that induces the plastic mechanism shown on figure 4.9.

To correct the curve and take and obtain the correct starting point of phase 3 in terms of N_{lost}, an additional step should be taken into account to determine which plastic mechanism will be the first to form in the DAP. However, as this issue has been outlined close to the end of this master thesis, in the following, the curve obtained with the analytical model will be shifted manually to make the starting point of phase 3 coincide with the theoretical value of the formation of the plastic mechanism.

4.6.4 Analysis of the corrected phase 3 obtained with the anaytical model

Figure 4.11 illustrates the structure's response of scenario 1 of structure Ia obtained with *Finelg* and the shifted third phase obtained with the analytical model followed by its manual shifting to make it starts at $939.86\,kN$, as it should be. First of all, the analytical model represents well phase 3 until $u = 0.6\,m$. Indeed, the two curves are almost superimpose until that point. However, further to $u = 0.6\,m$, the structural response obtained with the analytical model gains more rigidity that what the structure gain in rigidity in reality. After $u = 0.6\,m$, the analytical curve digresses from the *Finelg* curve. Furthermore, the model is

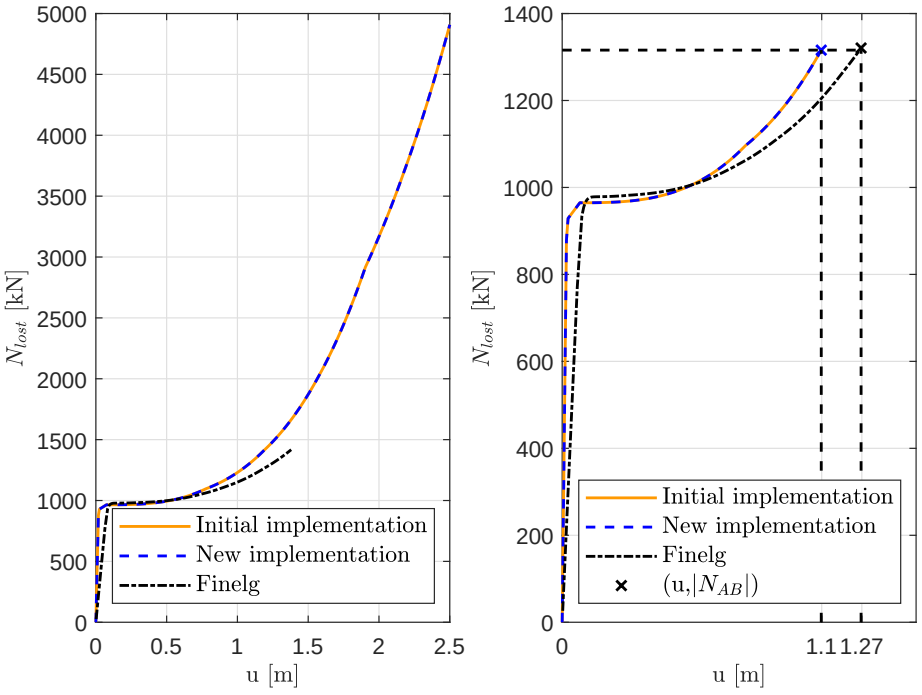

Figure 4.10 – Response of the frame when subjected only to the force simulating the column removal, N_{lost}, without the application of the initial loads.

not on the safe side as for the same force N_{lost} applied, the displacement determined with the analytical method is smaller than the one obtained with the *Finelg* simulation. The end of phase 3 is reached when $N_{lost} = 1314.5\,kN = N_{AB,design}$.

Going further by keeping increasing u in the analytical model results in applying an additional force pulling downwards at the top of the lost column after the latter has collapsed. This only has a numerical meaning. Another remarkable point after phase 3 corresponds to the kink marked with a dot on figure 4.12. This kink corresponds to the moment when the plastic hinges of the first story of the substructure reach its axial plastic resistance. From that point, the plastic hinge will axially extends without any possibility to carry any additional axial force. The first story is therefore more flexible, and by this way, the rest of the structure itself is more flexible, which is seen through the graph on the left of figure 4.12. Then, as the inclination of the axial internal force increases, its vertical projection gets larger. This vertical projection helps to carry some of the load applied, N_{lost} and by equilibrium, a larger force may be applied to the structure. These geometrical effects bring a supplementary axial stiffness to the structure which is seen on figure 4.12 with the increase of the slope.

Now that the analytical is corrected and validated, other structures are studied in the following to validate the new implementation.

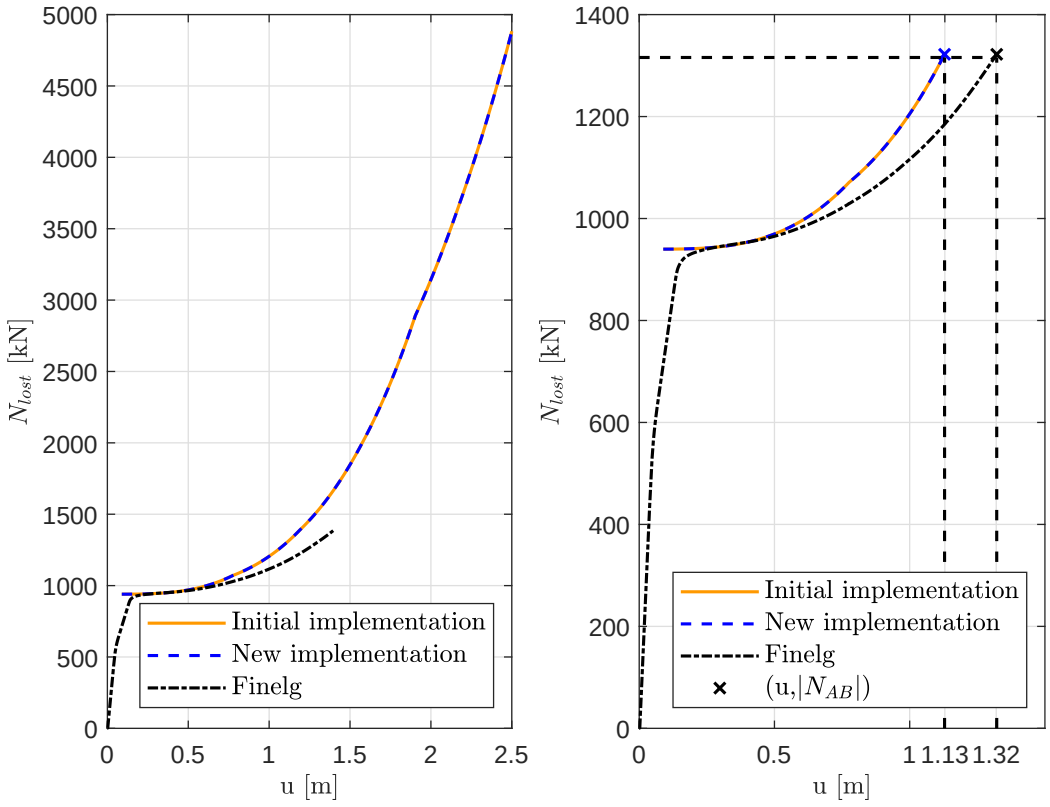

Figure 4.11 – Response of the structure Ia further to scenario 1. Evolution of the internal vertical force carried by the structure at the top of the lost column, so called, N_{lost} in terms of u, the vertical displacement above the lost column.

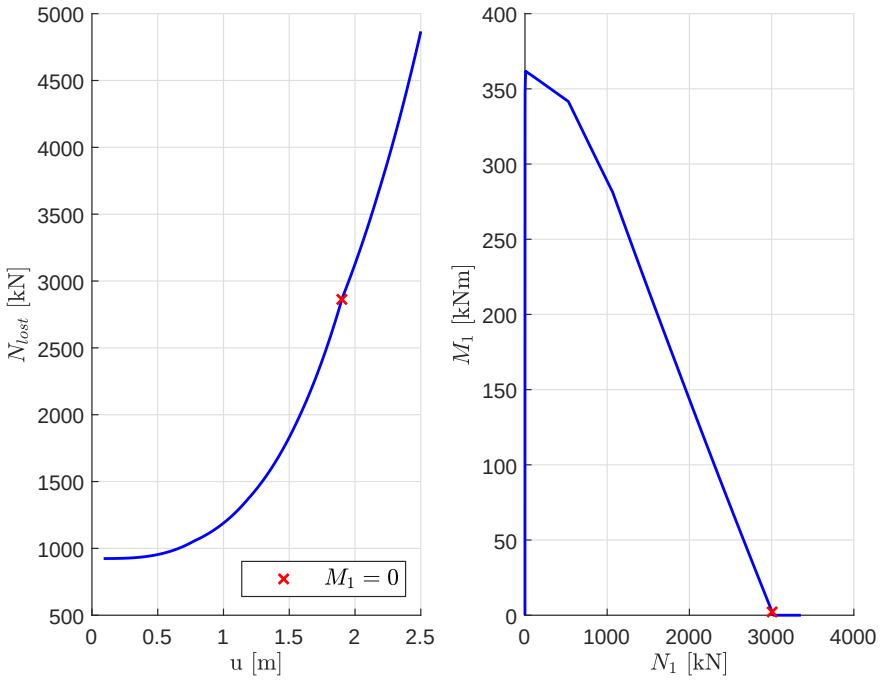

Figure 4.12 – Response of the frame further to the scenario 1. On the left, $M - N$ interaction in the beam's extremity (where the plastic hinge forms) at the first story of the DAP. On the right, evolution of the internal vertical force carried by the structure at the top of the lost column, so called, N_{lost} in terms of u, the vertical displacement above the lost column.

4.7 Validation of the new implementation and additional tests

In the following, the new implementation of the analytical model is validated through comparisons with the initial implementation. Furthermore, in the mean time, the analytcal model is validated through comparisons with *Finelg*. To do so, first, some situations that can be modeled with both the initial and the new implementations will be analyzed. For these situations, the results obtained with the initial implementation, the new implementation and the *Finelg* modeling are compared. Then, some situations that can only be modeled with the new model and for which the design is more realistic are analyzed. For those situations, only the new implementation and the *Finelg* modeling will be compared.

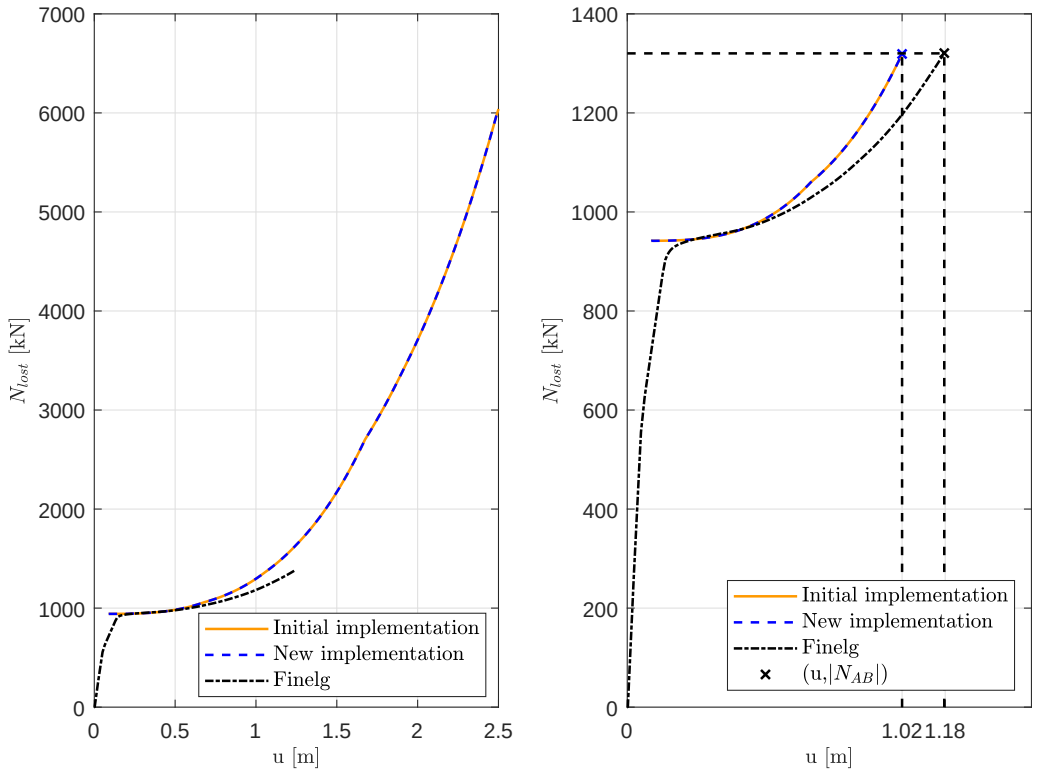

Figure 4.13 – Evolution of the internal vertical force carried by the structure at the top of the lost column, so called, N_{lost} in terms of u, the vertical displacement above the lost column. Comparison between the **corrected** initial implementation, the improved implementation and the *Finelg* modeling of the scenario 1 of structure IIa.

Figures 4.13 and 4.14 illustrate respectively the response of scenario 1 of structure IIa and scenario 2 of structure IIa (see section 3). In all these scenarios, it is one of the bottom columns that is removed. Therefore, as already explained, both the initial and the new implementation should lead to the same response. As it is illustrated for the different cases under study, both implementations lead indeed to identical response. Those results validate the new model.

Concerning the analytical model itself. Now that it has been shifted and that the phase 3 starts at the correct N_{lost} value, the representation of the phase 3 with the analytical model is accurate. Furthermore, the same observations than the ones already made regarding the scenario 1 of structure Ia may be made.

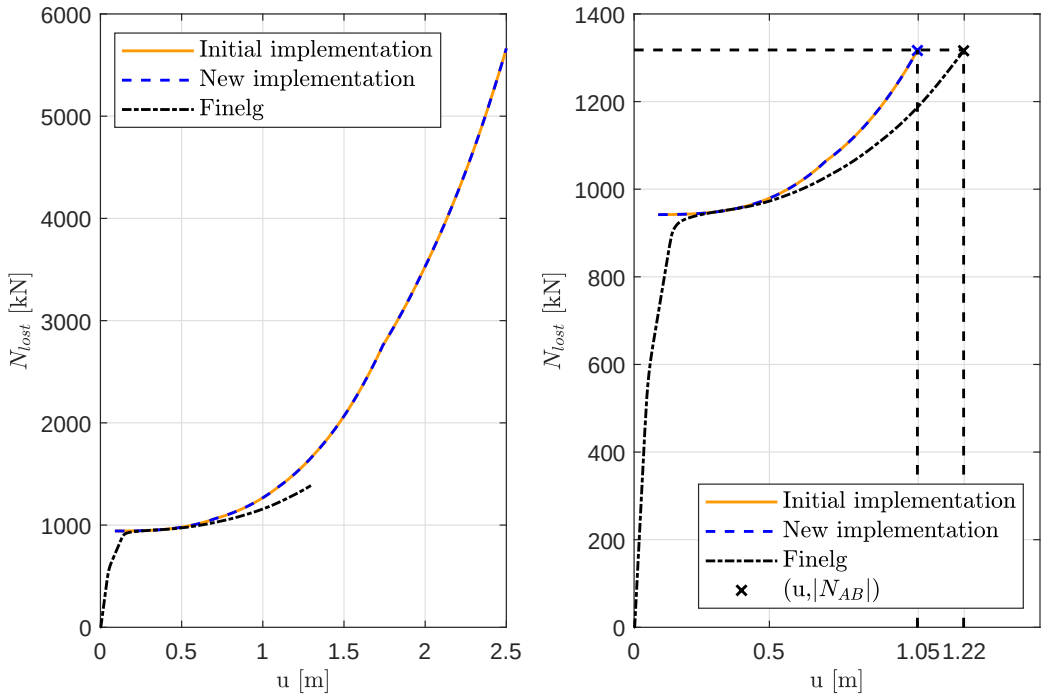

Figure 4.14 – Evolution of the internal vertical force carried by the structure at the top of the lost column, so called, N_{lost} in terms of u, the vertical displacement above the lost column. Comparison between the **corrected** initial implementation, the improved implementation and the *Finelg* modeling of the scenario 2 of structure IIa.

Furthermore, remark that, once the column is totally removed, the scenario 1 leads to larger vertical displacements at the top of the lost column for structure Ia than for the structure IIa, itself leading to larger u than for the structure IIIa. Indeed, in the case of scenario 1, the IAP of the structure Ia is softener than the IAP of structure IIa, itself softener than the IAP of structure IIIa (see section 3. Therefore, the restrain the IAP brings to the DAP is smaller in the case of scenario 1 of structure Ia in comparison to scenario 1 of structure IIa. Which lead to larger displacements in the case of scenario 1 of structure Ia with comparison with scenario 1 of structure IIa.

Now, using the new implementation, the designed 2D structures with different columns are analyzed. Figures 4.15, 4.16, 4.17 and 4.18 are respectively showing the response of the structure Ib further to scenario 1, structure IIb further to scenario 1, structure IIb further to scenario 2 and structure IIIb further to scenario 1. These situations cannot be modeled with the initial implementation of the analytical model, therefore, only the new implementation of the model is compared to the response obtained with *Finelg*. The phase 3 of the analytical curve correctly represents the phase 3 of the curve obtained with *Finelg*. The same observations may be drawn than those previously explained. Furthermore, comparing the end of phase 3 of scenario 1 of structure Ib with scenario 1 of structure Ia, the vertical displacements at the top of the lost column obtained with structure Ib are larger than those obtained with structure Ia. Indeed, structure Ib is composed of columns of the same type of structure Ia but also of columns of a type which is less stiff, for the columns that need less strength. Therefore the IAP relative to scenario 1 of structure Ib is softener than the IAP relative to scenario 1 of structure Ia. Therefore, scenario 1 of structure Ia leads to smaller displacements at the end

of phase 3 than scenario 1 of structure Ib.

In conclusion, both the new and the initial implementation, once shifted, are validated for the studied structures.

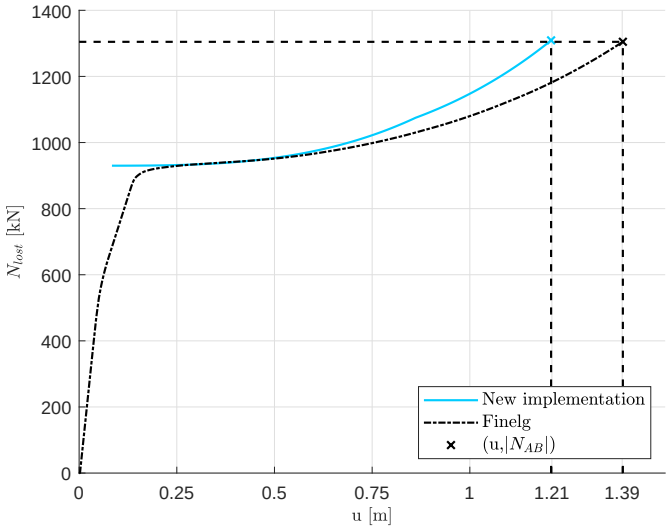

Figure 4.15 – Evolution of the internal vertical force carried by the structure at the top of the lost column, so called, N_{lost} in terms of u, the vertical displacement above the lost column. Comparison between the **corrected** initial implementation, the improved implementation and the *Finelg* modeling of the scenario 1 of structure Ib.

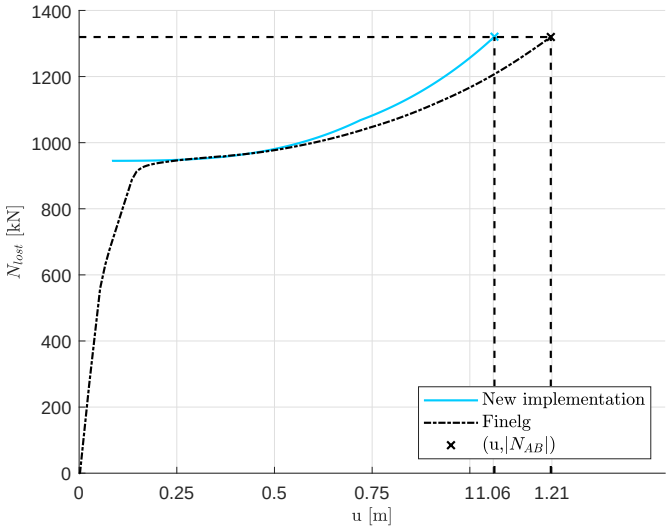

Figure 4.16 – Evolution of the internal vertical force carried by the structure at the top of the lost column, so called, N_{lost} in terms of u, the vertical displacement above the lost column. Comparison between the **corrected** initial implementation, the improved implementation and the *Finelg* modeling of the scenario 1 of structure IIb.

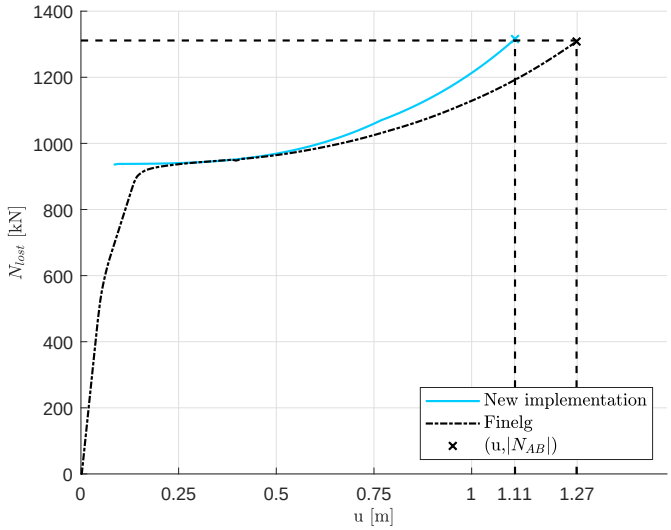

Figure 4.17 – Evolution of the internal vertical force carried by the structure at the top of the lost column, so called, N_{lost} in terms of u, the vertical displacement above the lost column. Comparison between the **corrected** initial implementation, the improved implementation and the *Finelg* modeling of the scenario 2 of structure IIb.

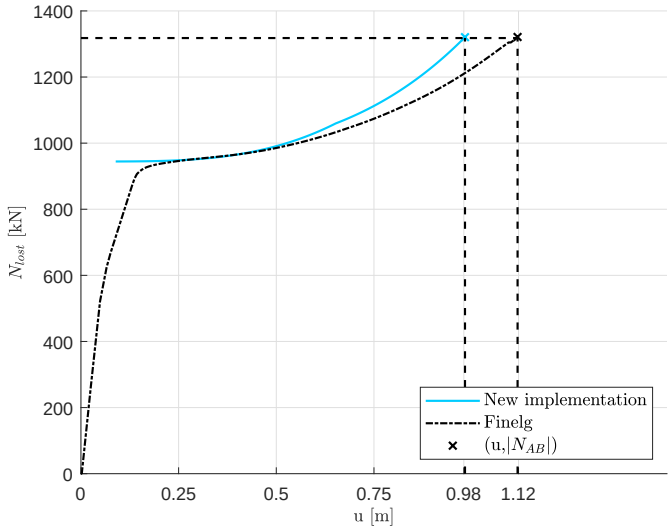

Figure 4.18 – Evolution of the internal vertical force carried by the structure at the top of the lost column, so called, N_{lost} in terms of u, the vertical displacement above the lost column. Comparison between the **corrected** initial implementation, the improved implementation and the *Finelg* modeling of the scenario 1 of structure IIIb.

4.8 Conclusive remarks

Before all, it worth mention the difficulties encountered during this second task. Different programs has been needed to learn, namely *BeamZ* and *Finelg*. Furthermore, the new implementation of the analytical model has been hard to verified as there was a mistake made on the initial implementation, to which the new implementation was compared. Moreover, the assumed plastic mechanism forming in the DAP was not the correct one. This mistake being

found a few days before the submitting deadline, its correction and its ad hoc explanations have been a supplementary work.

Despite, the initial model has been verified and validated through the study of several structures. It would be interesting to conduct a deeper parametrical study to criticize deeper the analytical model and to study its limitations.

Then, although this improvement added a supplementary step before the code execution, which is the modeling of the IAP in *BeamZ*, it allows more liberty on the design of the structure under study as no more restrictions exist on the columns of the whole structure. Indeed, the analytical model is independent of the columns of the DAP. Furthermore, the columns of the IAP modeled in *BeamZ* may be chosen to be different from one an other. Moreover, the columns of different stories may now have different heights. Besides, the supports may now be placed anywhere in the structure. Finally, the new implementation should improve the results in the case of a lost column that is not at the bottom stories of the structure.

Nevertheless, this analytical model does not reproduce correctly phase 2, which is only logical knowing it aims to reproduce phase 3. Furthermore, to reproduce the beginning of phase 3 correctly, the curve obtained with the model is shifted manually, as this mistake has been found shortly before the hand in. One of the possible future enhancements is the fusion of the model which reproduces phase 2 (see Hai's PhD thesis for more information) with the model reproducing phase 3, currently under study. This would lead to the possibility to represent both phases 2 and 3 correctly and would cancel the need to shift the curve as the mechanism under study in phase 2 would be the correct one. This matter is not under investigation in the present thesis but deserves further investigations in a future work.

Furthermore, a parametrical study could be conducted to study the improvement brought by the new implementation in terms of the determination of the flexibility matrices and the reproduction of the response of the stricture, with comparison with the initial model. This issue should be also investigated.

However, the analytical model is still based on the hypothesis that the elements composing the IAP stay in the elastic range. As previously mentioned, Dewez showed in his master thesis [8] that this hypothesis is not realistic in the case of the studied structures. This issue is addressed in the next chapter.

CHAPTER 5

Introduction of the yielding of the IAP in the model

In this chapter, a second improvement of the initial code, presented in chapter 2, is implemented. The motivation and strategy of this implementation are first presented, followed by the presentation of the theoretical, implementation and verification methodologies. Some results are then presented and commented. Finally, conclusive remarks are drawn on the staff contribution and the possible enhancements of the model.

5.1 Motivation and strategy of the improvement

The existing model is based on an IAP that does not yield. By assuming so, the flexibility matrices characterizing the horizontal shift of the extremities of the substructure shown in figure 2.6 are constant and the system of equations to solve in the analytical model is simpler. However, in reality, the IAP will often yield before the column is completely removed. Hence, the purpose of this implementation is to raise the fully elastic behavior assumption made on the elements composing the IAP and to introduce the yielding of the IAP. And therefore, this enrichment aims to improve the accuracy of the model with respect to the behavior of a real structure further to the loss of one column.

The strategy aims to keep the same implementation, determining the response of a structure with an IAP staying in the elastic regime. Then, an additional part is added to the latter code to take into account the yielding of the IAP and determine when a plastic mechanism is formed in the IAP which defines the breakpoint of the frame's response.

The additional part to implement is based on an analytical model developed by Dewez in his master thesis [8]. This latter analytical method is explained in the next section. However, the model developed is based on important assumptions, which are detailed as well in the next section. Furthermore, this analytical method is implemented through a coupling between *Matlab* and *BeamZ*.

5.2 Methodology followed to introduce the IAP yielding

The general philosophy of the methodology is to determine the breakpoint of the $u - N_{lost}$ curve, previously determined with the IAP assumed staying fully elastic, when the first plastic mechanism forms in the IAP. Its is also assumed that no local instabilities nor resistance failure occur in the IAP before the formation of this plastic mechanism. The $u - N_{lost}$ curve is therefore stopped at the u for which the IAP collapses due to the formation of a plastic mechanism. Note that if this plastic mechanism develops after the complete removal of the lost column, the curve $u - N_{lost}$ of a structure with an IAP that may yield is identical to

the curve of the same structure with the IAP assumed perfectly elastic. However, this case appears to be very unlikely.

Let's assume that the removed column is one of the bottom internal columns of a structure, such as the one shown in figure 5.1. The general appearance of the IAP of this structure is illustrated in figure 5.2. In this latter figure, the reaction forces of the DAP on the IAP during phase 3 are as well illustrated. These reaction forces come from the internal forces shown in figure 2.10.

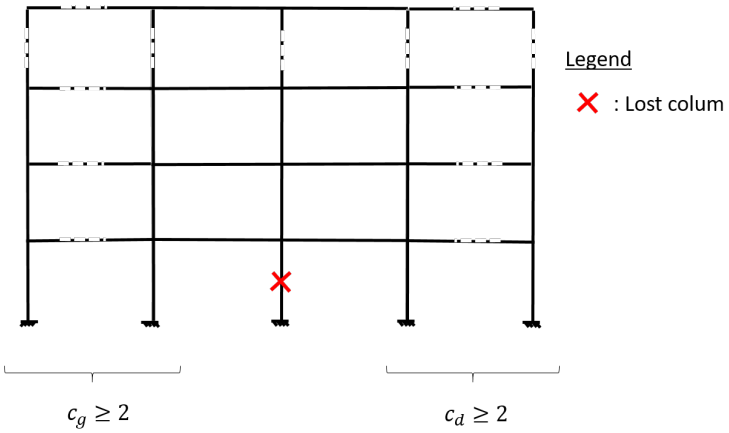

Figure 5.1 – Illustration of the positions of the lost column that are part of the field of application of the methodology applied.

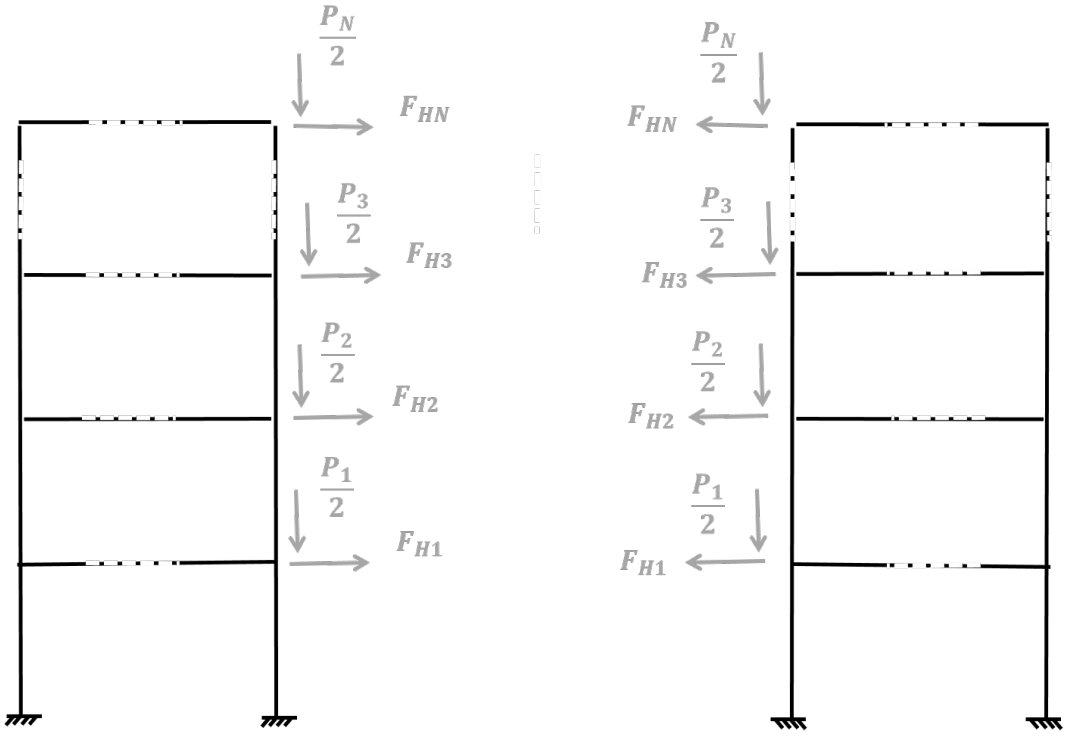

Figure 5.2 – Illustration of the IAP and the DAP reaction forces applied to the IAP during phase 3; where $F_{H\,i}$ and $\frac{P_i}{2}$ are respectively the horizontal and vertical reaction forces of the story i of the DAP on the story i of the IAP.

Through a parametric study with *Finelg*, Jerome Dewez showed in his master thesis [8] that the IAP collapses after the formation of the panel plastic mechanism illustrated on the left of figure 5.3 for the left part of the IAP. This observation is true even for frames composed of more than 5 spans. Moreover, this panel plastic mechanism is composed of $2\,c_g$ plastic hinges formed at the extremities of the bottom columns. Additionally, as illustrated on the left of figure 5.3, the top stories do not contribute to the panel plastic mechanism. Hence, the study of the panel plastic mechanism at the left of figure 5.3 is equivalent to the analysis of the one shown at the right of figure 5.3. In the latter substructure, H and V are the sum of respectively the horizontal and vertical reaction forces of the DAP on the IAP. The model determines the load factor related to the formation of the first panel plastic mechanism of the IAP, λ, for each step u. To do so, the substructure shown in figure 5.4 is studied through a non-linear rigid plastic analysis. In this figure, only the phenomenon which are playing a role in the formation of the panel plastic mechanism are illustrated. Namely, the reaction forces of the DAP on the IAP, λH and λV, and the displacement at the first story of the substructure illustrated in figures 2.6 and 2.9 in chapter 2, $\Delta_{H\,1}$. Note that the analysis is non linear as the displacement of the first story is taken into account in the analysis. Furthermore, a rigid plastic analysis is used as it is wished to determine the moment when the plastic mechanism is formed and as the elastic displacements are not wished to be determined. In figure 5.4, λ is determined through the application of the principle of virtual work to the substructure. The equality between the external and the internal works of the structure leads to the determination of λ, given by:

$$\lambda = \frac{\sum_{j=1}^{n_{hinge}} M_{N\,pl,j}}{H_0\ (H\ \cos\beta + V\ \sin\beta)} \tag{5.1}$$

where:

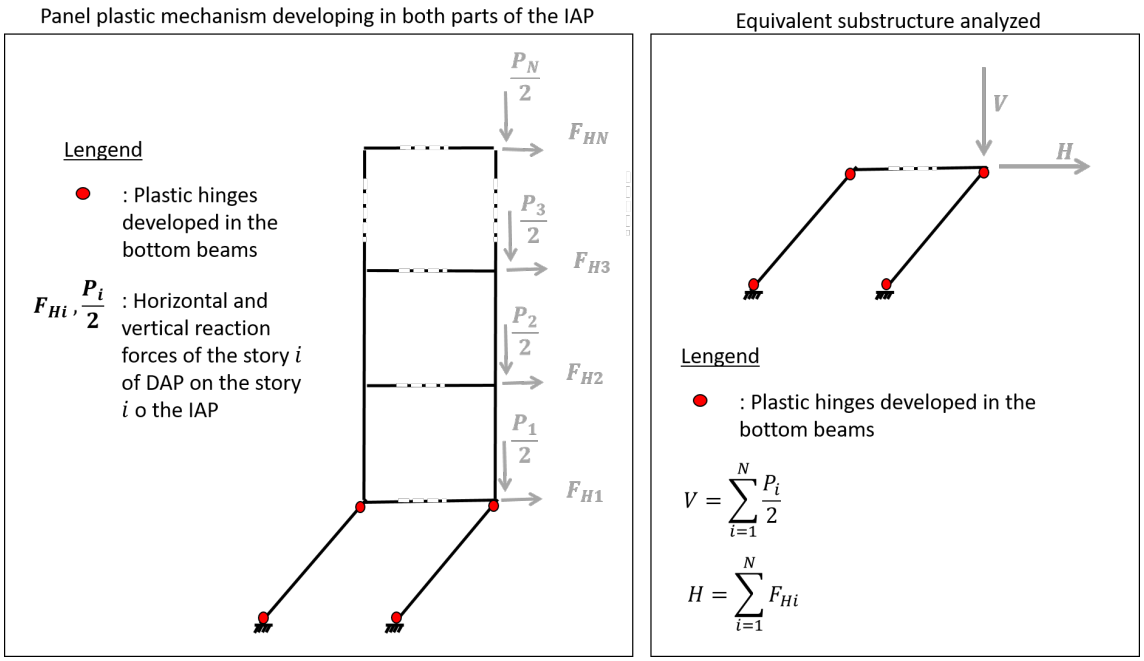

Figure 5.3 – Panel plastic mechanism. On the left, the real one. On the right, the equivalent one.

- n_{hinge} is the number of hinges composing the panel plastic mechanism. $n_{hinge} = 2\,c_g$ if it is the panel plastic mechanism at the left of the lost column that is under study or $n_{hinge} = 2\,c_d$ if it is the one at the right of the lost column,

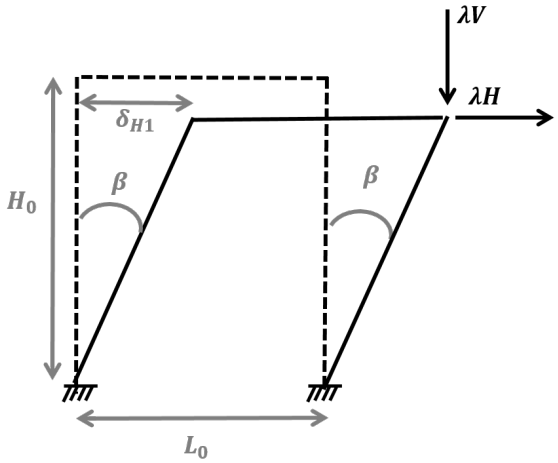

Figure 5.4 – Analyzed substructure for the determination of the load factor relative to the panel plastic mechanism.

- H_0 is the height of the bottom columns,
- $H = \sum_{i=1}^{N} F_{H\,i}$ with N being the number of stories of the substructure (see chapter 2 for more detail on this substructure),
- $V = \sum_{i=1}^{N} \dfrac{P_i}{2}$ with N being the number of stories of the substructure (see chapter 2),
- β is the rotation angle of the bottom columns caused by the horizontal shift of the IAP on the DAP at the first story of the substructure (see chapter 2 for more details on this substructure),
- $M_{N\,pl,j}$ is the reduced resistant plastic moment relative to the cross section where the i^{th} plastic hinge forms, determined by Villette in his PhD thesis [16] and is given in equations (5.2), (5.3) and (5.4).

$$M_{N\,pl,j} = \begin{cases} M_{N\,pl,1,j} \quad \text{if } 0 \leq \dfrac{N_j}{N_{pl\,j}} \leq \dfrac{A_{w\,1\,j}}{A_j} \\ \\ M_{N\,pl,2,j} \quad \text{if } \dfrac{A_{w\,1\,j}}{A_j} \leq \dfrac{N_j}{N_{pl\,j}} \leq 1 \end{cases} \tag{5.2}$$

$$M_{N,pl,1,j} = M_{pl\,j} \left(1 - \left(\frac{N_j}{N_{pl\,j}} \right)^2 \frac{1}{2\,\dfrac{h_j - t_{f\,j}}{h_j - 2\,t_{f\,j}} \left(1 - \dfrac{A_{w\,1\,j}}{A_j} \right) \dfrac{A_{w\,1\,j}}{A_j} + \left(\dfrac{A_{w\,1\,j}}{A_j} \right)^2} \right) \tag{5.3}$$

$$M_{N,pl,2,j} = b_j\,t_{f\,j}\,(h_j - t_{f\,j})\,f_y - 0.5\,(N_j - A_{w\,2\,j}\,f_y) \left(h_j - 2\,t_{f\,j} + \frac{N_j - A_{w\,2\,j}\,f_y}{2\,b_j\,f_y} \right) \tag{5.4}$$

Where:

- The subscript j stands for the properties of the j^{th} plastic hinge,

- $N_{pl\,j}$ is the normal plastic strength of the cross section in which the plastic hinge j forms,
- N_j is the internal axial force at the cross section in which the plastic hinge j forms,
- $A_{w\,1\,j}$ is the area of the web without taking into the fillet of the cross section in which the plastic hinge j forms,
- $A_{w\,2\,j}$ is the area of the web with the fillets of the cross section where the plastic hinge j forms,
- A_j is the area of the cross section in which the plastic hinge j forms,
- $M_{pl\,j}$ is the resistant plastic moment of the cross section in which the plastic hinge j forms,
- h_j is the height of the cross section in which the plastic hinge j forms,
- $t_{f\,j}$ is the flanges' thickness of the cross section in which the plastic hinge j forms,
- b_j is the length of the flanges of the cross section in which the plastic hinge j forms,
- f_y is the yielding strength of the column.

Furthermore, the loads that were carried by the lost column are assumed to be completely and equally redistributed to the two columns next to the lost column (i.e. the column at the right of the lost column and the one at the left of the lost column). Therefore, the internal axial force, N_j, is constant for all plastic hinges but those developing in the two adjacent columns of the lost column. For these two, the internal axial force is given by sum of the initial internal axial force to which $\frac{N_{lost}}{2}$ is added up[1]. Moreover, the variables depending on the vertical displacement at the top of the lost column, u, are β, H, V and N_j if the latter corresponds to a hinge forming in a column beside the lost column.

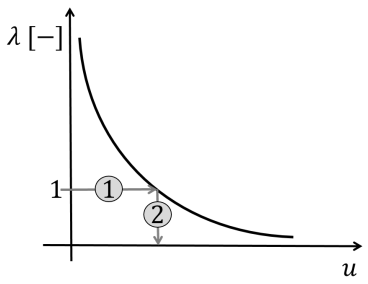

Figure 5.5 – Illustration of the global shape of the load factor of the panel plastic mechanism chosen in figure 5.4 in function of the vertical displacement at the top of the lost column, u.

Once λ, the load factor of the panel plastic mechanism, is determined for each u, the $u-\lambda$ curve may be plotted. Figure 5.5 illustrates the global shape of this curve. On the one hand λ tends to infinity when u tends to zero. Indeed, if the u is close to zero, then β is close to zero as well as H; hence, λ tends to an infinite value. On the other hand, λ tends to zero when u tends to infinity. Indeed, if u is very large, then β is very large as well as H due to the membrane force, therefore, λ tends to zero.

[1]Note that the gravity loads influence the panel plastic mechanism only in the determination of the reduced resistant moment.

Then, the next step consists in finding the u for which λ is equal to 1 on this curve (see figure 5.5). This u is the one for which the panel plastic mechanism forms. Note that if the IAP is not symmetric, the right and left panel plastic mechanism will not follow the same $u - \lambda$ curve. In this case, both curves are determined and the one for which $u = f(\lambda = 1)$ is the smallest characterizes the panel plastic mechanism that form first in the IAP. Then, the $u - N_{lost}$ curve determined with the IAP assumed to be perfectly elastic is cut at that u. At this point, the first panel plastic mechanism appears and the IAP is assumed to collapse right away.

5.3 Organization of the implementation

The global organization of the implementation is illustrated in figure 5.6. Two new parts are added to the implementation of the analytical model, compared to the one presented in the last chapter. First, an additional model has to be implemented in *BeamZ* before running the code. Secondly, an additional part is added in the analytical resolution after the resolution of the system summarized in table 2.3 in chapter 2. In the following, these new parts as well as the new inputs of the code are detailed.

The additional modeling in *BeamZ* aims to obtain the initial internal forces in the cross section of the elements composing the structure; namely the extremities of the columns in which the plastic hinges of the panel plastic mechanism form and the top of the lost column. The implementation of this model contains the nodes, elements (numbering, geometries and steel material) and the accidental combination of gravity loads of the structure. Note that the nodes and elements may be numbered in any order.

Moreover, the inputs of the code are detailed in table 5.1 and the new inputs with respect to the code developed in the last chapter are highlighted in grey. Those new inputs concern the modeling of the structure *BeamZ*, mentioned just before. More precisely, the exported file *file2.mat* will be used to export the initial internal forces. Moreover, $LoadCase$, $elem_g$ and $elem_d$, are used to export these internal forces of the concerned cross sections. The new input c_{lost} is there for the code to determine $N_{AB,design}$, the initial internal axial force at the top of the lost column when the structure is subjected to the accidental combination of actions.

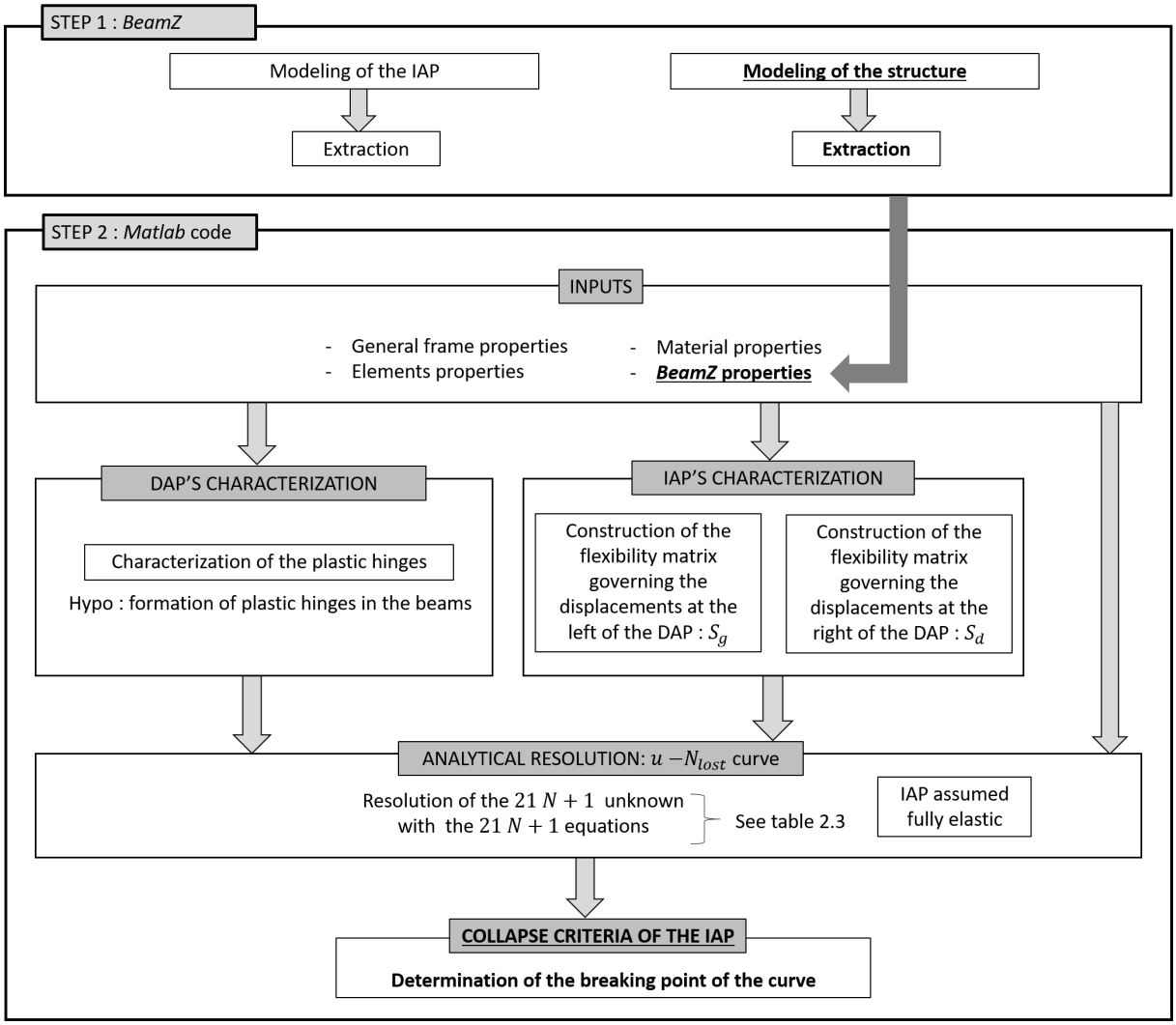

Figure 5.6 – Global organization of the new implementation of the analytical model.

Properties specific to the whole structure	
N	Number of stories above the lost column/ Number of stories composing the DAP/ Number of stories composing the substructure.
n	Number of stories below the lost column.
c_g	Number of columns at the left of the lost column (per story).
c_d	Number of columns at the right of the lost column (per story).
L_0	Length of the beams.
H_0	Height of the columns.
E	Young modulus of the steel.
f_y	Yield stress of the steel grade.
Properties specific to the DAP	
$beam_i$	Beams' type of the i^{th} $(i = 1, 2, ..., N)$ story of the DAP. For example 'HE 100 b'.
Properties specific to the IAP	
file.mat	*Matlab* file extracted from the BeamZ linear analysis of the IAP.
$Bracing_g$	If the user wants the code to automatically fix the horizontal DOF of the nodes of the left column of the structure. If yes $Bracing_g = 1$, if no $Bracing_g = 0$.
$Bracing_d$	If the user wants the code to automatically fix the horizontal DOF of the nodes of the right column of the structure. If yes $Bracing_d = 1$, if no $Bracing_d = 0$.
$Embedded$	If the user wants the code to automatically have embedded bottom columns. If yes $Embedded = 1$, if no $Embedded = 0$.
H_{fixed}	Vector manually provided by the user. It itemizes the nodes for which the horizontal DOF is fixed. The numbering is relative to the modeling of the IAP in *BeamZ*.
V_{fixed}	Vector manually provided by the user. It itemizes the nodes for which the vertical DOF is fixed. The numbering is relative to the modeling of the IAP in *BeamZ*.
R_{fixed}	Vector manually provided by the user. It itemizes the nodes for which the rotational DOF is fixed. The numbering is relative to the modeling of the IAP in *BeamZ*.
$node_{order}$	Vector provided by the user. It gives the numbering of the nodes in the order illustrated in figure 4.3.
file2.mat	*Matlab* file extracted from the *BeamZ* linear analysis of the structure with the loads inserted.
$elem_g$	Vector enumerating the columns in which the plastic hinges develop to form the panel plastic mechanism at the left of the lost column. The numbering is relative to the modeling of the structure in *BeamZ*.
$elem_d$	Vector enumerating the columns in which the plastic hinges develop to form the panel plastic mechanism at the right of the lost column. The numbering is relative to the modeling of the structure in *BeamZ*.
$LoadCase$	Load case that defines the accidental combination of gravity loads applied to the structure.
Properties specific to the column's removal	
u_{max}	Maximum vertical displacement necessary to reach for the drawing of the $u - N_{lost}$ curve.
$c_{lost} = [n_c\ n_{end}]$	n_c is the number of the column that is being removed. n_{end} characterizes if the top of the column is the starting point ($n_{end} = 1$) or the ending point ($n_{end} = 2$) of the element. The numbering are relative to the modeling of the structure in *BeamZ*.

Table 5.1 – Inputs of the *Matlab* code.

Besides, as already explained, the code is identical to the one developed in the last chapter except for the new step added in the analytical resolution after the resolution of the system summarized in table 2.3. This new part corresponds to the determination of the $u - N_{lost}$ curve for a structure with an IAP assumed elastic-perfectly plastic, based on the $u - N_{lost}$ curve of the same structure with the IAP assumed perfectly elastic. The global framework of this additional part is illustrated in figure 5.7. The $u - \lambda$ curves relative to the right and left panel plastic mechanisms are first determined, followed by the determination of the u for which λ equals 1. Then, the first panel plastic mechanism to be fully developed is determined by the one with the smallest $u(\lambda = 1)$. Finally, the $u - N_{lost}$ curve for a structure with an IAP assumed fully elastic is stopped at the u characterizing the first panel plastic mechanism to be fully formed. The cut curve obtained is the $u - N_{lost}$ curve for the structure at the end of which the IAP may yield.

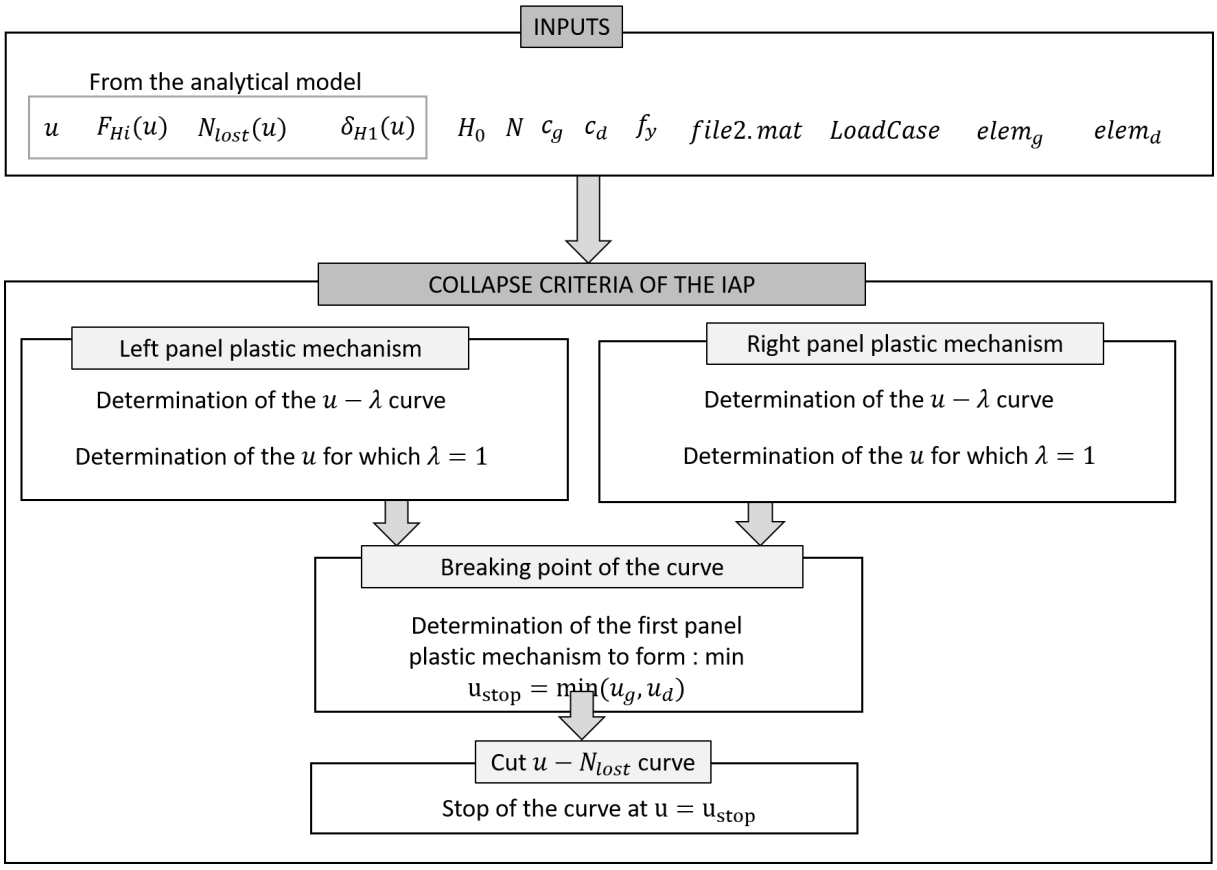

Figure 5.7 – Global organization of the model implementing the yielding of the IAP in the main model.

5.4 Verification of the implementation

To verify the implementation, some steps of the implementation are verified and commented. These checks are made on the scenario 1 of the structure Ib and are explained hereafter.

As all the steps before the introduction of the yielding of the IAP are identical to before, these steps do not need to be verified here. The first nearby step added in the framework is the determination of the $u - \lambda$ curves relative to both left and right panel plastic mechanisms (shown in figure 5.8). To do so, the reduced resistant plastic moment $M_{N\,pl}$ is first determined

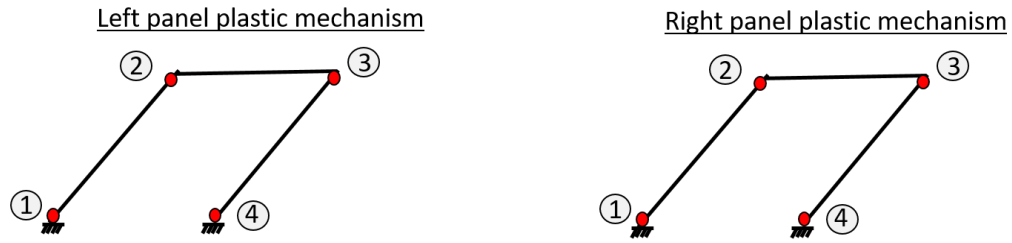

Figure 5.8 – Left and right panel plastic mechanisms of the scenario 1 of structure Ib, respectively on the left and right.

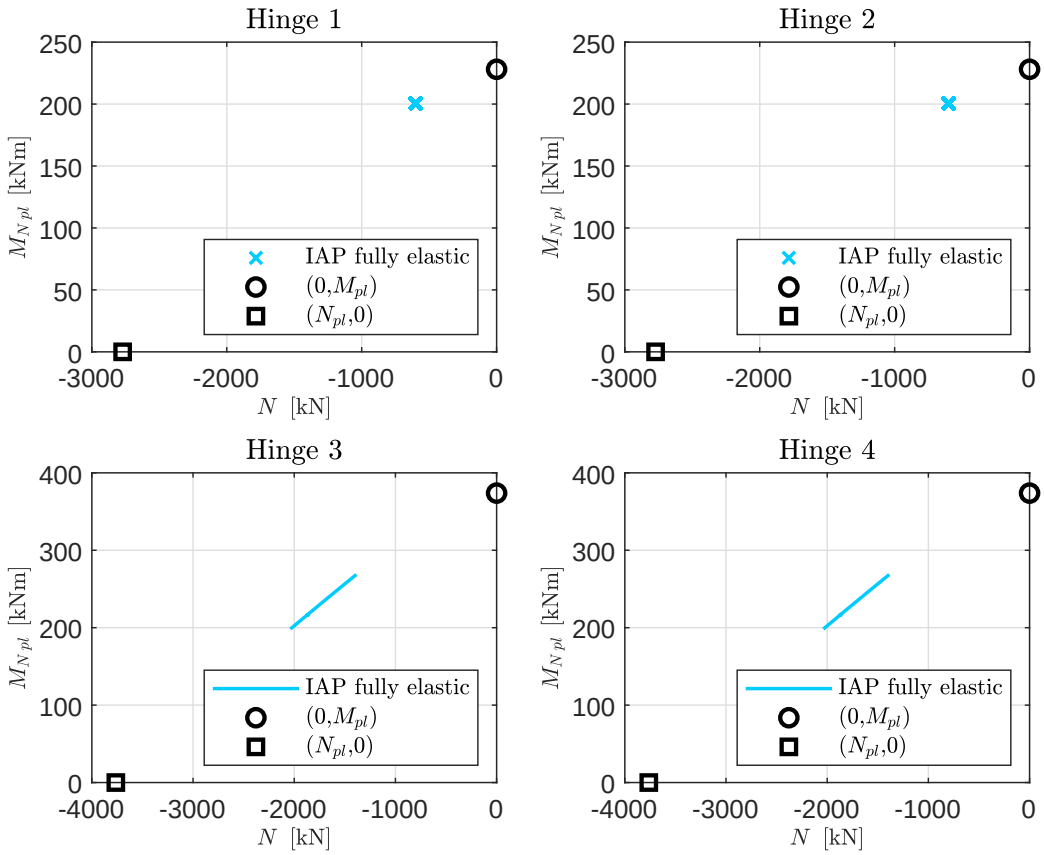

Figure 5.9 – Evolution of the reduced resistant plastic moment, $M_{N\,pl}$, with respect to the internal axial force, N, in the plastic hinges sections of the left panel plastic mechanism (see figure 5.8) of the scenario 1 of structure Ib.

for each step u. Figure 5.9 illustrates the evolution of $M_{N\,pl}$ in each plastic hinge in function of the evolution of the internal axial force in the plastic hinge's cross section. This latter internal force is a combination between the initial internal axial force and the supplementary axial force caused by the redistribution of the load during the removal of the lost column. Therefore these evolutions are based on the assumption that the IAP is perfectly elastic. Furthermore, these evolutions are shown from the beginning of phase 2, when the lost column starts to be progressively removed, until the end of phase 3, when the lost column has been fully removed. Note that the resistant plastic moment and the resistant plastic axial strength are highlighted as well on the graphs to have a mark point.

Let's first focus on plastic hinges 1 and and 2 for which the curve is resumed by a dot. Indeed, these plastic hinges form in a column which is not next to the lost one. As it has been assumed that the load that cannot be carried by the lost column anymore is redistributed completely and equally in the two side columns, all the other columns see no change in their internal forces. Hence, the internal axial force in the cross section of plastic hinges 1 and 2 is constant, in accordance with what has been observed in figure 5.9. Furthermore, the internal axial load is the one appearing when the accidental combination of action of the gravity loads is applied to the structure.

Now, let's look at the plastic hinges 3 and 4, appearing in the columns at the left of the lost column. In this case, the $N - M_{N\,pl}$ evolution is a curve for which the initial internal axial force is the internal axial force of the section when the accidental combination of the gravity loads is applied on the structure. Then, as the lost column is getting progressively removed, half of the load the latter was carrying is progressively redistributed to the column in which the plastic hinges 3 and 4 are forming. Therefore, the axial compression force in the hinges' cross section increases. As the axial force increases, the reduced plastic moment decreases, as seen on figure 5.9.

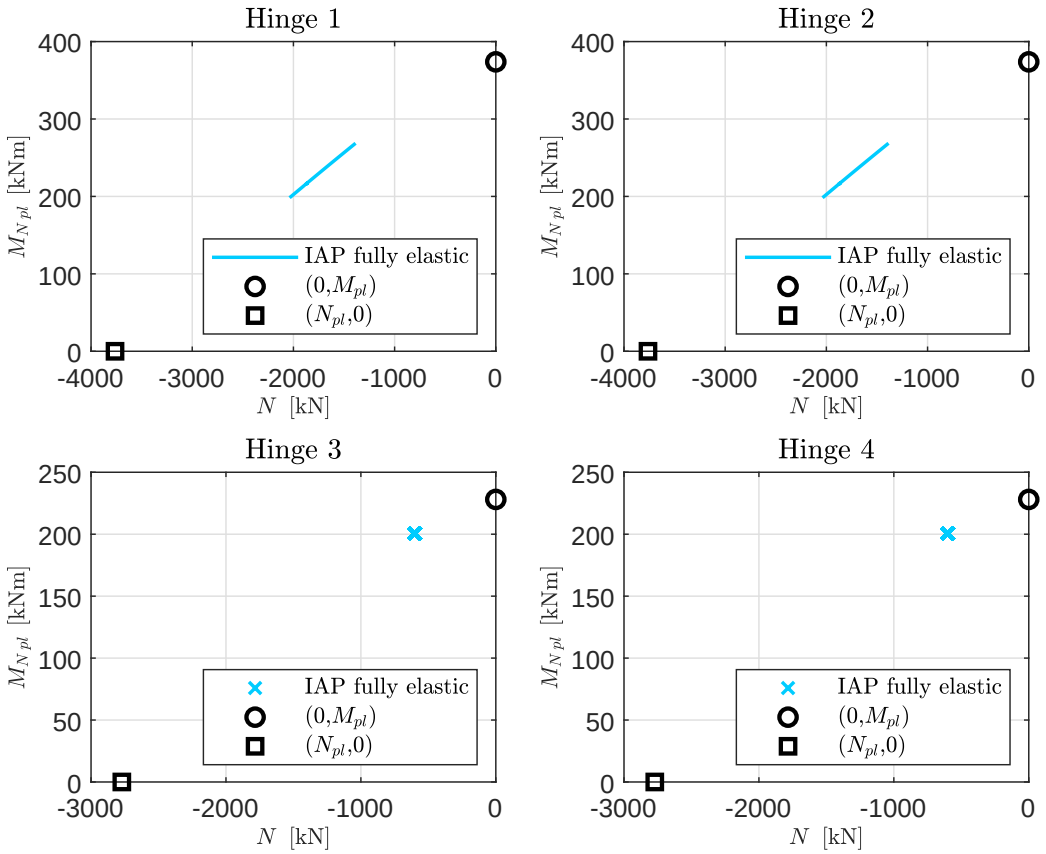

Figure 5.10 – Evolution of the reduced resistant plastic moment, $M_{N\,pl}$, with respect to the internal axial force, N, in the plastic hinges sections of the right panel plastic mechanism (see figure 5.8) of the scenario 1 of structure Ib.

The same conclusions are drawn for the left panel plastic mechanism for which the $N-M_{N\,pl}$ evolution's are illustrated in figure 5.10. Furthermore, the homologous plastic hinges of the

two panel plastic mechanisms are leading to the exact same $N - M_{N\,pl}$ evolution. Indeed, the structure is symmetrical. This is a way to verify that both calculations are not wrongly implemented, even if it is not a way to prove that these calculations are perfectly implemented.

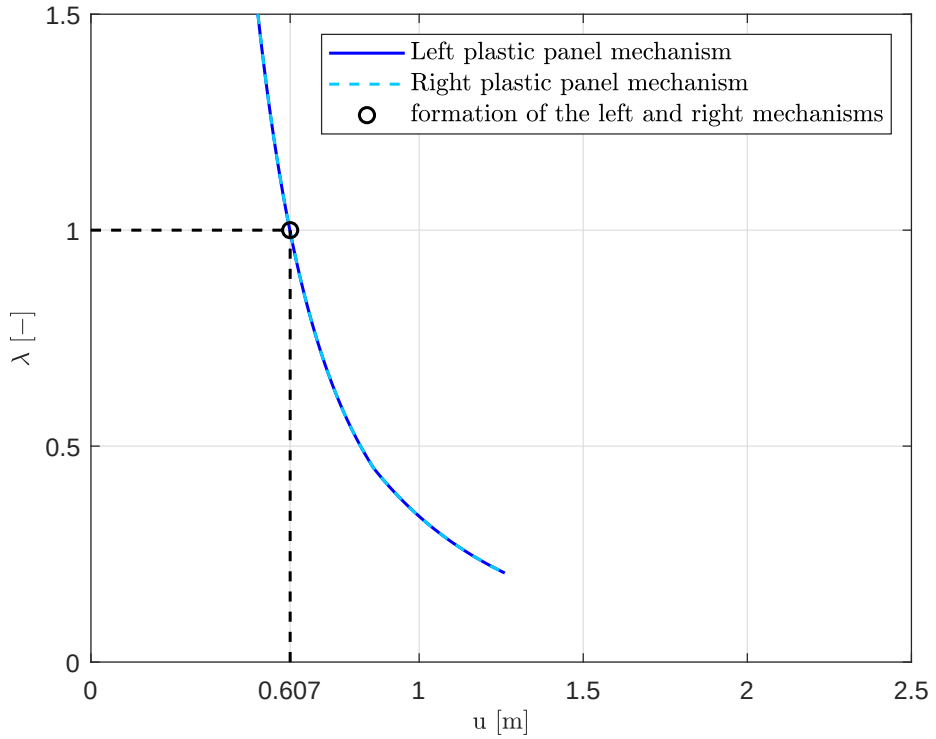

Figure 5.11 – Evolution of the load factor, λ, in function of the vertical displacement at the top of the lost column, u. Comparison between the load factor of the left and right panel plastic mechanisms.

Afterwards, the next step is the determination of the $u - \lambda$ curve of both the left and the right panel plastic mechanisms. These curves are shown in figure 5.11. First of all, both curves are identical. Indeed, as already mentioned, the left and right panel plastic mechanisms are leading to the same panel pastic mechanism as the IAP is symmetrical. Furthermore, the global shape of the curve makes sense compared to the theoretical curve shown in figure 5.5. Moreover, the value of u for which λ equals 1 is $0.607\,m$ which is close to the value obtained in the work of Dewez [8]. Indeed, in order to verify that his analytical method was going to lead to correct results, he applied it to structures using the *Finelg* software to output the curve based on a structure with a IAP assumed perfectly elastic (instead of implementing it in *BeamZ*). The graph he obtained is shown in figure 5.12 where the values of u for which $\lambda = 1$ is equal to 0.727 m. The differences between the two values are due to fact that in this master thesis the formula has been determined using the results from the system resumed in table 2.3; whereas Dewez used the real internal forces determined in *Finelg* to compute this curve.

Figure 5.13 illustrates the load factor, $\lambda_d = \frac{N_{lost}}{N_{AB\,design}}$ (see equation (1.1) in section 1.4), related to the structure's response with respect to the vertical displacement at the top of the lost column, u, for the scenario 1 of structure Ib. Three curves are highlighted in this figure. One is obtained from the analytical model with the IAP assumed fully elastic. Another one

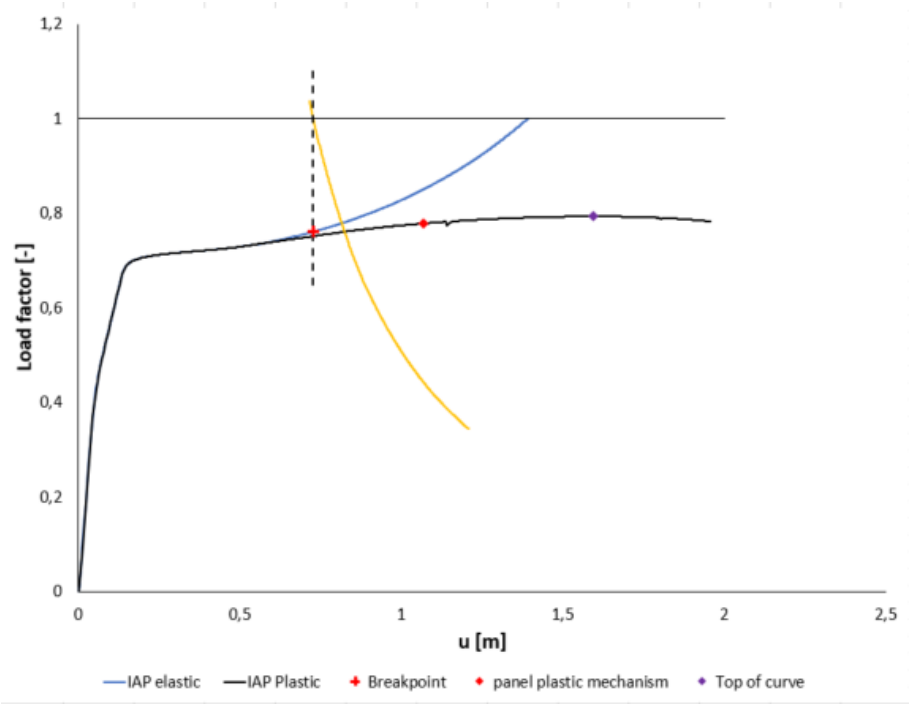

Figure 5.12 – Identified breackpoint of the scenario 1 of structure Ib determined in Dewez's master thesis with the software *Finelg* [8].

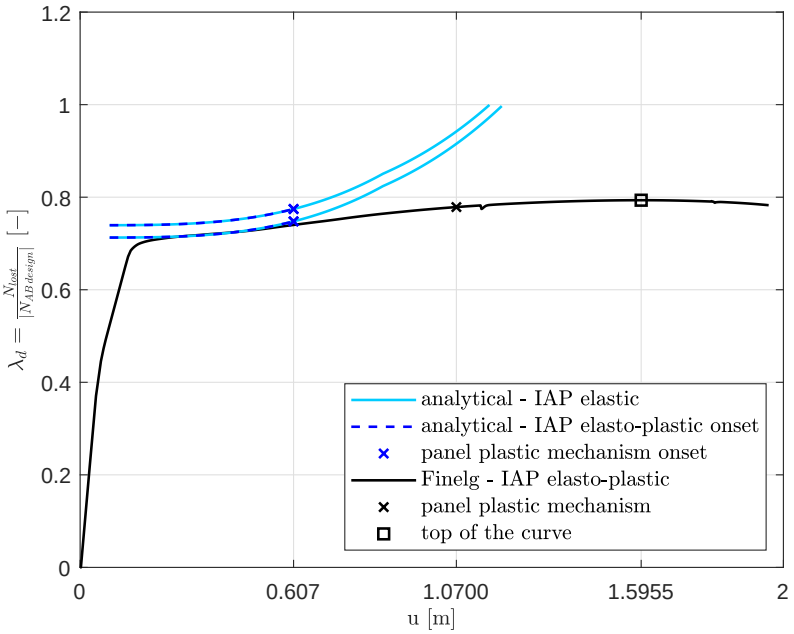

Figure 5.13 – Load factor related to the structure's response with respect to the vertical displacement at the top of the lost column, u, of the scenario 1 of structure Ib. Comparison between the analytical model and *Finelg*.

is obtained from the analytical model but assuming the IAP is elastic-perfectly plastic. The last one is obtained with the use of the software *Finelg* with the elements of the IAP assumed elastic perfectly plastic This graph may be compared to figure 5.12 for which the breakpoint

has been determined after the analytical model has been applied using *Finelg*. Both graphs leads to very similar results which lead to the conclusion of the good implementation of the model.

Furthermore, on the *Finelg* curve, two points are highlighted: the moment when the panel plastic mechanism forms and the top of the curve. Their means are explained in the next section. Besides, the $u - N_{lost}$ curve is shown in figure 5.14. On this curve, only the phase 3 of the $u - N_{lost}$ curve obtained with the analytical model is shown. Indeed, as already mentioned, the model aims to represent only the phase 3 of the structure's response. This curve is very similar to the one shown in figure 5.13. Indeed, it is the same curves except that the y-axis is multiplied by $N_{AB\,design}$.

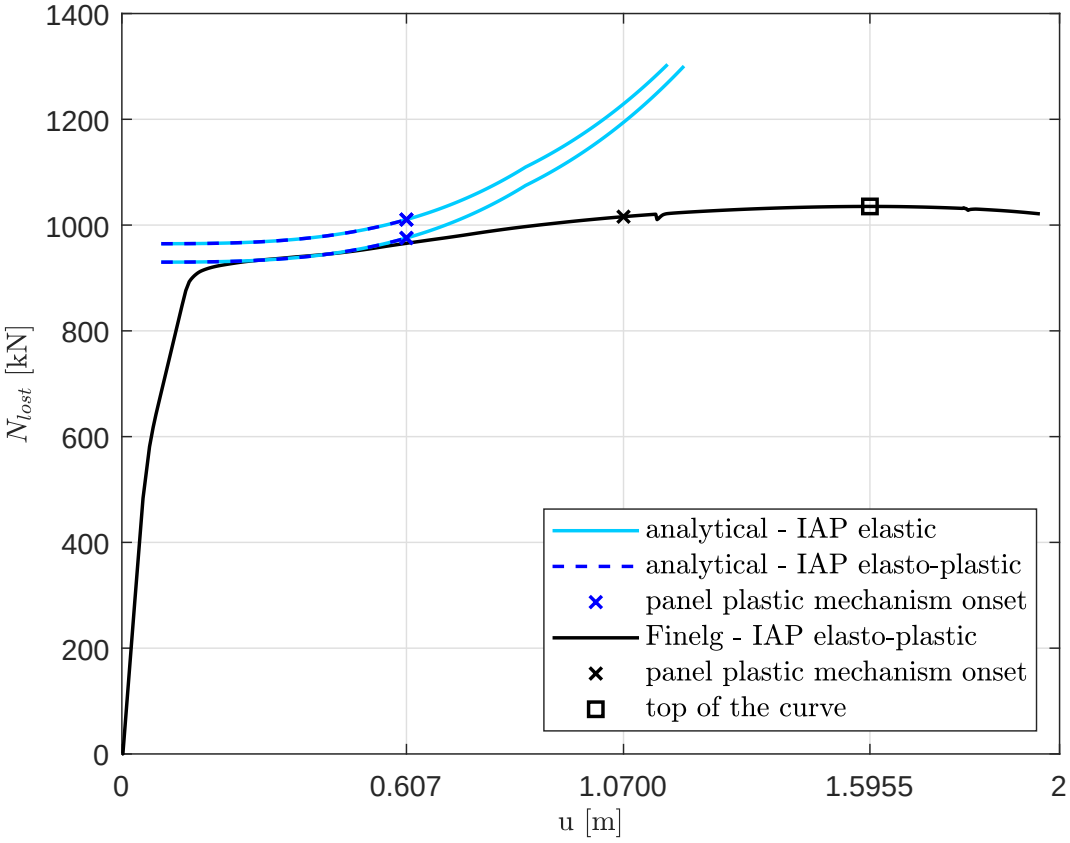

Figure 5.14 – Evolution of the load to be carried by the structure associated to the loss of the column, N_{lost}, in function of the vertical displacement at the top of the lost column, u.

In the next section the results of the scenario 1 of structure Ib are more detailed. Furthermore, other results are detailed to validate the model for other structures as well.

5.5 Validation of the new model

In this section, the response of the substructure obtained with the software *Finelg* is first detailed. Then, this response obtained with *Finelg* is compared with the response obtained with the new analytical model for different structures following the loss of a column.

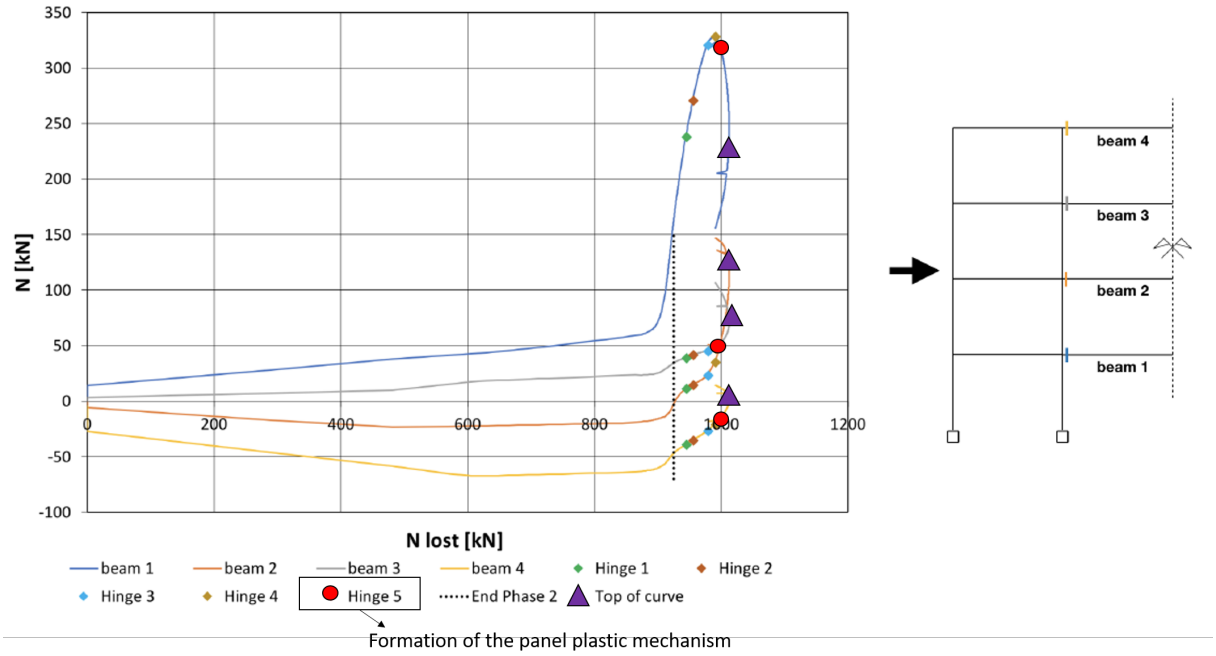

Figure 5.15 – Evolution of the normal forces in the cross section of the beams extremities of the DAP [8].

First, let's focus on the curve obtained with *Finelg* with the assumption that the elements of the IAP are elastic-perfectly plastic. Figure 5.14 illustrates this curve, on which two points are outlined: the moment when the panel plastic mechanism is formed and the moment when the top of the curve is hit. One would think that those two phenomenons should happen at the same time, however they do not. This phenomenon has been studied in Dewez's master thesis [8] and is explained hereafter. Figure 5.15 illustrates the evolution of the normal forces in the beams' cross section of the DAP in function of the load to be supported by the structure associated to the progressive loss of the column. First, at the end of phase two, a large increase in all the beams is observed. This is due to the development of the membrane forces, which are larger for the bottom stories than for the top stories. Moreover, the extremity of the top beam (beam 4) stays in compression when the catenary actions develop. This is in accordance with the theoretical explanations given on the curve in section 1.3. Then, as soon as the panel plastic mechanism is formed, the bottom beam of the DAP (beam 1), which was in high tension thanks to the activation of the catenary actions, is drastically decreasing. This behavior goes in accordance with the idea that the panel plastic mechanism and the top of the curve should be happening at the same time. However, the normal force at the extremity of beam 4 (the top beam of the DAP) is still in compression when the panel plastic mechanism develops. Therefore, when this latter forms and deletes the anchorage brought by the IAP, the top beams in compression bring a new anchorage on which the DAP may rely on. Therefore, while the internal force carried by beam 1 has drastically decreased, the internal axial forces in beams 2 and 3 have drastically increased. Therefore, these middle beams are able to carry the tension force that could not be carried anymore by the bottom beam and they are the reason why the top of the curve is not happening right after the panel plastic mechanism forms. In conclusion, the existing lateral restrain after the formation of the panel plastic mechanism is due to the arch effect, detailed previously in section 1.3.

Now, the collapse criteria accuracy is now commented. To do so, the moment when the plastic hinges 3 and 4 form according to the results obtained with *Finelg* is compared to the moment when these plastic hinges are forming in the analytical model. Figure 5.16 illustrates the $N - M_{N\,pl}$ curve determined with the analytical model for the scenario 1 of structure Ib. The figure highlights the moment in the analytical model when the panel plastic mechanism forms and, which corresponds to the moment when the hinges are assumed to form. Furthermore, this latter figure shows as well the internal forces obtained with the *Finelg* simulation in the plastic hinges sections. When these internal forces cross the $N-M_{N\,pl}$ curve, the plastic hinge forms in the *Finelg* modeling of the situation. As seen on figure 5.16, the analytical model thus represents correctly the panel plastic mechanism onset, which is identical to the once predict by *Finelg*, as analyzed in Dewez's master thesis [8].

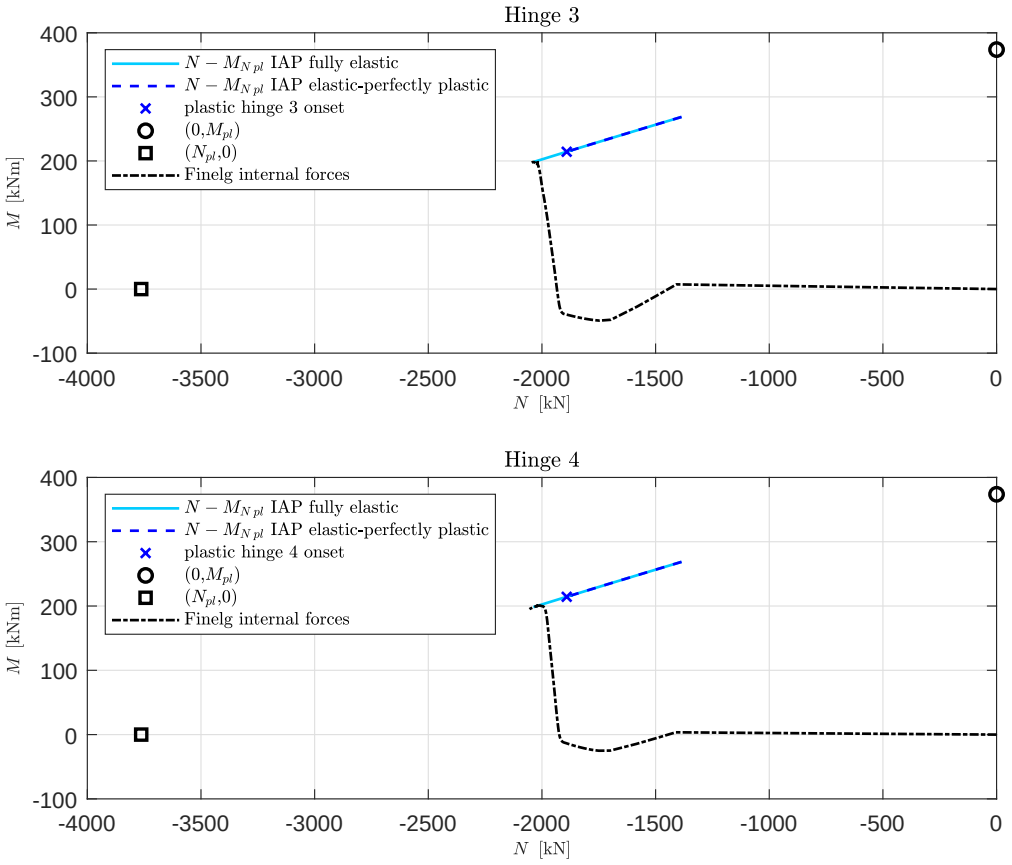

Figure 5.16 – Comparison of the moment when the plastic hinges form in reality (with *Finelg*) and the moment when they are assumed to form in the analytical model.

Let's then focus on the response of the frame Ib further to scenario 1, resumed on figure 5.17. To do so, let's define different error measures:

- The "error 1" is the relative absolute error in terms of displacements between the breaking point of the analytical curve and the panel plastic mechanism onset of the *Finelg* curve,
- The "error 2" is the relative absolute error in terms of displacements between the breaking point of the analytical curve and the top of the *Finelg* curve,

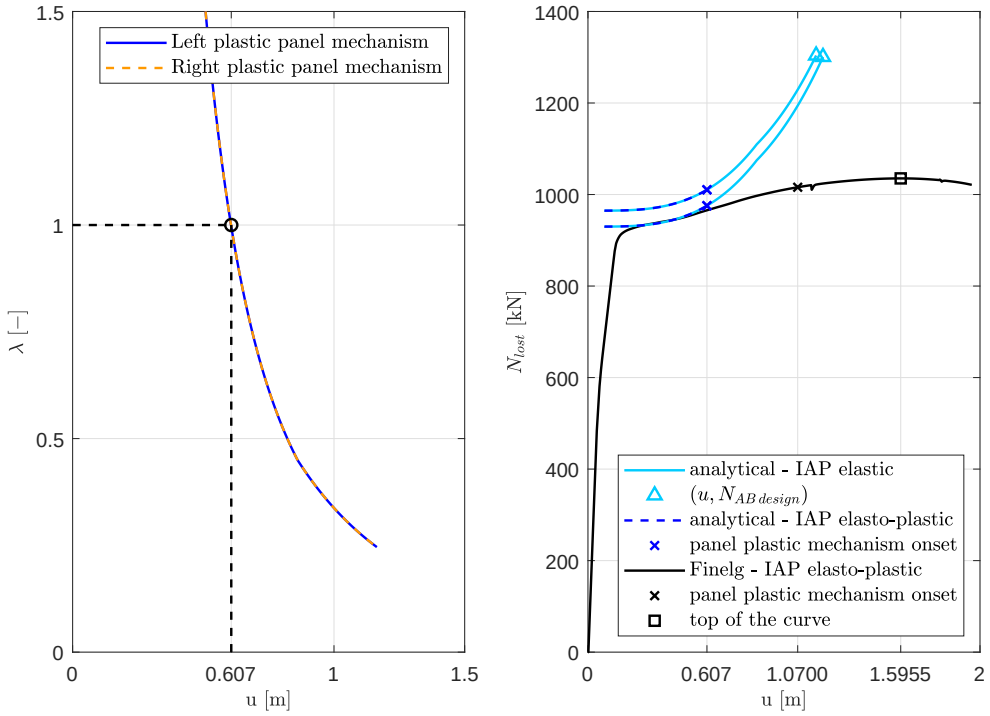

Figure 5.17 – Response of the structure Ib further to scenario 1.

- The "error 3" is the relative absolute error in terms of forces between the breaking point of the analytical curve and the point of the *Finelg* curve corresponding to the same displacement,
- The "error 4" is the relative absolute error in terms of displacements between the breaking point of the analytical curve and the point of the *Finelg* cure corresponding to the same force.

Figure 5.17 illustrates the results obtained with the analytical model after correcting the DAP plastic mechanism, as well as the results of the analytical model before the correction. The results with the non corrected DAP plastic mechanism lead to accurate results in terms of N_{lost}. Indeed, an error of 0.5% is made through the evaluation of the panel plastic mechanism onset (error 1) and an error of 2.4% is made for the evaluation of the top of the curve (error 2). Furthermore, the results, in terms of N_{lost} are on the safe side. However, it leads to non accurate displacements at all: by assuming the breaking point is part of the structure response, an error of 40% (error 4) is made in terms of displacements. Moreover, these non accurate displacements are not on the safe side. Indeed, the evaluated displacements are smaller than those that will appear for such a N_{lost} in reality. These cannot therefore be used to verify such a structure.

However, using the curve with the corrected DAP plastic mechanism onset, the obtained results are a lot more accurate and useful for future practice verification methods to be provided to the design desks. Indeed, a larger error is brought in terms of displacements for the evaluation of the panel plastic mechanism onset (4.1 % error, see table 5.2), as well as in terms of displacements for the evaluation of the top of the curve (6.1%). But the point obtained with the analytical model is almost exactly on the curve. Therefore, by assuming

this point is on the real curve, a smaller error is made on in terms of displacement and force. By assuming the structure collapses for that load, the model is on the safe side as in reality the structure collapses for a load about 6% higher. Furthermore, for that load, the error in terms of displacements is of 13%, which is 27% less than with the non corrected analytical model. This model could be applied to other structures and a the importance and variation could be discussed.

In the following, the response of different structures following the loss of a column determined with the analytical model are compared with the response obtained with the *Finelg* curve. Figure 5.18 shows the response of structure IIb further to scenario 1, figure 5.19 summarizes the response of structure IIb further to the scenario 2 and figure 5.20 illustrates the response of the structure IIIb further to the scenario 1. Furthermore, table 5.2 gather the evaluation of the differet error for the different structures under investigation.

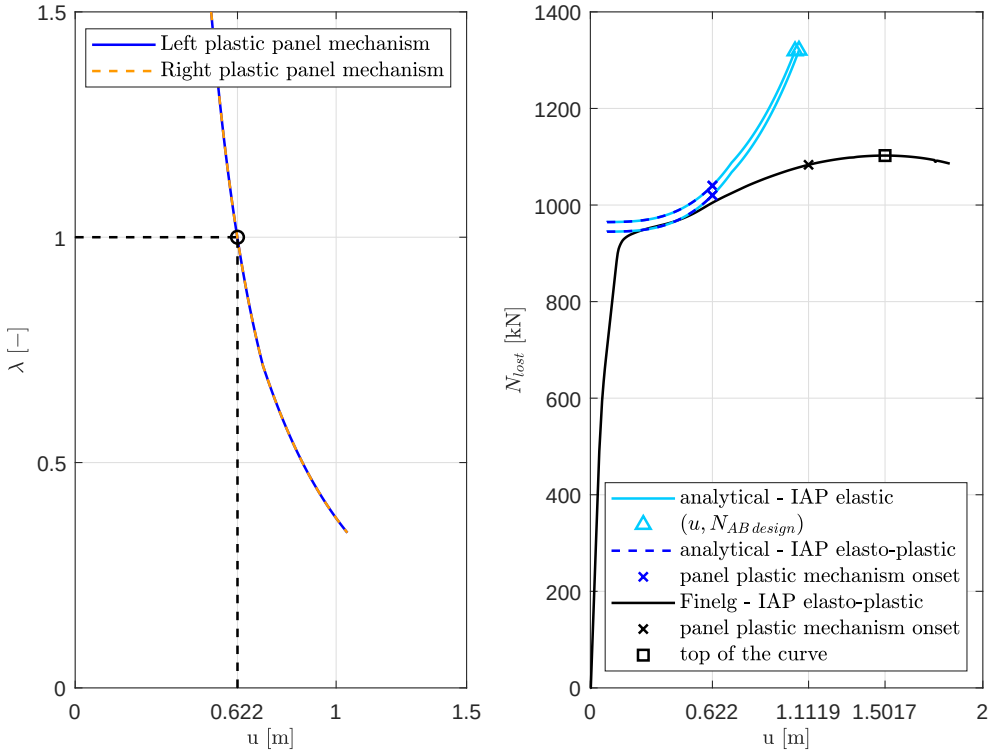

Figure 5.18 – Response of the structure IIb further to scenario 1.

		error 1 [%]	error 2 [%]	error 3 [%]	error 4 [%]
After the shift	structure Ib scenario 1	4.1	6.1	0.02	13
	structure IIb scenario 1	6.2	8.1	0.04	10.9
	structure IIb scenario 2	1.5	2.3	0.09	18.1
	structure IIIb scenario 1	7.8	9.9	0.13	12.4

Table 5.2 – Numerical value of the four errors explained earlier and applied to the model after the correction of its DAP plastic mechanism.

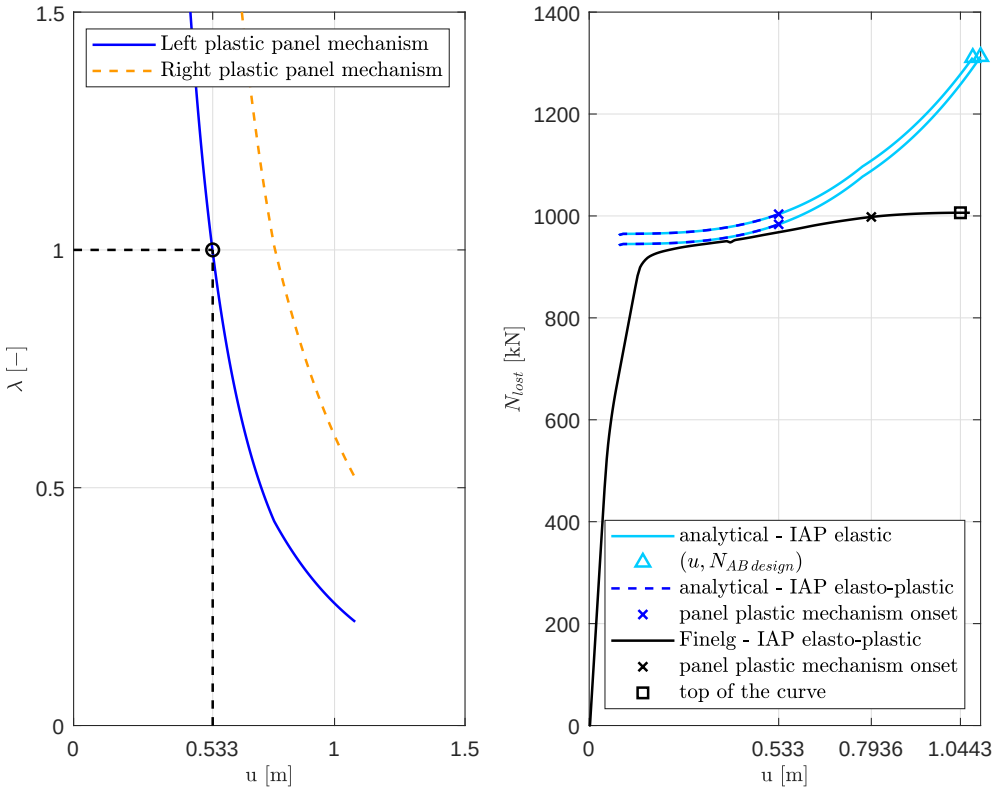

Figure 5.19 – Response of the structure IIb further to scenario 2.

From these results, the same observations and conclusions can be drawn regarding the responses of the analytical model relative to the uncorrected and corrected DAP mechanism. Furthermore, the error made in terms of loading with respect to both the panel plastic mechanism onset and the top of the curve (i.e. error 2) tends to increase with the number of spans of the structure. Indeed, the more the spans, the higher the restrain brought by the IAP to the DAP is and the less flat the *Finelg* curve is. However, this error is on the safe side for the situations under investigation because the value of N_{lost} obtained with the analytical model is smaller than the value of N_{lost} obtained with the modeling in *Finelg*. Besides, in terms of displacement and force accuracy by assuming the pannel plastic mechanism onset obtained with the corrected analytical method ay be reached by the structure, the breaking point is assumed to be one point of the real curve. No conclusion may be yet drown. More structures should be analyzed deeper in future work.

Furthermore, figure 5.19 shows well that when the IAP is non symetrical, the two panel plastic mechanisms do not form at the same time and it is the one forming first that governs the end of the $u - N_{lost}$ curve.

Moreover, remark that all the studied structures in this section collapse before the end of phase 3. Indeed, the analytical curve representing the structure with the possible yielding of the IAP stops before the end of phase 3, i.e. before the reach of $|N_{AB,design}|$. Further analyses and studies needs to be done to study the validity of the model on such structures behavior.

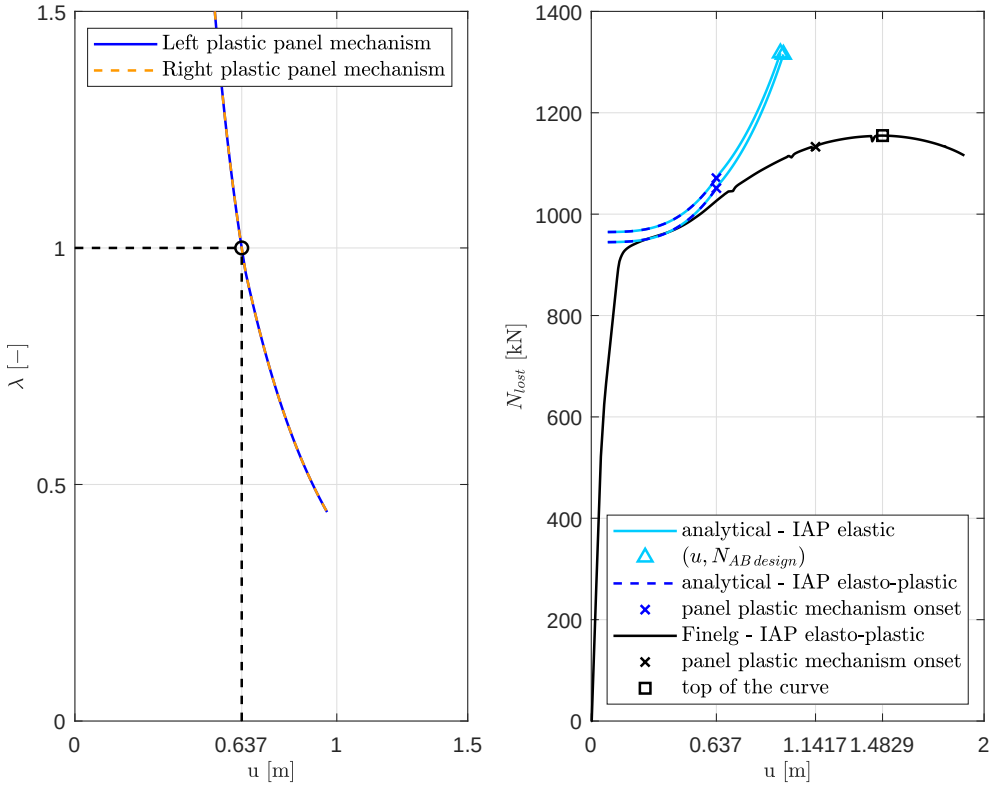

Figure 5.20 – Response of the structure IIIb further to scenario 1.

5.6 Personal conclusive remarks

Before all, it worth mention the difficulties encountered during this task. These latter have been linked to the desired automating of the method. Furthermore, the initial assumed DAP of the analytical model has been analyzed to be wrong just a few days before the deadline. Therefore changing the results and letting not much time to analyze deeper the different curves.

Despite everything, the new model implemented allows the determination of the response of a structure within which a panel plastic mechanism may form in the IAP. The evaluation of the panel plastic mechanism onset has been analyzed to carry on well with the new model. This improvement of the initial model is important in order for the model to be able to simulate realistic structures. Furthermore, at first sight, the analytical model seems to be a good alternative to characterize the structural integrity of a structure faced to an exceptional event leading to the loss of a column. The small parametrical study helped to verify the model and validate it for some structure.

However, none of the tested design structure has kept its structural integrity faced with these exceptional events. It would be interesting to redesign the preceding studied structures in order for them to keep their structural integrity faced to those exceptional events. Besides, this new implementation is only applicable in the case of the loss of a bottom column. Otherwise, one should verify that the involved plastic mechanisms are still identical. Therefore, it is only natural that one of the next steps will be to study the cases in which the loss column is not

a bottom column and to enlarge the field of application of this model. Moreover, it would be helpful to conduct parametrical studies in order to comment in more details the accuracy of the model and to determine its limits. Finally, it would be interesting to automate the strength verification of the concerned elements, now that the initial internal forces may be obtained with *BeamZ* and used in the model implementation. More details are given on the perspectives of this master thesis.

CHAPTER 6

Conclusion and perspectives

6.1 Conclusion

In the present work, a contribution to the analytical model developed by Liège University to investigate the robustness of structures is presented. Indeed, after a contextual introduction, some important robustness general principles defined in the Eurocodes 1-7 [2] have been explained. In particular, the "alternative load path method", a method consisting of the analysis of a structure further to the loss of one of its structural elements after being faced to an exceptional event, have been detailed. Then, a closer look has been given to the general principles governing the response of a structure further to the loss of a column. Finally, the analytical model developed by Liège University to represent the phase 3 of the structure response (see figure 1.17 in section 1.3, the topic of this master thesis, has been introduced.

This analytical model and its implementation developed so far have been first analyzed in chapter 2. Within this chapter, the hypotheses at the basis of the model, the code organization, the system of equations governing the analytical model, and their origin are clearly detailed and explained. Furthermore, their implementation have been verified and mistakes existing in the initial implementation have been highlighted.

Afterward, a first enhancement of the model implementation has been carried on in chapter 4 to extend its field of applications. This latter consisted of the combination of *BeamZ* and *Matlab* to replace the initial determination of the flexibility matrices, S_g and S_d, characterizing the IAP in the substructure defined in section 2.1.2. Both the new and the initial implementations lead to the same results for the structures that are part of the field of application of both implementations. During the verification process, the analytical model turned out to be based on the wrong DAP plastic mechanism. It has been corrected and validated by comparison with *Finelg* simulations. At the end of the day, the model represent well the beginning of phase 3. However, it quickly diverges from the *Finelg* curve. Besides, the hypothesis that the IAP stays elastic during the whole phase 3 is unrealistic, as concluded in Dewez's thesis [8].

This issue has been addressed in the last objective of this thesis in chapter 5. The yielding of the IAP (see figure 1.9 in section 1.3) is introduced through the implementation of the analytical method developed in Dewez's master thesis [8]. This method, and the way to integrate it in the code, has been first explained. The results have been then verified and validated trough comparison with *Finelg* simulations. The corrected analytical model combined with this improvement lead to accurate results in terms of loading but not so accurate and unsafe in terms of displacements (about 10% lower).

6.2 Perspectives

The first improvement of the analytical method, concerning the determination of the flexibility matrices, allows a lot more flexibility on the choice of the structure. More realistic structures may be modeled with the analytical method, which open a lot of possibilities for parametric studies. However, although the model has been validated trough several simulations, only the case of the loss of a bottom column has been studied. It would be interesting to qualify the accuracy improvement of the new implementation, with respect to the initial one, for situations in which the lost column is not a bottom column.

Concerning the analytical model taking into account the yielding of the IAP, this model has been validated through several structures, however it would be interesting to perform parametric studies to investigate the accuracy and the limitations of the IAP yielding prediction. Furthermore, as none of the studied structures had enough structural integrity faced to those events, it would be interesting to redesign these structures to enhance their structural integrity and reapply the model to these redesigned structures to qualify how the model reflects the behavior of these non collapsing structures. Note that the first elements to redesign are the columns in which the plastic hinges of the first panel plastic mechanism onset. Besides, other elements should be studied to verify the absence of any instabilities nor resistance failures. Another further investigations subject could be to investigate the IAP plastic mechanism when the removed column is not a bottom column in order to determine the break point in those cases and to enlarge the method in an automatic way.

Moreover, concerning the general analytical method itself, the analytical model of the phase 3 could be merged with the one to reproduce phase 2 in order to automate the shifting of the curve (i.e. the correction of the starting point of phase 3). Furthermore, the strength verification could be automated in the implementation of the model. Finally, but not only, the limits of the formation of the complete mechanism in the DAP should be studied. To do so, parametric studies could be conducted to determine when all the stories are not involved in the plastic mechanism onset of the DAP.

In conclusion, several researches still need to be performed on different aspects or hypothesis of the model. In any case, by improving and studying the validation of the model, step by step, Liège University gets closer to the final objective that is to propose design requirements to ensure an appropriate robustness under the loss of a column.

Bibliography

[1] J.-F. Demonceau, J.-M. Franssen, B. Mihaylov Conception et exécution des bâtiments. Partie dédiée à la robustesse des structures. Liège University course. Liège, Belgium, 2008.

[2] European committee for standardization. EN 1991-1-7: Eurocode 1: Actions on structures - Part 1-7: General actions - accidental actions. Brussels, Belgium, 2006.

[3] J.-F. Demonceau Steel and composite building frames: sway response under conventional loading and development of membrane effects in beams further to an exceptional action, PhD thesis presented at Liège University. Liège, Belgium, 2008.

[4] L. N. N. Hai Structural response of steel composite building frames further to an impact leading to the loss of a column, PhD thesis presented at Liège University. Liège, Belgium, 2008.

[5] MSM department Greish info s.a. Finel user's manual - Non linear finite element analysis program - Version 8.5. Liège, Belgium, 2002.

[6] Denoel V. BeamZ: structural analysis - special version.

[7] Duchêne Y. and Guisse S. WnOSSA2D: computation software for 2D structures - User's manual (in French). Liège, Belgium, 1995.

[8] J. Dewez. Robustness of steel structures further to a column loss: influence of the yielding of the indirectly affected part on the global response of the structure, Master thesis presented at Liège University. Liège, Belgium, 2018.

[9] C. Huvelle. Contribution à l'étude de la robustesse des structures de bâtiments, Master thesis presented at Liège University. Liège, Belgium, 2011.

[10] S. Kulik. Robustness of steel structures: consideration of couplings in a 3D structure, Master thesis presented at Liège University. Liège, Belgium, 2014.

[11] C. Huvelle, J.-P. Jaspart, J.-F. Demonceau. Robustness of steel building structures following a column loss, scientific article. Helsinki, Finland, 2013.

[12] C. Huvelle, J.-P. Jaspart, J.-F. Demonceau, V.-L. Hoang. Complete analytical procedure to asses the response of a frame submitted to a column loss, scientific article. Oxford, United Kindom, 2015.

[13] L. Comeliau. Effects of the dynamic behavior of steel structures further to a column loss (in French), Master thesis presented at Liège University. Liège, Belgium, 2009.

[14] L. Comeliau, B. Rossi, J.-F. Demonceau. Robustness of steel and composite buildings suffering the dynamic loss of a column.

[15] W.F. Chen, G. Yoshiaki, Liew J.Y. R., Stability design of semi-rigid frames. John Wiley & sons, INC, 1996,p.162-163.

[16] Villette M. Analyse critique du traitement de la barre comprimée fléchie et propositions de nouvelles formulations, PhD thesis presented at Liège University. Liège, Belgium, 2004.

[17] Hjeir F. Robustness of steel structures further to a column loss: identification of the structural requirements through parametrical studies, Master thesis presented in Liège University. Liège, Belgium, 2015.

[18] European commitee for standardization. EN 1990: Eurocode - Basis of structural design. Brussels, Belgium, 2002.

List of Figures

List of Tables